Studies on OFDM Signal Recognition in Cognitive Radios using MachineLearning

Hang Liu

Department of Communication Engineering and Informatics

The University of Electro-Communications

A thesis submitted for the degree of

Doctor of Philosophy in Engineering

2019 September

Chairperson: Professor Takeo Fujii

1. Member: Professor Xi Zhang

2. Member: Professor Yasushi Yamao

3. Member: Professor Koji Ishibashi

4. Member: Professor Toshiharu Kojima

Day of the Pre-defense: 21th May, 2019

Day of the Final defense: 6th August, 2019

Abstract

In the traditional wireless communication systems, the access way to the spectrum resources is static, which means the allocation of the available frequency bands is unchangeable and pre-reserved; thus the systems often result in inefficient utilization of the valuable frequency bands. The cognitive radio (CR), as a raised paradigmatic solution to the frequency-scarceness, recycles the idle bands left by the static distribution and enables the coexistence of the licensed and unlicensed user without compromising the communication quality. A primary user (PU) is the entitled with the privilege, or higher priority, to use the frequency bands. Meanwhile, a secondary user (SU) is equipped with cognitive radio capabilities that cannot only sense the spectrum reliably to detect if it is occupied by a primary user, but also alter certain related parameters to exploit the unused spectrum. In such an execution platform, the spectrum sensing through the physical layer takes the task of being aware of the current utilization status of the spectrum or the existence of the primary user. Therefore this technology normally includes determining the spectral content, recognizing the occupied signal and obtaining the usage characteristics across multiple dimensions such as time, space and code.

The orthogonal frequency division multiplexing (OFDM) modulated signal is able to achieve high spectral efficiency while survive from the narrow-band co-channel interference, as well as the inter-symbol interference and fading caused by multipath propagation. The benefactor is the special frame-by-frame signal structure of OFDM modulation that contains pilot tones, a cyclic prefix, and preambles. The OFDM-based CR system inherits the flexibility of the OFDM signals

and tends to be easily modified to meet the on-demand transmission. Then inspired by a feasible conventional method of the spectrum sensing, the cyclostationary feature detection, this dissertation focuses on the cyclic spectral signature which can be extracted from the mentioned built-in structures of the OFDM modulation scheme. Among those, the pilot-tones-based spectrum sensing is emphasized more than the other two due to its robustness of cyclostationarity against harsh transmission environments.

The objective of this dissertation is to develop and provide advanced OFDM signal-identification schemes to perform the spectrum sensing in the CR system. In order to achieve this, an efficient data analyzing process is necessarily executed after the cyclostationary feature extraction. The term cognitive involves obtaining knowledge and comprehension by perception, learning, reasoning to problem-solving, which links itself to a trendy technology of machine learning with similar features. It performs the "cognition" by extracting patterns and exploiting deeper connections from massive amounts of raw data. Furthermore like the focused spectrum sensing, the machine learning senses the environment and internal states, classifies and generalizes needed information and achieves goals and decision-making. On the one hand, massive sets of data help to increase the learning accuracy during the training process, which means the machine learning performance is strongly dependent on the selection of data expression/representation. For this reason, a proper data transformation, such as the mentioned cyclostationary feature extraction, is able to effectively support and localize the machine learning into the spectrum sensing. On the other hand, the implementing competence of the data processing task depends on the classifier architecture of the neural networks of machine learning. This dissertation particularly pays attention to how the network constructions, including the layer, node, type, etc., affect the data processing results.

A classification problem is usually the purpose of a machine learning network. Therefore, to integrate the machine learning and spectrum sensing together, a fundamental implementation frame is proposed to convert the signal recognition into classification. The statuses of licensed user are considered as different classes of data. More specifically, this dissertation discusses two converted implementation schemes. Firstly, for unlicensed user terminals that utilize the full-duplex (FD) mode where severe self-interference will be encountered, the cyclostationary periodogram generated by OFDM pilots is exhibited in the form of images. These images are subsequently plugged into convolutional neural networks (CNNs) for classifications owing to CNNs strength in image recognition. More importantly, to realize spectrum sensing against residual self-interference, noise pollution, and channel fading, this dissertation uses adversarial training, where a CR-specific, modified training database was proposed. This dissertation analyzes the performances exhibited by the different architectures of the CNN and the various resolutions of the input image to balance the detection performance with computing capability. This dissertation also proposes a design plan of the signal structure for the CR transmitting terminal that can fit into the proposed spectrum-sensing scheme while benefiting from its own transmission. The simulation results prove that the proposed method has excellent sensing capability for the FD system; furthermore, it achieves a higher detection accuracy than the conventional method. Secondly, an ensemble learning (EL) framework is adopted for cooperative spectrum sensing (CSS) in an OFDM signal based CR system. Each unlicensed user is accordingly considered as a base learner, where the local spectrum sensing is for investigating the probability of the licensed user being inactive or active. The CNN with simple architecture is applied for the limited computation ability of each unlicensed user, while the cyclic spectral correlation feature is still utilized as the input data. As for the supervised learning, the bagging strategy is helped to establish the training database. For the global decision, the fusion center employs the stacked generalization for further combination learning the SU output of the probability predictions of the PU status. The proposed method shows significant advantages over conventional CSS methods in term of the detection probability or false alarm probability performance.

Simulations are performed to test whether the proposed schemes can provide better spectrum sensing performances than conventional methods. Comparisons are usually conducted with the energy detection and cyclostationary feature detection: the former for its well-recognized symbolic while easy realization, the latter for the fact that it is using the same feature for sensing as the proposed schemes. All the results show that the proposed schemes can possess capabilities of better OFDM signal recognition. Other inner comparisons are also performed within each proposed scheme to identify the best structure for data processors, the most suitable number for SU cooperative system, etc.. Such simulation results are given and carefully analyzed for future references. As long as machine learning technologies have drawn a lot of attentions in various fields including advanced researches, manufactures, etc., one can only expect such a situation to keep moving forward. In the future, learning may more orient to system management in order to directly learn from the actual user terminal and integrate the data in the first place. Meanwhile, from the technology level, both the hardware and software will face more challenges; for example, the cognitive radio user may need a processor with stronger computing ability but smaller body size. Therefore, revolutions in the system integration mode, central processor or individual terminals are expected to happen.

Acknowledgements

This research was completed with the guidance and help of my supervisor Professor Fujii. I would like to express my sincere gratitude. Professor Fujii's profound professional knowledge, rigorous academic attitude and professionalism have set a good example for me as an excellent researcher and a model for me to learn. He not only teaches me to study, but also teaches me how to do things, and also gives me a lot of care in my life in Japan. I would like to extend my sincere respect and sincere gratitude to Professor Fujii.

In the three and half years of study, I received the care, guidance, encouragement and help from all the faculties, staffs and fellow students in AWCC. They make me feel welcomed not only to the lab but also to this country. I would like to express my thanks to all them who help learn and fit in this new environment.

Thanks to every scholar involved in this paper. This dissertation draws on the views and arguments of most scholars. If there are no scholars' research results to provide me with guidance and help, I will not be able to successfully complete this dissertation. I would like to express my sincere gratitude to every scholar.

Finally, I want to thank my family. Only under their support, I was able to go this far. Thanks to all those who care and help me.

In short, during these three and half years of doctoral studies, I not only exercised my ability in academic research, but also enriched my life experience. I will always cherish this campus time.

Contents

List of Figures

LIST OF FIGURES

List of Tables

Acronyms

AI	artificial intelligence
BPSK	Binary Phase Shift Keying
CFD	cyclostationary feature detection
CIR	channel impulse response
CNN	convolutional neural network
CP	cycle prefix
CR	cognitive radio
CSS	cooperative spectrum sensing
DNN	deep neural network
ED	energy detection
EL	Time Complexity
FCC	Federal Communications Commission
FD	full-duplex
FFT	fast Fourier transform
ICI	inter-code interference
IFFT	inverse fast Fourier transform
INR	interference-to-noise ratio
ISI	inter-Symbol interference
MUSIC	multiple signal classification
ML	machine learning

MMSE	minimum mean square error
N-QAM	N-Quadrature Amplitude Modulation
OFDM	orthogonal frequency division multiplexing
p_d	probability of detection
p_f	probability of false alarm
PHY	physical
p_m	probability of miss detection
PU	primary user
QoS	quality of service
QPSK	quadrature phase shift keying
ROC	receiver-operating characteristic
RSI	residual self-interference
SCD	spectral correlation density
SCF	spectral correlation function
SNR	signal-to-noise ratio
SS	spectrum sensing
SU	secondary user
SVM	support vector machine

Chapter 1

Introduction

At the beginning of the thesis, this chapter introduces the study about orthogonal frequency division multiplexing (OFDM) signal recognition in the cognitive radio (CR) using machine learning (ML). The structure of this chapter is as follows. In Section 1.1, the background of the research as well as some critical technologies related to the applications in the cognitive radio is introduced. Section 1.2 explains the motivation as well as problems that inspire applying the machine learning in an OFDM signal-based cognitive radio system. Section 1.3 lists both the contributions and novelties of this dissertation. Section 1.4 gives scope and objectives. The dissertation organization, as well as the overviews of all chapters, are stated in Section 1.5 at the final of this chapter.

1.1 Background

From the moment that only-voice communications evolve into multi-media applications, such kinds of devices with high data rate is developing in an explosive growth speed. Taking into account the nature spectrum limitations, obviously, the previous static spectrum allocation strategy in wireless communication cannot provide enough transmission channels and serve the massive number of the mentioned high data rate devices. Therefore, innovative technologies that are able to offer a new distribution approach of the available spectrum bands is desired. Being a promising solution to the congestion problem, *cognitive radio* can offer the opportunistic utilization to recycle not heavily occupied entitled bands

[1, 2]. Since there seems no unified common understanding of the general concept of CR, recently it has been exploited to contain different definitions for an individual specific background. However, this dissertation uses the definition that employed by the FCC (Federal Communications Commission), that the cognitive radio refers to a smart radio mechanism which can be aware of its interesting transmission environment then automatically operate self-modifying to guarantee a free channel for the secondary markets and upgrade the max throughout [2]. This means the CR system offers new spectrum accesses through automatically exploring locally unused frequency bands.

The cognitive radio must observe its operating environment and understand its current situation, then make in-place decisions based on their observations, expectations, and experiences, and finally perform intelligent adjustments to maximize its utilities subject to many limitations. It is inspired by a learning process, "cognition cycle", as shown in Figure 1.1. In order to execute thusly, the cognitive radio should possess the ability to measure, sense, learn and understand parameters that are related to characteristics, availability and operating environment for spectrum channels, user policies, networks, as well as other operational limitations. On the one hand, a primary user (PU) is entitled with higher priority or privilege for the utilization of a particular portion of the spectrum bands. On the other hand, a secondary user (SU) with lower priority can access to the entitled spectrum bands only when it will not cause any interference to the primary user. Hence, the SU requires to have CR functions of diagnosing the interested frequency band to make sure if its current utilization status from the PU then changing the related transmission schemes to take advantage of such band portion.

It is worth mentioning that a survey conducted by the FCC revealed a fact that, in the frequency bands below 3 GHz, the utilization situations of the radio spectrum are very different from each other, and their occupancy rates are from 15% to 85% [2]. Driven by this real survey results, interleave cognitive radio models are widely applied among industrial standardization bodies, which is led to not only because interleave cognitive radio with the capability of recycling low utilization parts of the radio spectrum, but also because the models can take full advantage of the spectrum while reasonably ensure quality of service

(QoS). Therefore, many communication protocols including the IEEE 802.22 and 802.11af protocols as well as Ecma-392 were constructed to employ interleave cognitive radio models. Because of the dramatic number increasing of application of such interwoven CR models, this dissertation focuses on enabling technologies for this model. To implement this model, essential components including spectrum sensing, spectrum analysis, and spectrum decision making must be equipped.

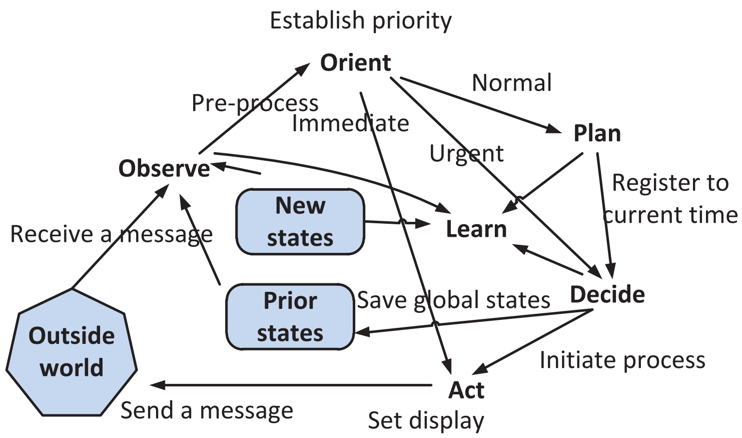

Figure 1.1: Ideal cognition cycle.

The CR ought to detect the operating environment and dynamically adapting itself according to the observation, as it shown in Figure 1.2. Therefore, the tasks realized by the cognitive radio should include,

- *Spectrum sensing (SS)*: SS is considered to be the most crucial while fundamental function for performing the cognitive radio and is twofold. First of all, the interested frequency bands have already been assigned to the primary user according to a static protocol without a doubt. The spectrum sensing performs an inspection to confirm whether some or all of the frequency band resource is free over time, frequency, space, and code or angle domain. Secondly, according to the sensed results, the secondary user adjusts its radio parameters to be able to access these free spectrum bands to complete its own transmission [3, 4, 5, 6].

- *Spectrum management*: It is performed by the cognitive radio is to guarantee the secondary user can obtain the most appropriate available frequency band, enabling data transmission to meet user and QoS requirements. One can verify whether the current frequency band has good transmission performance while guarantees transmission quality by considering indicators such as hold time, uncertain noise power, transmission loss, and error/delay in the radio media.

It consists of two basic parts including spectrum analysis and decision. The spectrum analysis posses the capability of analyzing and estimating characteristics from white space has been determined. The SD selects the best spectral position from the effective results provided through SA, so that current selection can meet the communication requirements of the required QoS while balancing cost-effectiveness [7, 8, 9].

- *Spectrum mobility*: The ability of this function is that it can cause the SU to quickly leave the band to ensure that the SU does not interfere with the PU transmission, when the PU in question is detected it arrival for reuse the spectrum bands. In another word, the cognitive radio can move from the currently borrowed frequency band to another frequency band, thereby ensuring a smooth transition of the CR [10, 11].

- *Spectrum sharing*: It is performed to set up sound utilization arrangement of the spectrum as well as fair and sound spectrum allocation strategy among several secondary users. It is implemented in conjunction with spectrum access and transceiver handshake operations [12, 13].

Spectrum holes, also known as spectrum opportunities, are parts of the radio spectrum initially allocated but currently free. In this dissertation, the SS is to gain an understanding of the interested band usage and presence of primary users, in other works to obtain awareness about the spectrum holes, as shown in Figure 1.3. The focal point of this dissertation is then the SS executed in CR since it has a broader range of applications but lower infrastructure requirements. It can also function to recognize the types of signals that are transmitted by PUs through the interested spectrum bands, including the signal modulation, waveform, bandwidth, carrier frequency, etc.. However, the execution may require certain prior information, powerful signal analysis methods or extra computational complexity.

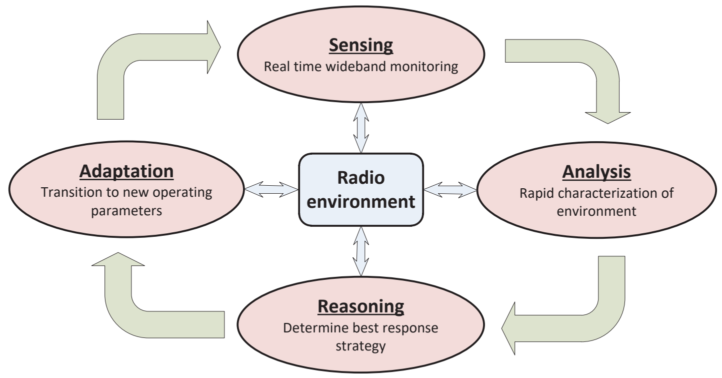

Figure 1.2: Basic function of a cognitive radio.

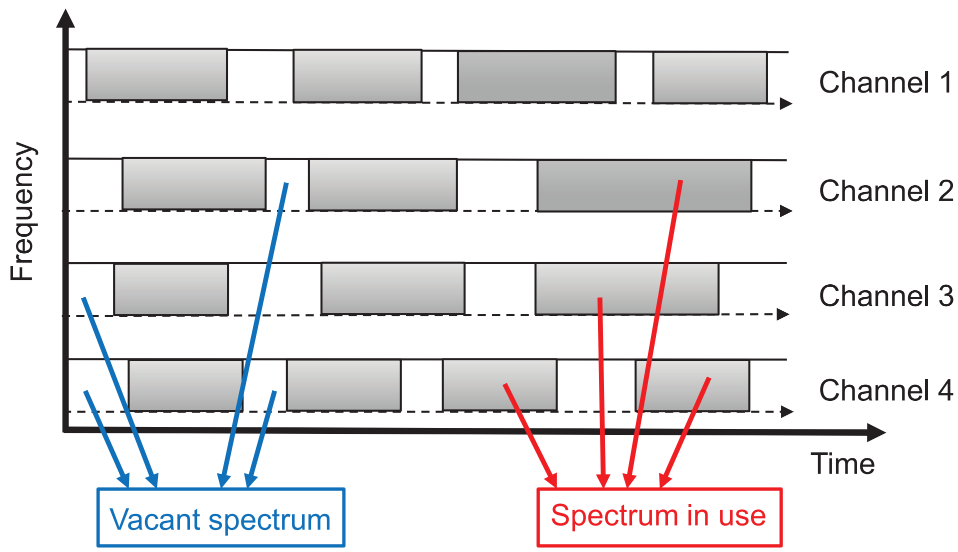

Figure 1.3: Access scheme to spectrum holes.

1.2 Motivation and Objection

Researchers have invested significant effort in establishing the cognitive radio models, then addressing serious challenges of realizing the key models and finally solving the problems encountered during actual implementation. Thanks to a significant amount of surveys and works, it is possible for this dissertation to review the summarized problems and their corresponding solutions. Research on practical solutions for actual system implementation has become the key to actual system deployment.

As mentioned before, the cognitive radio should have the capability to learning beneficial information from the operating environment, including the natural transmission environment as well as the primary user activities. That is the reason why the spectrum sensing is the main ingredient at this point. In the past few years, the spectrum sensing in the cognitive radio have come across many challenges and had to adjust its study directions accordingly. Researchers have proposed practical technologies from various starting positions and processing styles [14, 15, 16]. Among those, the energy detection, matched filter detection, cyclostationary feature detection, wavelet detection, and covariance detection represent the major research fields and therefore are considered to be the "conventional spectrum sensing methods" [17, 18, 19, 20, 21, 22]. However, as stated in [8, 11, 15, 18], when establishing the spectrum sensing scheme, performance degradation is caused by practical imperfections which include uncertainty from signal, noise, interference and channel, transceiver imperfections, channel correlation, etc..

Up till now, the practical implementation of the deuterogenic, advanced versions of conventional spectrum sensing methods are still at the front stage of the investigation. These solutions have been recognized as the update or even revolution of existing technologies. For example, on the one hand, some of these sensing methods are able to provide high detection precision with the support of specified extra complexity and sensing time, which are called spectrum scanning; on the other hand, some of these sensing methods can take complete efficient and high-speed sensing procedure with a slight sacrifice of the detection accuracy such as methods with downsampling scheme regarded to the Nyquist sampling rate. The work teams are still putting efforts on strengthening the current algorithms and implementation schemes every day to obtain almost perfect sensing methods which can balance among the detection accuracy, monitoring time and computing complexity [23]. Furthermore, the spectrum sensing/monitoring while performing cognitively transmission is another attractive issue which is objective to become the solution to the throughput problem of the secondary network. Cooperative spectrum sensing scheme is also developed to integrate each thin detection ability to improve the global accuracy as well as address the problem of the hidden terminal which is commonly inherent in the wireless communication network [24, 25, 26]. Besides, from an industrial perspective, there are some new standards introduced for discussion, including IEEE 802.11af and 802.15.4m protocols, which are counting on the interweave network. They contribute to bringing in not only new definitions but also the new challenges brought by execution perspective. It is a truth that a lot of solutions with novel aspects have revolutionized the traditional spectrum sensing technologies.

Inspired by those ways of thinking, advanced technology from another field may also assist in raising the spectrum sensing performance. A CR is expected to be a smart wireless communication system that possesses learning ability by nature to understand and built from the interactions with the environment. Such characteristics of the learning and reasoning capabilities indeed make the cognitive radio "cognitive". In recent years, it becomes more and more popular and promising to apply machine learning algorithms into the cognitive radio applications. The strength of coordinating the thoughts and actions make the machine learning a nearly perfect core to be embedded in a cognitive engine. Typically, the learning mechanism becomes more critical if a particular unknown factor from the input data affects the accuracy of the output in a given system [27]. It means that learning can suggest an appropriate input scheme to make a regression curve of the input-output function better. To fit into the modern wireless communications, the cognitive radio system has to develop with more complicated structure as well as more degrees of freedom [28]. At this point, multiple dimensional parameters as well as policies, such as coding and modulation scheme, sensing algorithm and policy, communication protocols, etc., may need to cooperate and to be adjusted simultaneously. These requirements frame the conventional rule-based methods of model establishing to a disappointing position, since there is no simple function to describe the complex interactions within the CR system under the impact of these factors. Back to the signal identification for the spectrum sensing, the influences from outside or inside the CR system, such as uncertainty of signal, noise, interference and channel aspects, transceiver imperfections, channel correlation, severely cost the detection capability of the spectrum sensing. However, if the machine learning is employed to estimate the channel characteristics, or to determine the specific coping technologies, or to find out the relationship between the received data and the sensing results, such executions are able to allow efficient the spectrum sensing to guarantee the fundamental principle of the cognitive radio.

In order for the realize the intelligence for a machine, there are three necessary conditions: perception, which collects valuable information from from the surrounding or internal states for further processing; learning, which analyzes data and deduces specific relationship or pattern model hidden inside the data; reasoning, which contribute results in the forms of classification or policy-making, as shown in Figure 1.4. Obviously, learning is the core of any intelligent system, especially CR. Researchers have proposed several implementation schemes to intercept the machine learning into the CR system, including both supervised learning and unsupervised learning [29, 30, 31]: approaches based on neural network or support vector machines (SVMs) for the former and approaches based on reinforcement learning (RL), game theory, etc.. It has been proven that these methods can efficiently perform a parameter optimization or refine a cognitive engine framework for the operating channel state even comparatively high application requirement. Needless for extra description, the autonomous learning in the partially observable environment will be the match point. Based on this idea, this dissertation conducts studies to link the available information to accurate sensing results through the assist of machine learning.

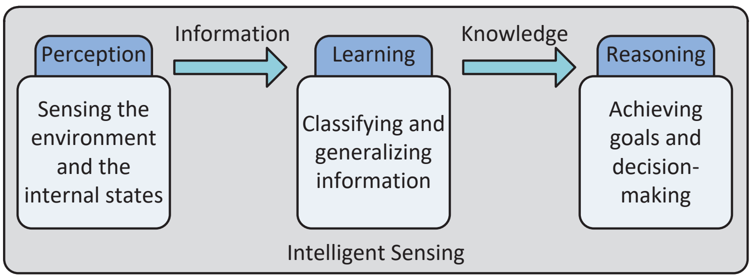

Figure 1.4: Implementation of intelligent sensing.

1.3 Contributions and Novelty

As the research background is the cognitive radio, the machine learning technologies, whose main idea is to wisely understand and build interactions within the operating environment, are therefore applied throughout this thesis considering their consistency and similarity in solving specific problems. The detection of the primary user, or spectrum sensing, can then use the classic classification function of ML after accordingly converting the signal recognition scheme, where the absent PU and present PU scenarios are treated as two classes.

This thesis firstly would like to exploit the capability limitation of the proposed scheme, in another word how capable the ML technology is in solving spectrum sensing problem. Therefore, the secondary user equipped with the full-duplex (FD) mode is set to be the operating system since it has one of the most complicated and harsh transmission environment where not only the additive noise and fading effects but also self-interference effect, are demanded to be considered. Secondly, after verifying the effectiveness of the proposed scheme, this thesis then would like to consider a more practical situation where the common SU as a sensing terminal in the CR system, only has limited computing power meaning the huge computing complexity that required in the FD mode cannot be met. In this case, the SU can only use a neural network with simple structure which limits its sensing ability. In order to again reach the fine performance as the one of the FD situation, several spatially distributed SUs should work together as in the cooperative spectrum sensing scheme. In summary, to test the proposed scheme, Proposal 1 is conducted to maximum the sensing performance from simple simulation level, and Proposal 2 is conducted to research on the balance between the performance and computing power from practical application level.

The two proposed machine learning based spectrum sensing schemes support the contributions and novelties of the thesis. Aiming for two practical implementation plans of spectrum sensing, proper machine learning algorithms are selected to fit into the cognitive radio system with the full-duplex (FD) mode, and the cooperative spectrum sensing (CSS) structure.

For the full-duplex equipped CR scheme, the contributions and novelties are as follow:

- For spectrum sensing in the FD mode, a novel implementation scheme, as well as its specific adversarial training strategy which establishes a modified training database to cope with residual self-interference (RSI) are given. Simulation results prove the improved sensing under RSI effects and even other transmission influences;

- A thorough theoretical analysis of the spectral cyclic signature brought by the OFDM signal applied in the full-duplex is presented, particularly the pilot peak coordinates in the spectral periodogram;

- To determine a balance between the computing limitation and detection performance, the input image formations with two different resolutions as well as various CNN architectures are proposed and analyzed, while their leading performances are evaluated;

- In order to realize a better secondary transmission with full-duplex mode, which means the SU data transmission plan has to consider the SS in the same time, a signal design focusing on the pilot arrangement is proposed.

For the cooperative spectrum sensing structure, the contributions and novelties are as follow:

- aiming at an OFDM signal based cooperative spectrum sensing, the ensemble deep learning is employed due to the similar characteristic between these two structures. The proposed scheme shows an improved sensing performance compared to classic sensing approaches;

- advanced execution strategies from the ensemble learning including the bagging for the supervised learning in local sensing and the stacking generalization for the combination strategy for the fusion center are borrowed and set for the cooperative spectrum sensing to expect better sensing performance;

- both hard and semi-soft strategies are proposed to optimize the fusion method.

- various types of weak learner network including changing in SU number and structure are also tested to conduct a quantitative analysis on their brought affects.

1.4 Scope

A complete cognitive radio system should contain several layer-wise functions including the spectrum sensing, spectrum management, spectrum mobility, and power control, as mentioned before. However, the spectrum sensing detecting the spectrum holes through the Physical (PHY) layer is considered to be the given study confine. More particularly, the spectrum sensing can perform from multiple dimensions containing the time, frequency, spaced and code domain. In this dissertation, only the spectrum sensing from the time domain is focused. It means the primary user is continuously utilizing one certain frequency with the invariable bandwidth and center frequency, in the meantime the secondary users only pay attention to this entitled frequency band and access to it from time to time.

Although hardware conditions, system network plan, signal model, etc., appear in various formations in CR systems. From the signal aspect, signal and multiple carrier modulation are both widely used. However, to meet the requirement of high data rate, the latter one attracts more attentions. In particular, the orthogonal frequency division multiplexing is quite popular in CR systems owing to its higher data rates and reliability; nevertheless, studies on such structure are still developed because of the consideration of the system complexity. In this study, the OFDM modulation is the main research object.

With the development of artificial intelligence (AI), several branches have been evolved, such as machine perception, knowledge representation, and machine learning, etc. However, for this study and the proper usage for the CR system, only the machine learning will be employed and discussed in detail considering the mentioned strength of learning capability. Specifically, the two key learning mechanism will be paid extra attention to, including supervised learning and unsupervised learning. The advantages and limitations of each learning paradigms will be taken into account and carefully analyzed particularly under the framework of the cognitive radio application. Furthermore, for special task/context of the cognitive radio, both centralized learning as well decentralized learning will be described.

1.5 Organization of the Thesis

The dissertation provides recent researches about single-device as well as cooperative spectrum sensing schemes. For both circumstances, proper machine learning algorithms are carefully selected and localized according to their particular requirements and implementation contexts. This dissertation consists of six chapters as the following description.

- Chapter 1 gives the introduction about the background, motivation as well as objection. The contributions, novelty, as well as research scope of the proposed researches are also described.
- Chapter 2 explains the specific operating system models of the spectrum sensing in this research. Several representative spectrum sensing methods are listed for their advantages and limitation in order to conduct further comparison among those and the proposed methods. After that, in the spectrum sensing background, the OFDM modulation signal model, especially its cyclostationary feature is analyzed for data collection phase in classification.
- Chapter 3 gives an overview of the recently revealed implementation schemes of adapting the machine learning into the spectrum sensing context. Both supervised and unsupervised learning, as well as their classic algorithms for various purposes are discussed. The aim is to conduct the fundamental work for to-be-discussed proposals.
- Chapter 4 explains a classification-converted sensing based full-duplex sensing method. The spectral cyclic signature induced by the pilot structure of OFDM modulation acting as input image data is put through the CNNs for classifications. Moreover, in order to survive from residual self-interference, noisy and fading channel, a sensing-oriented adversarial training of a localized training database was presented.
- Chapter 5 presents a cooperative spectrum sensing scheme assisting by the ensemble learning framework to ease the local computation power tense

while remaining a good sensing performance. Each SU is accordingly considered as a base learner. Then in order to better apply supervised learning for sensing, a bagging strategy from the ensemble learning is invited here for building databases. The fusion center employs a stacked generalization for further raise the sensing accuracy.

- Chapter 6 gives the conclusions of the dissertation and summarize the conducted research contributions in chapters 4 and 5.

Chapter 2

System Model and Signal Model

In this chapter, the system mode, which is the in-question spectrum sensing scheme, and the signal model, which is the considered OFDM modulation signal are carefully stated to lay the groundwork for the to-be-discussed proposed methods. The spectrum sensing is considered to be the most critical component for its capability of preparing the groundwork which is executed nicely so the following step can be built upon it. Methodologies for the spectrum hole detection have already been established as a soundest system. Among those, some main concerned problems such as performance increasing, environmental uncertainty, etc., have been challenged. According to these, specific efficient mathematical formulas have been constructed as valuable references. However, even under such great help, insufficiencies that need more devoted efforts and novel ideas are always left behind. Then, as one of the most widely applied modulation type, the OFDM modulation signal also helps further raise the channel utilization situation, since it supports high data rate transmission. Open- to- public protocols for its formation as well as usage regulated the transmission style, which in some way even make the spectrum sensing more valid than before. As a result of its particular structure, the induced cyclostationary feature can be extracted for its better detection.

This chapter is organized as follow. Section 2.1 describes the system mode of the spectrum sensing. Concretely, the general formation and its related concepts and applications are given in section 2.1.1; the mathematical expression is presented in section 2.1.2; several representative spectrum sensing methods and their advantages and limitations are listed in section 2.1.3. Section 2.2 carefully explains the OFDM modulation model: the protocol of the OFDM modulation signal that regulates the specific forms as well as parameters, are stated in detail in section 2.2.1; in section 2.2.2, the model induced cyclostationary feature is analyzed for data collection which will be discussed later. Section 2.3 summarizes this chapter.

2.1 System Model of Spectrum Sensing

2.1.1 Spectrum Sensing Hypothesis

As stated before, factors like uncertainty from signal, noise, interference and channel, transceiver imperfections, channel correlation, make the spectrum sensing a real challenge. Besides that, the temporal sensing for a primary user signal relates to a seriously complicated signal processing problem. Furthermore, in particular circumstance, the secondary users may be required to evaluate the channel conditions to refrain from causing interference towards the primary user. Since there is no information interchange between the primary and secondary users, the signal recognition or channel exploitation is supposed to be very tough.

The spectrum sensing query generally distinguishes between the PU statuses of existence(presence) and inexistence(absence), or in another word, the busy/idle situation of the aim band. The sensing results are mainly evaluated or measured with the formation of two probabilities which are the probability of detection (p_d) and the probability of false alarm (p_f).

Previous studies provided a binary hypothesis mechanism to describe the SS [8], where H_0 stands for quiet PU and H_1 stands for busy PU, respectively. Its mathematic expression is considered as

$$\begin{aligned} &\mathrm{H}_0 : x = n, && \text{Absent PU} \\ &\mathrm{H}_1 : x = hp + n, && \text{Present PU} \end{aligned} \tag{2.1}$$

where p and x stand for the original transmitted signal from the primary user terminal and the received signal at the SU terminal, respectively. h and n is channel coefficient and the additive noise (Throughout this dissertation, the additive white Gaussian noise, AWGN, is the only considered, which is with mean of zero and variance of σ_n^2 so that $n \sim CN(0, \sigma_n^2)$). Moreover, if π_0 represents the probability when the PU is absent, i.e. true for H_0, and π_1 represents the probability when the PU is present, i.e. true for H_1, and as $\pi_0 + \pi_1 = 1$, then two types of error may be encountered for the sensing results:

- *Error Type 1*: as defined in p_f, the secondary user mistake H_1 when H_0 is actually true;
- *Error Type 2*: the probability of miss detection (p_m), as the opposite of p_d ($p_m = 1 - p_d$), the secondary user mistake H_0 when H_1 is actually true.

2.1.2 Classic Spectrum Sensing Approaches

As described in the last section, obviously, the underlying problem for the spectrum detector is to select the sensing plan then establish a proper threshold of γ. Methodologies of the detection theory have built up a sound system to an idea with such issue. The scheme of the classical statistics and Bayesian statistics [32] are the two main implementation plans of detection theory. For the implementation scheme of the traditional statistics, the prior information is the hypnosis results which means H_0 or H_1 is deterministically known, while the aim of the execution is to maximum p_d according to a fixed p_f. However, for the implementation scheme of the Bayesian statistics, based on a certain priori information, the hypotheses are randomly set to be true. Then the aim of the execution is to minimize the Bayesian cost.

This section will list several most traditional spectrum sensing schemes that are often compared with as the benchmarks and instruct most of the recent research for further exploring the detection performance.

2.1.2.1 Energy Detection

Energy detection (ED) is a widely developed non-coherent signal detection approach for the SS owing to the comparatively low computing complexity [33, 34, 35, 36, 37, 38]. It is mostly applauded by the fact that it requires no priori information about the primary user nor the channel status compared to other methods. The result will be given out only by comparing the energy accumulation value calculated by the detector with the threshold depended on the noise floor [39]. However, such simple strategy may leave out some challenges for performing the spectrum sensing: the threshold calculation error when the noise uncertainty occurs, the difficulty of distinguishing the inference from the primary user or noise, the poor detection performance under harsh transmission environment, i.e. low signal to noise ratio (SNR=σ_s^2/σ_n^2) value and the inefficiency for detecting the wide-band signal [38, 40, 41].

As stated before, when the primary user is currently occupying the interested spectrum band, the received signal is in the form of

$$x = hp + n, \tag{2.2}$$

where h is considered to be 1 here. Then, the energy accumulation value will be set to be the decision metric as

$$M = \int_0^T x(t)^2, \tag{2.3}$$

where T stands for the testing period of the considered received signal part. Then the sensing results will be obtain after compared the metric M with the pre-decided fixed threshold Λ. The decision for Λ should a perfect balance between p_d and p_f. However, such Λ may require both noise and PU signal information. Therefore in actual execution, the threshold is set to guarantee a certain value of p_f, resulting in the only required information is the noise power.

To simplify the analysis, besides the noise, the signal term is also set to be the Gaussian distribution, i.e. $s\left(n\right) = N(0, \sigma_s^2)$. However if the fading effect is also considered, the signal model $s(n)$ will be much more complicated. Upon on these settings, the metric M then behaves as the chi-square distribution with the freedom degrees of $2N$, χ_{2N}^2, as in

$$M = \begin{cases} \frac{\sigma_w^2}{2}\chi_{2T}^2 & H_0, \\ \frac{\sigma_w^2+\sigma_s^2}{2}\chi_{2T}^2 & H_1. \end{cases} \tag{2.4}$$

Then the p_d and p_f can be written as [42]

$$p_{fa} = 1 - \Gamma\left(L_f L_t, \frac{\lambda}{\sigma_w^2}\right), \tag{2.5}$$

$$p_d = 1 - \Gamma\left(L_f L_t, \frac{\lambda}{\sigma_w^2 + \sigma_s^2}\right), \tag{2.6}$$

where Γ is the half gamma function.

The energy detection needs to set a noise power based threshold, where even a small variance estimation of the noise may cost the sensing performance. At this point, the multiple signal classification (MUSIC) algorithm which divide the received data into signal and noise spaces, can be applied for reducing the estimation error. The MUSIC calculates the autocorrelation matrix of the received data and chooses the smallest eigenvalue to be the noise variance which is also chosen according to the set p_f.

2.1.2.2 Matched Filter Detection

As a part of communication theory, a matched filter normally have the objective of the maximizing the received SNR in the AWGN channel. Therefore, for the spectrum sensing, such detector is proven to take full advantage of the coherent condition [43, 44]. If the cognitive user knows about not only the necessary parameters of the signal establishing as well as the entire PU signal structure, the coherent technology can well function. The specific execution is that: the detector will calculate the cross-correlation between the received and pre-mastered primary user signal; then if there is a true correlation peak (confirmed after comparing it to the set threshold) appears, the detector makes a decision of active primary user; otherwise the decision will be inactive primary user. Actually, as long as the cognitive system applying the signal with certain synchronization structure of the preamble, pilots, or spreading codes, the coherent feature is prepared and guarantee the matched filter detection.

In contrast to the energy detection, the matched filter detection leave an impression of well behaving in the low SNR environment, which make it more desirable to sense the weak signal [45, 46]. Based on this characteristic, the matched filter is often used to detect the mistaken transmission during a silent period, in spite of its comparatively high computing complexity. Besides these, the matched filter has also been used to estimate the power of the primary user signal.

Even though the matched filter detector is able to provide an excellent performance, such detection capability builds on the well known of the primary user network. Only a few spectrum sharing schemes are able to meet this requirement, such as the spectrum trading circumstance where the entitled user will rent the band for the silent period. However, it is not the most common scenario for the cognitive radio system. Besides, during the actual implementing phase, the lack of information of the fading channel parameters or the frequency/time offset, the matched filter detection may degrade due to the unfortunate correlation situation.

2.1.2.3 Cyclostationary Based Detection

When the primary user applying a signal with the cyclic spectral signature, the cyclostationary based detection can be adopted in a given, interested spectrum bands [47, 47, 48, 49, 50, 51, 52, 53]. The cyclostationarity can be explored from the periodicity in a signal or its related statistics such as autocorrelation. In some circumstances, the cyclostationarity can be deliberately installed into the signal structure to apply the cyclostationary based detection. This sensing method is able to distinguish the signal from the background additive noise due to the fact that the primary signal applying the modulated signal with spectral periodic correlation while the noise is a wide sense stationary with no correlation at any point over the time domain. At this point, the cyclostationary based detection can also be applied for differentiate among several primary users as long as they apply signals with different types of the cyclostationarity.

Assume that $c\left(n,m\right)$ stands for the OFDM symbol sequences, where n and m denote the symbol and carrier number. The expression of variance is as:

$$\sigma_d^2 = E\left\{c\left(n,m\right)c^*\left(n,m\right)\right\}. \tag{2.7}$$

Then the auto-correlation is

$$\begin{aligned} R_{xx}(t,\tau) = &\sigma_c^2 \cdot Re[\\ &\sum_{n=-\infty}^{\infty}\sum_{m=0}^{M} d(t-nT_s)d(t-nT_s+\tau)\cdot \\ &exp\left(-j2\pi\left(m-\frac{M-1}{2}\right)\Delta f\tau\right)\cdot \\ &exp(-j2\pi f_c\tau)], \end{aligned} \tag{2.8}$$

where M and T_s denote the total carriers number and symbol duration. Δf and $d(t)$ are the carrier spacing and rectangular pulse. T_s is centered at 0. Then,

$$\begin{aligned} a(\tau) &= \sum_{m=0}^{M-1} \cdot exp\left(-j2\pi\left(m - \frac{M-1}{2}\right)\Delta f\tau\right) \\ &= \frac{sin(\pi\Delta f M\tau)}{sin(\pi\Delta f\tau)} exp\left(\frac{-j\pi\Delta f(m+1)}{2\tau}\right). \end{aligned} \tag{2.9}$$

Applying the above equation, the original auto-correlation can be rewritten as:

$$\begin{aligned} R_{xx}(t,\tau) = &\sigma_c^2 a(\tau)\cdot \\ &Re\left\{\sum_{n=-\infty}^{\infty}\sum_{m=0}^{M} d(t-nT_s)d(t-nT_s+\tau)\right\}. \end{aligned} \tag{2.10}$$

Normally, a signal used for data transmission can be viewed as the integrate of a series of weighted spectrum ingredients. Due to such fact, the statistical periodicity analysis can be utilized to decompose the interested signal back into several weighted cosine waves. Accordingly, signals in different modulation types can be formed by a group of different cosine functions for their specific intrinsic periodic characteristics. Sometimes the received signal does not directly show periodicity from appearance, however, various transformation algorithm like the Fourier or inverse Fourier analysis can help reveal the inner periodicity features. In this dissertation, the second order spectral transformation, such as the mentioned auto correlation, is applied to analyze the cyclostationarity. For further explore the periodicity spectrally from the time domain formation of $x(t)$, the cyclic auto correlation function of $x(t)$ can be written as

$$R_x^\alpha = \lim_{T\to\infty}\frac{1}{T}\int_{-T/2}^{T/2} x\left(t+\frac{\tau}{2}\right)x\left(t-\frac{\tau}{2}\right)e^{-j2\pi\alpha t}dt, \tag{2.11}$$

where α is the amount of shift, also as know as the cycle frequency. The expression for the spectral correlation as a Fourier transformation of the cyclic auto correlation, can deeply exhibit the frequency correlation spectrally. The spectral correlation function (SCF) can be written as,

$$
\begin{aligned}
S_x^{\alpha}(f) =& \int_{-\infty}^{+\infty} R_x^{\alpha}(\tau) e^{-j2\pi f\tau} d\tau \\
=& \int_{-\infty}^{+\infty} \lim_{T\to\infty} \frac{1}{T} \int_{-T/2}^{T/2} x\left(t+\frac{\tau}{2}\right) x\left(t-\frac{\tau}{2}\right) e^{-j2\pi\alpha t} e^{-j2\pi f\tau} dt d\tau \\
=& \lim_{T\to\infty} S_{X_T}^{\alpha}(f)
\end{aligned}
\tag{2.12}
$$

where f is the frequency, and $S_{X_T}^{\alpha}(f)$ is the cyclic periodogram of the spectral correlation. $S_{X_T}^{\alpha}(f)$ is:

$$
S_{X_T}^{\alpha}(f) = \left[X_T\left(t, f+\frac{\alpha}{2}\right) \cdot X_T^{*}\left(t, f-\frac{\alpha}{2}\right)\right] /T. \tag{2.13}
$$

Then the spectral coherence density (SCD) of $x(t)$ is defined as:

$$
S_{X_T}^{\alpha}(f)_{\Delta t} = \frac{1}{\Delta t} \int_{-\Delta t/2}^{\Delta t/2} \frac{1}{T} X_T\left(t, f+\frac{\alpha}{2}\right)^{*} X_T^{*}\left(t, f-\frac{\alpha}{2}\right) dt. \tag{2.14}
$$

X_T here is fitting for the $x(u)$ local spectral representation written as:

$$
X_T(t, v) = \int_{t-T/2}^{t+T/2} x(u)^{*} e^{-j2vfu} du, \tag{2.15}
$$

where f is the general frequency and v is the cyclic frequency, respectively. Meanwhile the limit SCD is expressed as $\lim_{T\to\infty} \lim_{\Delta t\to\infty} S_{X_T}^{\alpha}(f)_{\Delta t}$.

2.2 Signal Model of OFDM Modulation

2.2.1 OFDM Modulation

At first, the frequency division multiplexing was proposed to assign channel for different purposes of data transmission. The OFDM modulation signal developed such idea but multiplexed in the frequency domain to create a certain number of subcarriers to apply them all to transmit data from one channel. The modulation scheme is to divide the data over parallel low rate orthogonal subcarrier, which should be modulated using traditional single carrier modulation plan from BPSK (Binary Phase Shift Keying) to N-QAM (N-Quadrature Amplitude Modulation) for guaranteeing high data rate and sound transmission in the integrated channels. The subcarriers of orthogonality can be divided through applying correlation techniques, which can reduce inter-Symbol interference (ISI) between subcarriers. The bandwidth on each subcarrier is smaller than relevant bandwidth, resulting in the fact that subcarriers can be regarded as flatness fading and thereby eliminating inter-code interference (ICI). Since the sub-bandwidth only takes a small portion of original bandwidth, the channel equilibrium becomes comparatively easy. The OFDM modulation and demodulation are realized based on IFFT and FFT respectively, and the lowest complexity makes the OFDM modulation the widest application. The OFDM modulation is even able to apply dispersed free frequency bands in order to distribute transmission, owing to the capability to reshape and integrate subcarriers. The good quality and adaptability of the OFDM modulation signal result in such technology currently being adopted in forms of Wi-Fi, Wi-Max, DVB-T, etc. in many radio systems.

For this dissertation, here are some reasons why among all of the data modulation technology, the OFDM modulation is the best choice for the CR system. As stated before, the cognitive radio as a software-defined radio system, relies on the flexibility of the digital domain means flexibility and demands a high level of programmability. Meanwhile, the characteristics of the OFDM modulation allow it to step into different spectrum bands and meet different transmission requirement by adjusting the specific implementation parameters, which again meet the definition of the CR system. Furthermore, the spectrum sensing from the physical layer is often realized by FFT which has already built within the OFDM modulation and can be shared by the spectrum sensing technology.

To measure the OFDM application in the CR, the advantages and disadvantages of OFDM should be mentioned:

Advantages:

- High channel utilization and effectively resist interference between signal waveforms make the OFDM modulation suitable for high-speed data transmission in multipath environments and fading channels, which is especially important in wireless environments with limited spectrum resources;

- High resistant to narrow-band interferences, since these interferences only affect a small fraction of subcarriers. In a single carrier system, a single fading or interference can cause the entire communication link to fail, but in a multi-carrier system, only a small fraction of the carriers are subject to interference;
- Strong anti-fading ability. Through the joint coding of subcarriers, the modulation utilizes the frequency diversity, and if the fading is not particularly severe, there is no need to add a time domain equalizer. Error correction codes can also be used for these subcarriers for error correction. Meanwhile, when frequency selective fading occurs, only the subcarriers falling in the band recess and the information carried by them are affected, and other subcarriers are not damaged, so the overall BER (bit error ratio) performance of the system is better.

The OFDM modulation requires a amount of the orthogonal multiple subcarriers closely spreading over certain spectrum band, which is intently invited to avoid the interference while reduce the total bandwidth. The complex subcarriers would be modulated then loaded with 2 bits in the BPSK modulation case, 4 bits in the QPSK and 2^n in the N-QAM modulation case, as

$$S_c(t) = A_c(t)e^{j[2\pi f_c t+\phi_c(t)]}, \tag{2.16}$$

It is a time-vary signal with magnitude and phase. N sets of this signal consist the entire OFDM modulation definition, which expresses as

$$S_s = \frac{1}{N}\sum_{n=0}^{N-1} A_n(t)e^{j[2\pi f_n t+\phi_n(t)]}. \tag{2.17}$$

Throughout a complete OFDM symbol, the amplitude and phase stay still

$$S_s(t) = \frac{1}{N}\sum_{n=0}^{N-1} A_n e^{j[2\pi f_n t+\phi_n]}. \tag{2.18}$$

Since the subcarriers centralize around one certain central frequency of f_0 leading $f_n = f_0 + n\Delta f$, and when $f_0 = 0$ for reference, $f_n = n\Delta f$. In the mean time, a discrete time domain makes $t = KT$, where T is the whole sampling period. Then

$$S_s(KT) = \frac{1}{N}\sum_{n=0}^{N-1} A_n e^{j[(2\pi n\Delta f)KT+\phi_n]}. \tag{2.19}$$

A further transformation is written as

$$S_s(KT) = \frac{1}{N}\sum_{n=0}^{N-1} A_n e^{j\phi_n} e^{j[(2\pi n\Delta f)KT]}. \tag{2.20}$$

Such mathematical equation expresses a similarity to the IFFT where $A_n e^{j\phi_n}$ clearly represents the frequency domain

$$x[n] = \frac{1}{N}\sum_{n=0}^{N-1} X_k e^{j2\pi\frac{nk}{N}}. \tag{2.21}$$

It describes the integrate of orthogonality subcarriers over the frequency domain by the IFFT definition, which is also a condition to guarantee the orthogonal exponentials of $2\pi\Delta f nKT = 2\pi n\frac{k}{N}$. For the to-be-transmitted data stream which is in the form of complex modulation expression, $d_n = a_n + jb_n$ where the values of a_n and b_n are based on the chosen scheme of BPSK, QPSK or N-QAM. Substitute N of the complex data, the expression of the OFDM modulation over the time domain can be rewritten as

$$S_s(KT) = \sum_{n=0}^{N-1} d_n e^{j[2\phi n f_n t_k]}. \tag{2.22}$$

The real part of the OFDM symbol after complex multiplication is

$$Re\left\{S_s\right\} = y(t) = \sum_{n=0}^{N-1}\left[a_n cos(2\pi f_n t_k) + b_n sin(2\pi f_n t_k)\right]. \tag{2.23}$$

The establishment of the OFDM modulation is shown in Figure 2.2.

2.2.2 OFDM Structure Induced Cyclostationarity

On the one hand, the OFDM modulation is also valued for its robustness against multi-path fading effect, which provides by its unique design of the structure of the cyclic guard intervals. Such a featured design makes it easy to modify to

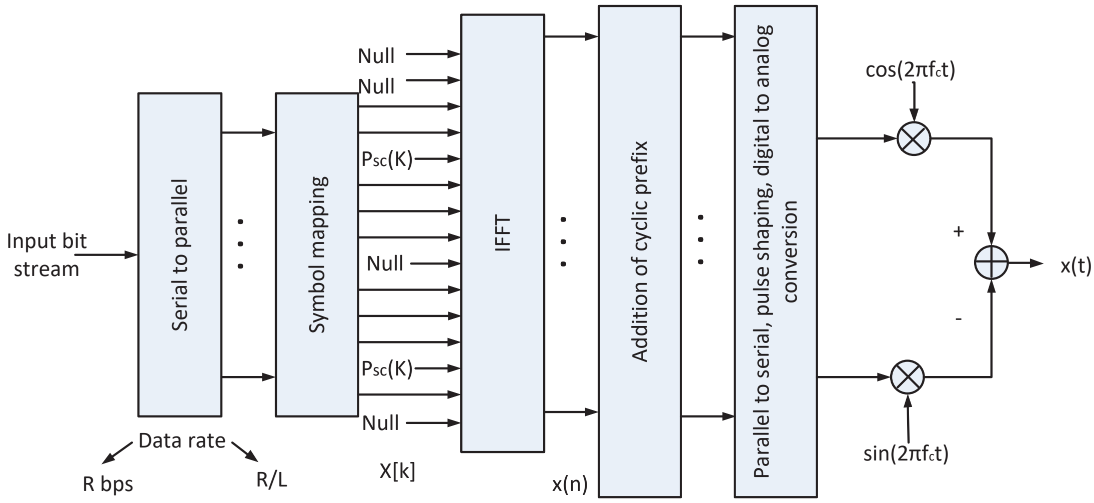

Figure 2.1: Establishment of OFDM modulation.

suit various transmission. On the other hand, the OFDM modulation needs high synchronization not only over the frequency and time domains but also from the aspect of the channel estimation. The mentioned cyclic guard intervals including the pilots, preambles and cyclic extensions, enables the receive terminal to achieve urgent synchronization demands, as shown in Figure 2.3.

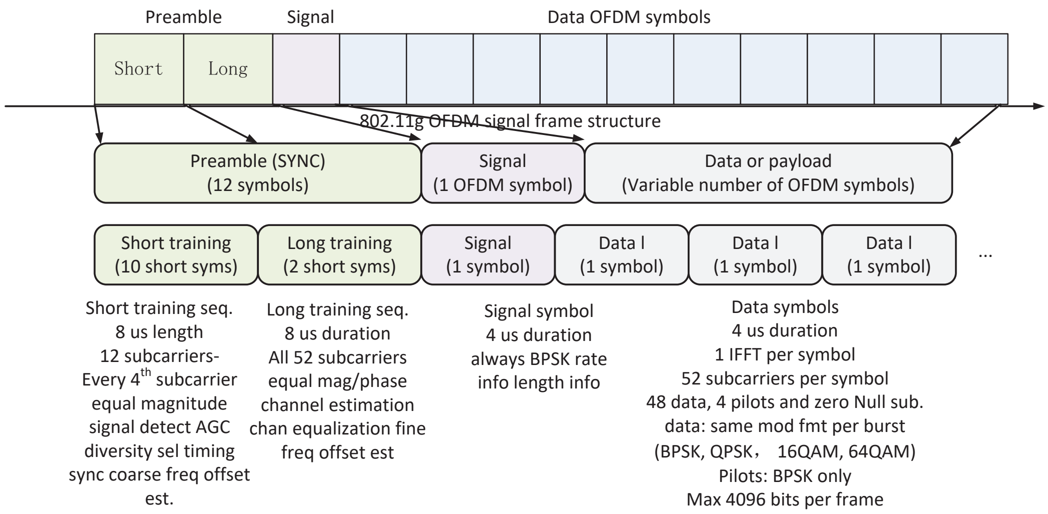

Figure 2.2: OFDM modulation frame structure of IEEE 802.11g.

- *Cycle Prefix*: Due to the existence of the multipath fading, delays of different OFDM symbols in one same frame can be caused by different propagation paths for the frame. In the relevant frequency domain, the cross interference between the subcarriers is caused, which affects transmission performance. A good modulation design must include some efficient structure to avoid the mentioned inter-symbol and inter-carrier interference which may be caused by the frequency selective fading, or at least suppress them to an acceptable level. In the OFDM system, that is to select a sufficient cycle prefix (CP) to prevent the ISI and ICI.

The CP structure deliberately copies certain length of the last portion of an OFDM symbol and add it at the beginning of the symbol, and such extension version of the original symbol would be the final transmission applied form. The extension portion between each symbol within one frame is known as guard interval. An appropriate length of the extension should be selected to be longer than the channel impulse response (CIR) then to eliminate the ISI. In addition, because of the cyclic prefix, the IFFT FFT operation turns the original linear convolution into a circular convolution, which greatly simplifies the corresponding signal processing complexity;

- *Preamble*: Synchronization of the system is an important issue due to the Doppler shift and Doppler change rate of the radio system. The preamble sequence is designed to solve this problem. The preamble sequence consists of a special synchronization sequence for solving the problem of the time synchronization and the estimation of the Doppler shift and its change rate. In addition, the OFDM modulation scheme encodes the preamble sequence to implement information feedback between the point-to-point communication. The transmitting and receiving terminals are both well known about the parameter of the preamble, and it can play an important role when the receiving terminal approximately estimates the interference of the transmitting channel. That is, for the equalizer to generate a channel model including the channel estimation, frequency offset estimation and to search for the starting point of the OFDM signal.

  The preamble must be able to possess correlation properties, and in order to perform recovery tasks smoothly, it must avoid a complex algorithm.

Therefore, the task of searching for the starting point of the OFDM signal is completed by correlating the input data with the reserved preamble copy. The frequency offset estimation between the transmitting and receiving terminals is completed by multiplying the input signal by the conjugate of the reserved preamble copy;

- *Pilots*: The sequence as the commonly known information for both the transmitting and receiving terminals is evenly inserted in the time-frequency two-dimensional domain, so that the receiving terminal can conveniently extract the corresponding transmission channel information for the channel estimation, frequency estimation, data management, and space-time decoding. An unfixed number of the subcarriers functioning as such sequence is the well-known pilot tones; meanwhile, they are modulated by BPSK or QPSK (quadrature phase shift keying). However the number, modulation, etc. are given in the design parameters for a specific frame format.

  Considering the channel change in time and frequency, the pilot insertion must also be uniform, which can correctly reflect the average channel variation in an information resource block. The receiving terminal digs out them then utilizes the minimum mean square error (MMSE) criterion for maximum likelihood channel estimation. In fact, the previous researches have revealed various pilot schemes. Several design schemes are mostly utilized, including using pseudo-random values to avoid frequency lines, using pilot tones at the same frequency position of every OFDM symbols, and moving the pilot tones among the symbols to the current position. Notice that in any case, the design scheme of the scattered or fixed pilot tone must be inserted at the same power and guarantee the cyclic spectral signature over the whole OFDM symbol or frame. However, for the actual implementation, the pilot design has to consider its effect on increasing the power to peak average ratio.

As the OFDM modulation signal is adopted in the CR system, its excellent characteristics of the flexibility and modifiability can be transferred and passed on to the CR system. All the built-in structure of the OFDM modulation, as mentioned above the cycle prefix, preamble and pilot tones can devote for the on-demand transmission. Among these three structures, this dissertation pays more attention to the pilot tones and utilizes them for the spectrum sensing. The reasons are: on the one hand, the cycle prefix generally cannot provide the comparatively better detection performance due to its short length and being easily disturbed by the frequency selective channel [55]; on the other hand, the cyclic stability of the preamble is usually interrupted by the transmission mode of its random WiFi packet [22, 56].

According to the mathematical expression of the spectral correlation density as in

$$S_{xx}^{\alpha}(f) = \int_{-\infty}^{\infty} R_{xx}^{\alpha}(\tau) \cdot e^{-j2\pi f \tau} d\tau. \tag{2.24}$$

From this equation, the bi-frequency plane with the horizontal and vertical axises of the frequency f and cycle frequency α can be visualized by the magnitude of the spectral correlation density $|S_{xx}^{\alpha}(f)|$, and be utilized as the to-be-processed data for the spectrum sensing. The cyclostationarity induced by the pilot tones is shown in Figure 2.4

2.3 Chapter Summary

This chapter introduces the system mode of the spectrum sensing. Several typically considered spectrum sensing scheme is listed. Then since the time dimension sensing is the focus of this dissertation, the mathematical expressions are then presented for future discussion and reference. Conventional spectrum sensing are also listed and compared each other with their strengths and limitations.

This chapter also introduces the signal model of the OFDM modulation and its utilization for the in-question cognitive radio system. The underlying mathematical expressions are given, and so are its cyclostationarity. Inspired by the cyclostationary feature detection, the bi-frequency plane will act as the image data for the future process.

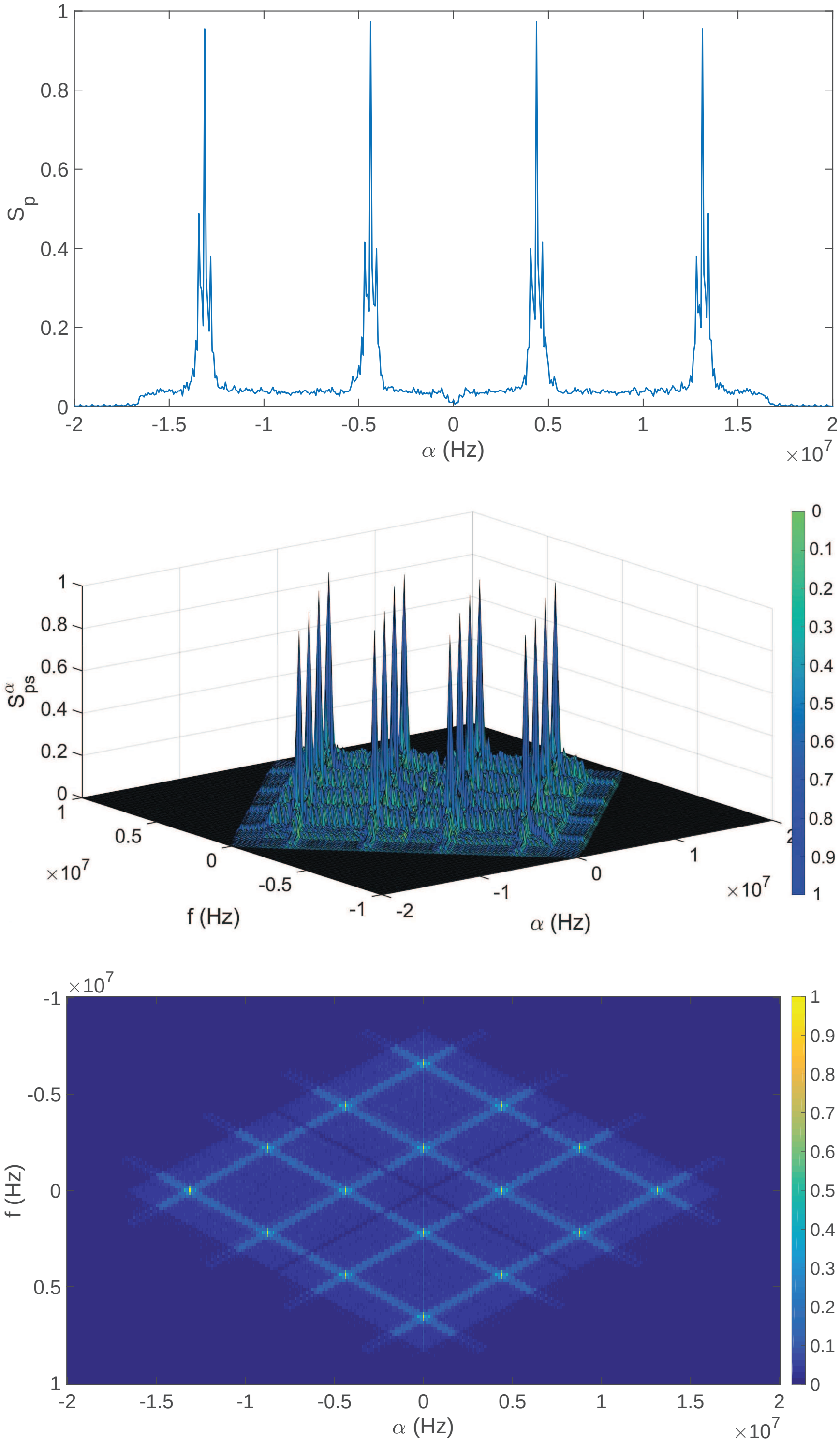

Figure 2.3: spectral correlation density of pilot tones induced cyclostationarity.

Chapter 3

Machine Learning for Signal Recognition

Machine learning is a multidisciplinary subject containing disciplines of probability theory, statistics, and convex analysis, etc.. It specializes in making machines simulate or implement human learning customs for obtaining new information or skills. The ML is the crucial technology of AI, and its applications span over all fields of AI. Currently, the ML is mostly applied in the induction and synthesis rather than deduction.

At this stage, the scope of applications with various machine learning methods has been expanding, and some of them have already formed commodities. Knowledge acquisition tools of the induction learning have been widely used in diagnostic subtype expert systems. Connection learning is dominant in acoustic image recognition. The analytical learning has been used to design integrated expert systems. The genetic algorithm and reinforcement learning have a good application prospect in engineering control. The neural network connection learning coupled with the symbol system will play a role in intelligent enterprise management and intelligent robot motion planning.

Particularly for the signal process, in fact, some research in the field of signal processing does not only focus on simple analysis, but also considers reasoning factors. At present, the signal processing algorithms and techniques have borrowed a lot from the development of machine learning, to solve many problems that traditional algorithms cannot solve and to achieve performance indicators that are not easy to achieve. As the field of machine learning is relatively new and has more opportunities, more signal processing research is beginning to be integrated into machine learning research. This dissertation is inspired by such kind of idea of utilizing the machine learning to help raise the performance of signal recognition for the spectrum sensing.

This chapter is organized as follow. The introduction about the data collection scheme that specifically designed for the SS is in Section 3.1. The interception-based as well as simulation-based detection which are explained in Sections 3.1.1 and 3.1.2. For Section 3.2, the machine learning, particularly the signal recognition relate part, is introduced. Section 3.2.1 introduced the two main learning schemes of the supervised and unsupervised learning. Section 3.2.2 considers the consumption of the neural network and presents the calculation method of the computing complexity. Section 3.2.3 gives the examples and simulation results showing how the network structure affects the final performance. Section 3.3 summarizes this chapter.

3.1 Data Collecting

The main task of the SS is to detect if the PU is transmitting its signal nor not. No matter implementing this in a conventional way or a new way, data is needed to be received and to be pre-processed. In this dissertation, the machine learning is applied into the spectrum sensing to help with the primary user signal recognition.

Being able to accept support from the cognitive radio system, the supervised learning which will be explained later, is invited to complete the signal processing task. Therefore, the data preparation or data collection is important to build up the supervised database to train the classifier. Under the framework of the OFDM based CR system, various prior information about the PU signal, channel situation, etc. provide various beginning conditions and lead to various implementation flows of the signal recognition. In this dissertation, two data collecting scheme is discussed including the interception-based as well as a simulation-based collection for training database establishment.

3.1.1 Interception based Data Collection

Interception based data collecting means data can directly be intercepted from the real transmission process of the PU for training. Two kinds of data with different contents, such as the only noise existing data and the primary user signal mixed with noise data, must happen in different periods and can be intercepted for establishing different training database. Although these should not be any interaction between the primary and secondary users and will not be any opportunities of obtaining such kinds of data, a two-step sensing scheme then can be utilized in this scenario [9, 57]. The implementation flow is as following:

- Performing a comparatively more complex and accurate spectrum sensing method to precisely assure the periods for different activity statuses of the primary user;
- Sum up and extract certain parameters and information about the signal or channel condition, or for the case that discussed in this dissertation, record the required data to establish the training database;
- Execute a time-saving spectrum sensing method but still be able to remain the high sensing performance thanks to the prior information obtained from the above step.

The specific implementation flow is shown in Figure 3.1, and recently it has been employed in most of the standard CR system. For instance, the draft fo IEEE 802.22 standard allows an inter-frame period with duration time up to 158ms, and an intra-frame period with duration time up from 5ms to 10ms [58]. Based on these supportive conditions, ECMA 392 standard uses a conventional sensing period of more than 5ms, and further spectral measurements are made with a selectable desired sensing time [59]

At this point, the proposed machine learning based SS is considered executing in the rapid sensing period, because of the fact only a few or even one OFDM symbol is enough to implement the spectrum sensing, which will be described in detail later). The exceptional sensing period is used for performing another time-consuming high-capability method to confirm the signal transmission periods of

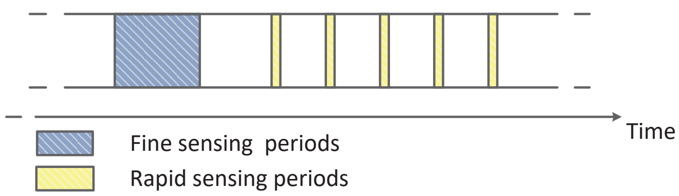

Figure 3.1: Implementation flow of two step sensing scheme.

the PU and collect datasets for the active as well as inactive periods. After collecting the data, it can be further pre-processed including the de-correlation, de-mean, etc., and then be sent to the final data-processing/signal-recognition phase.

3.1.2 Simulation based Data Collection

Nowadays, the OFDM signal utilization has been utilized to accomplish higher information rates and quality in the rapidly developed CR system. To fully utilize the limited wireless spectrum, the established transmission scheme protocols, for example, IEEE 802.11 protocol [58], have already employed by major communication companies and organizations. Since the protocol is widely acknowledged, more and more specific parameters and information about the transmission signal are open to share with the public and academic research. The simulation based data collection is, therefore, executable. In this dissertation, assume IEEE 802.11g protocol is obeyed by the primary user for its data exchange, which make this research can directly use the information about the modulation mode, signal structure, etc. for simulating the primary user signal. Database for training the classifier then can be built by just loading such kinds of simulation data samples. Moreover, instead of performing the pre-processing for the raw intercepted data, the simulated data can directly appear in the forms that are desired for the research.

3.2 Data Processing

The ML is invited to help with raising the performance of signal recognition in the cognitive radio system, due to its strength in data processing compared to

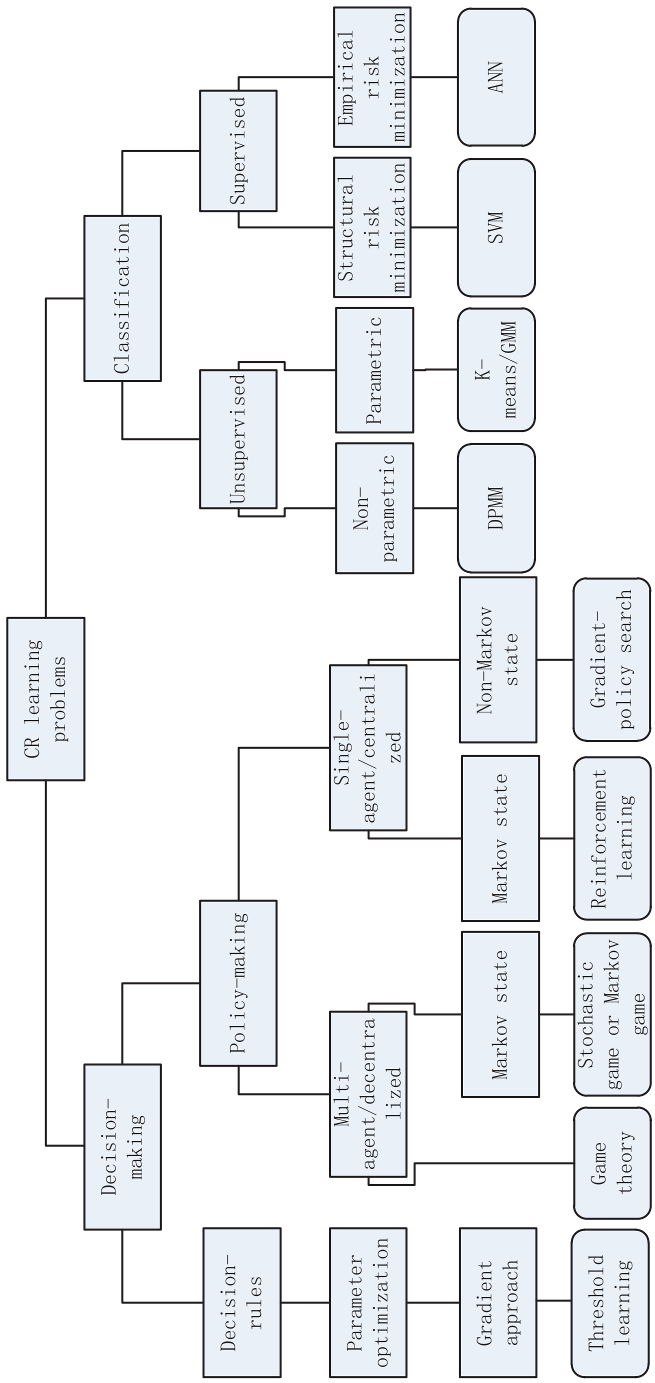

Figure 3.2: Machine learning based solutions to classic problems in cognitive radio system.

other conventional methods. Most of the machine learning inspired methods aims for tasks of classification or decision-making, as shown in Figure 3.2.

As long as this thesis focuses on the SS which is all about detecting if the primary user signal is in the interested band or not, as stated before, it is easily transformed as classification issue when data received in both active and inactive primary user is counted as two classes of data. The spectrum sensing task of detecting the signal being there or not is converted into a classification task of classifying/dividing two mentioned data classes. Focus on the branch of the classification in Figure 3.2, the supervised and unsupervised learning is needed to be discussed in detail.

3.2.1 Learning Paradigms

Typically ML contains two learning paradigms: supervised or unsupervised. The simple way to distinguish between the two is to look at the added information for the data. Whether it is supervised, it depends on whether the input data has a label. If the input data has a label, it is supervised learning, and if there is no label, it is unsupervised learning.

The middle of these two is semi-supervised learning which is proposed recently for meeting the new challenges. At this point, part of the training data is labeled and the other part is not labeled, and the amount of unlabeled data is often greater than the amount of tagged data (which is also true). The basic rule hidden under semi-supervised learning is that the distribution of data is not entirely random. Through some local features of tagged data and the overall distribution of more unlabeled data, an acceptable or even outstanding classification result can be obtained.

3.2.1.1 Supervised Learning

For supervised classification learning, the input training data has features and labels. The essence of so-called learning is to find the relationship between features and labels. In this way, when there is a characteristic and unlabeled unknown data input, we can get the unknown data label through the existing relationship. The supervised learning is a machine learning method in which a training model can be learned or established; then another new instance can be inferred from this model. Training data should contain designed input of vectors as well as the expected output of label. Usually, the output is either a relationship function as known as regression analysis or a prediction of a classification label also known as the classification. For a supervised learner, after observing some training paradigms (inputs and expected outputs), predicts the output of this function for any possible input values. To achieve this goal, learners must generalize from existing sources to non-observed situations in a "reasonable" manner. In human and animal perception, it is often referred to as concept learning.

The main concerns of supervised learning are the computing complexity and trade-off variances and deviations. Please note that both are interrelated. The appropriate computing complexity usually depends on the nature of your training data. If your data volume is small, or if your data is inconsistently distributed in all possible situations, you should choose a learning algorithm with computing complexity. This is because high complexity models will be overused if used on a small number of data points. Over-fitting means that the learning function is very suitable for your training data, but it will not be able to assimilate other datasets. One rigorously learn to generate training database under no understanding of tendency or structural output. In theory, you can use any degree of function, and one will carefully adopt another complicated model while using linear functions.

From the view of this dissertation, there are various types as well as capabilities of classifiers. The classification accuracy is primarily related to the data expression to be classified. Various rules of experiences are used to compare the performance of the classifier and to find data characteristics that will determine the performance of the classifier. Deciding a classifier that fits a problem is both an art and a science.

3.2.1.2 Unsupervised Learning

Usually, the main goal of unsupervised learning is to cluster the data. The unsupervised means one only need to provide the data without a label for the learning algorithm and let it find out the inner relationship lying within the data. Here, different the execution scheme of the supervised learning, the comparison among various learning algorithms is hard to conduct.

3.2.1.3 Semi-supervised Learning

Part of the training data for semi-supervised learning is labeled, and the other part is unlabeled, and the amount of data without labels is much more substantial than the amount of data with labels. The basic rule hidden under semi-supervised learning is that the distribution of data is not entirely random. Through some local features with tag data and more overall distribution of unlabeled data, you can get acceptable or even outstanding classification results. The basic idea of this learning scheme is to use the model assumptions on the data distribution to create a learner to label unlabeled samples.

3.2.2 Computing Complexity

Since the research method of this dissertation is to use the simulation results to verify the effectiveness of the proposed method and evaluate its performance. Assume that the hardware device meets the requirements required for the study and does not need to be discussed in the dissertation as a focus. Therefore throughout this dissertation, the computational complexity here refers to the time complexity rather than the space complexity (access stock) which is a measurement of the amount of storage space temporarily occupied by an algorithm during its operation.

The time complexity is the number of operations of the model can be measured by **FLOPs**, which is the floating-point operations. A floating point operation can be defined as one multiplication and one addition (although sometimes a floating point operation will also be defined). Since the spectrum sensing, in this research, is to recognize the OFDM modulation signal as it is assumed to be applied by the primary user transmission. Its cyclostationary feature then will be adopted as the final form from the data collecting to plug into the classifier. As stated before, the cyclostationarity appears in the form of a bi-frequency plane, i.e., a piece of image data. The requiring of the image processing ability push this research to employ the convolutional neural network as the data processor or classifier. Therefore, let us take the CNN as an example to show the specific calculation process of the time complexity.

- Time complexity of one single convolutional layer:

$$Time \sim O(M^2 \cdot K^2 \cdot C_{in} \cdot C_{out}), \tag{3.1}$$

where M is the side length of each convolution kernel output feature map, K is the side length of each convolution kernel. C_{in} is the number of channels per convolution kernel, which is the number of input channels, also known as the number of output channels of the previous layer, and C_{out} is the number of convolution kernels that this convolution layer has, which is the number of output channels. It can be seen that the time complexity of each convolutional layer is completely determined by the output feature map area M^2, convolution kernel area K^2, input channel C_{in} and output channel C_{out}.

The input matrix size determines the output feature map size itself X, the convolution kernel size K, *Padding*, and *Stride*, which are expressed as follows:

$$M = (X - K + 2 * Padding)/Stride + 1. \tag{3.2}$$

Notice here, in order to simplify the number of variables in the expression, and it is assumed here that the shapes of the input and convolution kernels are all square. Meanwhile, strictly speaking, each layer should also contain one bias parameter, which is omitted here for brevity.

- Time complexity of one complete convolutional neural networks:

$$Time \sim O(\sum_{l=1}^{D} M_l^2 \cdot K_l^2 \cdot C_{l-1} \cdot C_l), \tag{3.3}$$

where l is the convolutional layer index of the neural network, D is the total number of the convolutional layers belonging to the neural network, which is the depth of the network. C_l is the number of the output channel C_{out} of the lth convolutional layer, which is the number of convolution kernels. For the lth convolutional layer, the number of input channels C_{in} is the number of output channels of the $(l-1)$th convolutional layer.

In summary, for conventional calculations, the nonlinearity function is usually not considered, then the computing complexity for convolution operations is calculated as [60]

$$FLOPs = 2 \cdot H \cdot W \cdot (C_{in} \cdot K^2 + 1) \cdot C_{out}, \tag{3.4}$$

where H, W and C are the height, width and channel. It can be seen that the overall time complexity of the convolutional neural network is not mysterious, but the time complexity of all convolutional layers is cumulative. In short, the layers are multiplied and accumulated between layers.

From this calculation, the computing complexity of the full connected neural network, taking bias into account, is according to

$$FLOPs = 2 \cdot I \cdot O, \tag{3.5}$$

where I and O is the numbers of input and output nodes.

3.2.3 Deep Neural Network

3.2.3.1 Structure of Deep Neural Network

Suppose we have a system S with n layers $(S_1, ...S_n)$ whose input is I and whose output is O, which is represented graphically as: $I => S_1 => S_2 => ...... => S_n => O$, if the output O is equal to the input I, that is, there is no information loss after the input I changes through this system. The information remains the same, which means that input I passes through each layer of S_i without any loss of information, i.e., in any layer of S_i, it is another representation of the original information, i.e., input I. That is the basic information flow in the deep neural network (DNN). It is needed to learn the features automatically, assuming having a bunch of input I, such as a bunch of images or text and having designed a system S with n layers. The parameters are also required to be adjusted in the system, so that its output is still inputted I.

For deep learning, the idea is to stack multiple layers, that is, the output of this layer as the input to the next layer. In this way, the input information can be hierarchically expressed. In addition, the front is to assume that the output is strictly equal to the input. This limit is too strict. One can relax this restriction slightly. For example, one only need to make the difference between input and output as small as possible. This relaxation will lead to another kind of different deep learning method.

Deep learning itself is a branch of machine learning, which can be understood as the development of the neural network. About twenty or thirty years ago, the neural network was once a particularly hot direction in the ML field, but it slowly faded out, including the following:

- It is easier to overfit, the parameters are harder to tune, and it may need special tuning tricks;
- Learning speed is relatively slow, while the effect is not better than other methods when the level is relatively small (less than or equal to three).

The same is true for deep learning. It uses a similar hierarchical structure of neural networks. It contains a multi-layer network consisting of input, hidden (multilayer), and output layer. Joined nodes have connections. Each layer then is regarded as a logistic regression structure; this hierarchical model is closer to the structure of the human brain.

In order to overcome the problems in neural network training, deep learning uses a training mechanism that is very different from neural networks. In the traditional neural network, the back propagation method is adopted. In simple terms, an iterative algorithm is used to train the entire network, the initial value is randomly set, and the output of the current network is calculated, and then The parameters of the previous layers are changed according to the difference between the current output and the label until convergence (the whole is a gradient descent method). Deep learning as a whole is a layer-wise training mechanism. The reason for this is because, if the back-propagation mechanism is employed, for a deep network, the residual propagation to the foremost layer has become too small, and a so-called gradient diffusion occurs.

3.2.3.2 Trade-off of Deep Neural Network

In this section, certain simulation results are conducted to reveal the trade-off between the DNN or computing complexity and classification accuracy. In order to quantitatively analyze the relationship between the network structure and sensing performance, a full connected neural network known as the stacked denoising autoencoders (SDAEs) are selected to be the classifier, since it is more intuitionistic to see the performance gaps caused by different numbers of layers and nodes. IEEE 802.11g is considered to be the PU applying signals. For the supervised learning scheme, five training databases are prepared here as in Table 3.1.

Table 3.1: Training datasets under various SNR conditions

Training database	**Training datasets of C_0/C_1 (Transmission condition)**	**Number of datasets**
1	C_0: pure noise	10,000
	C_1: PU signal under SNR 5 dB	10,000
2	C_0: pure noise	10,000
	C_1: PU signal under SNR 0 dB	10,000
3	C_0: pure noise	10,000
	C_1: PU signal under SNR -5 dB	10,000
4	C_0: pure noise	10,000
	C_1: PU signal under SNR -10 dB	10,000
5	C_0: pure noise	10,000
	C_1: PU signal under SNR -15 dB	10,000

Based on previous research and experiments, one should consider altering the structure of the neural network to obtain or maintain good performance when there are changes in the number of input/output units, the number of training datasets, the complexity of the function, background noise situation, etc. Obviously, in this research when the target background becomes noisier, i.e., the C_1 training-data situation becomes worse, the data structure of C_1 becomes more similar to that of C_0, which makes the classification harder to realize. Therefore, to maintain the good SDAE situation from the training, a more powerful, deeper and wider SDAE network structure, i.e. structure with an increasing number of hidden layers and their nodes, should be considered. Figure 3.3 provides the specific values of the determined hidden layer number and hidden node number of each layer. As shown here, to achieve a better performance, a more sophisticated structure is required.

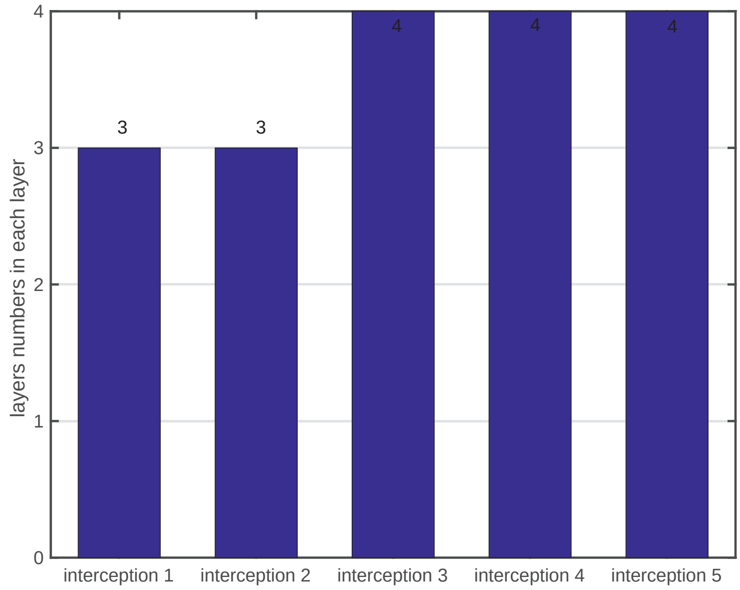

(a) Hidden layer number for each training database condition

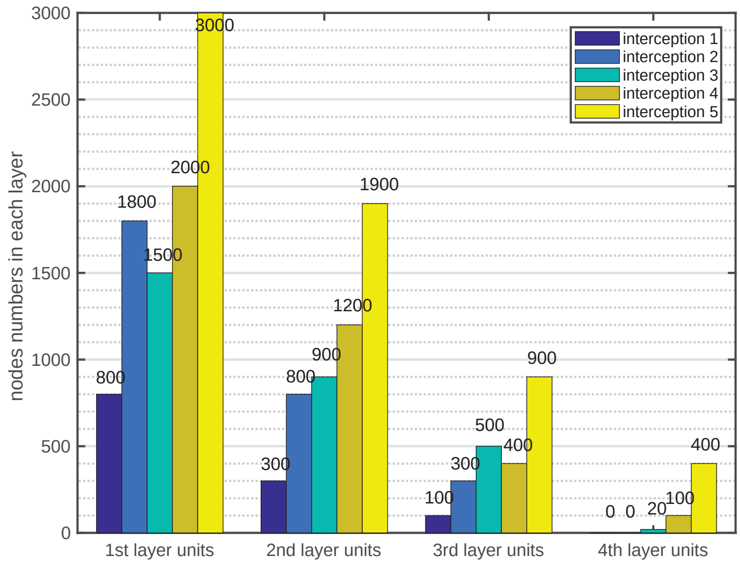

(b) Hidden node number for each training database condition

Figure 3.3: Structure of SDAE network for each training database condition

Different training strategies lead to different training duration, which is consistent with the network structure analysis. Therefore, another evaluation index of the training phase would be the elapsing time, as shown in the second column of Table 3.2. The training datasets are split into small batches for each iteration to calculate model error and update model coefficients. Therefore, the elapsing time is measured in every iteration under a suitable mini-batch value of 100, which was decided by the training phase. The number of the training datasets, as well as the epoch that represents the pass times over the whole training datasets, can be varied for a different accuracy demands or computing power status. Only the duration of one iteration under a certain structure is worth being provided a serviceable reference. Although minutes may be required for one iteration in the training phase, such an assignment could be done beforehand without delaying the actual signal classifying process for the CR system. Still, due to worse C_1 training-data condition, a longer elapsing time will be required corresponding to the more complicated SDAE structure. In conclusion, the complexity of the SDAE structure as well as the training time consumption should both be considered when optimizing the detection performance.

Table 3.2: Elapsing time of each training database condition

Training database	**Training phase (s)**	**Testing phase (ms)**
1	79.7	0.5
2	201.2	1.1
3	219.0	1.3
4	302.4	1.4
5	498.4	2.0

Once the training phase is done with the five C_1 training databases under different interception conditions, the five training-decided SDAE structures are then ready to be employed. On one hand, for the detection performance curve, as the C_1 training data is from worsening transmission conditions, the general downward trend is accelerating. This dividing line also changes along the training data conditions. On the other hand, owing to the training procedure, although the training data condition is deteriorating, it can provide an increasingly superior performance. For example, when detecting the testing data under a SNR of -10 dB, the training procedure of Database 4 guarantees that such data can be detected. However, for Databases 1, 2, and 3, the data can be detected because of the high tolerance and flexibility of the SDAE network. In any case, the proposed method shows a higher detection capability compared to energy detection. This is attributed to the training datasets intercepted from an actual communication environment. In addition, the superior performance of the proposed method is rational, because it can be obtained as an integration of the higher-order cumulants, spare autoencoders, and a softmax classifier. The higher-order cumulants suppress Gaussian noise. The autoencoders extract feature from the higher-order cumulants. Then, the softmax classifier provides maximum likelihood classifications. In terms of the specific values, the energy detection shows a p_d of $> 77\%$ at a SNR of -4 dB. The proposed method, Database 1 shows a p_d of $> 95\%$ at -4 dB, Database 2 shows a p_d of $= 100\%$ at -4 dB, Database 3 shows a p_d of $= 100\%$ at -8 dB, Database 4 shows a p_d of $= 100\%$ at -10 dB, and Database 5 shows a p_d of $= 100\%$ at -14 dB.

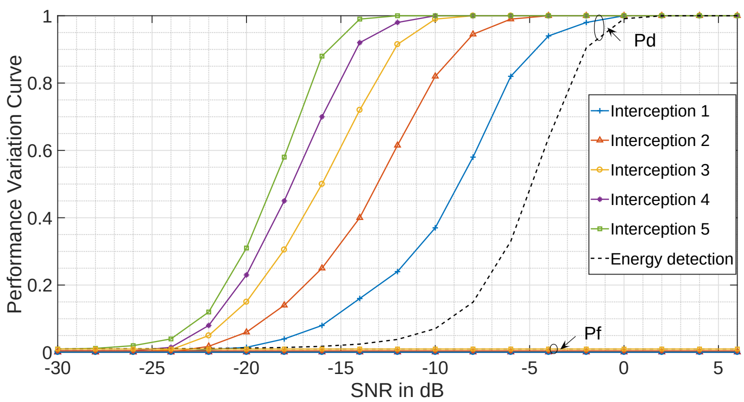

Figure 3.4: Performance comparison of the proposed method of each training database condition and energy detection for various SNR of the testing data

The false alarms probabilities are affected by the fitting situation of the SDAE network training. As shown in Figure 3.4, the p_fs of Databases 1, 2, and 3 are under 0.001, and the p_fs of Databases 4 and 5 are 0.0046 and 0.005, respectively. Databases 1, 2, and 3 reached an almost perfect fitting situation from the SDAE network training, as reflected in the classification accuracy approximately equal to 100% in the pretesting mentioned before. It guarantees that for these three training schemes, the pure AWGN will be perfectly and accurately classified into C_0 most every time, resulting in the pure AWGN also being classified into C_0 in the final testing phase, i.e., a low false alarm probability. Though the classification accuracy values of Databases 4 and 5 are comparatively big, there is still just a small probability of the AWGN being mistakenly classified into C_1. These two training scheme are still effective enough to provide low false alarm probabilities compared to some conventional spectrum sensing methods. In fact, the low false alarm probability is actually one of the advantages of the proposed method.

3.3 Chapter Summary

In this chapter, firstly since the CR system allows either monitoring the primary user activity or announcing key parameters of the primary user signal, the supervised learning is adopted for this research. The data collection procedure of collecting and preparing data samples for establishing the training database both interception-based and simulation-based, is introduced. Then the theory and characteristic of the machine learning are well described to explain how its advantage can assist the spectrum sensing. The learning schemes, computing complexity, and neural network establishment are discussed in detail as the reference for the future researches.

Chapter 4

Full-duplex Spectrum Sensing using Convolutional Neural Network

This chapter introduces an advanced spectrum sensing method for SU terminal with full-duplex (FD) technology. The proposed sensing scheme can provide an excellent detection performance even under a severe self-interference. The implementation flow is executed following a ”classification-converted sensing” framework. The spectral cyclic signature brought by the OFDM modulation structure is treated as input image data, then the convolutional neural network is employed as the image data processor. In the implementation process, in order to perceive residual self-interference (RSI), noise pollution and channel fading effect, the proposed method modifies the conventional adversarial training to built a CR-specific, training database. Meanwhile, to balance the computing ability and the detection performance, different input data formation as well as different CNN structures are discussed to decide a suitable combination for this research. Several SU structure designs are also proposed to benefit the spectrum sensing and its own transmission [61, 62, 63].

This chapter is organized as follow. Section 4.1 introduces of the background and the proposed scheme. Section 4.2 explains the system model and the implementation framework of the proposed method. Section 4.3 gives the mathematical derivation of the pilots induced cyclostationarity in the FD mode. In Section 4.4, the theory and architecture of the CNN, and the corresponding adversarial training plan are presented. In Section 4.5, the performances given by the different CNN architectures and image resolutions are analyzed and balanced with the computing capability; meanwhile, signal designs that can fit into the proposed method while benefiting SU transmission is presented. Section 4.6 summarizes this chapter.

4.1 Introduction

Currently, most of conventional sensing approaches are designed especially for SU equipped with half-duplex mode, which means it can only alternately perform spectrum sensing and data transmission. Such SUs are unable to utilize the required spectral band fully: the SU wastes precious data-exchanging time when performing independent SS, and would not be able to adjust itself in time if PUs suddenly arrive because of the divided sensing periods. However, if the SU adopted FD mode which functions the channel sensing and data sending at the same time, the utilization of the sensed free band will be more efficient [64]. SU equipped with FD mode is capable of identifying spectrum occupation statuses even during data exchanging period.

The biggest obstruct for FD widely be applied due to the severely self-interference from its own data transmission. However, such worrying situation has been improved from both the analog and digital scheme of the SU terminal [64, 65, 66, 67, 68]. Even so, residual self-interference cannot easily ignore. Most of the work on FD improvement primarily mostly pays attention to refine the full-duplex execution scheme [68, 69] or providing better allocations of executing the SS and data sending slots [70, 71]. Previous studies [72, 73] about FD-mode spectrum sensing under the RSI effect prefer to focus on the mathematical analysis from physical transmission aspect and lack in offering detailed problem-solving methods. For the OFDM modulation applied by the PU in this study, related researches are still in the development [74, 75].

Aiming for the mentioned challenges, this dissertation provides a novel SS method which posses an effective combination of solving RSI problem, surviving from harsh transmission environment and maintaining highly accurate sensing performance. The machine learning assisting SS is the basic framework converting the signal recognition into classification. Two main steps are required here: the cyclostationary feature generated by the pilot structure of OFDM modulation is considered to be collected image data [76, 77, 78, 79]; therefore, in order to sufficiently explore the inner construction of the input image, the convolutional neural network is then applied as the data processor/classifier [77]. Specialized adversarial training is assisting through the two-step in order to further improve the SS performance [80].

4.2 System Model and Implementation Framework

4.2.1 System Model

The in-question CR model is shown in Figure 4.1. Assuming that the considered SU equipped with FD module functions as a base station in the CR system, which means it has the capability and duty of SS towards the PU and exchanging data with other affiliated ordinary SU with FD module [69]. Without saying, the SS of the base station SU must be degraded for the RSI.

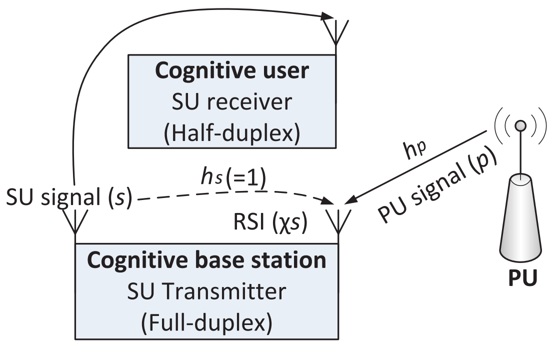

Figure 4.1: Basic system model of full-duplex in CR system

Putting aside the data exchanging between the SUs, which can only be processed after the status of sharing band being identified, the SS is still the priority mission. Therefore, based on the working position of PU, the mentioned binary hypotheses can be established as:

$$\begin{array}{c}\mathbf{H_0}\\ \textit{PU absent}\end{array} \qquad x = \begin{cases} n, & \mathrm{H}_{00}\ \text{SU silent,} \\ \chi s + n, & \mathrm{H}_{01}\ \text{SU busy,} \end{cases} \tag{4.1}$$

$$\begin{array}{c}\mathbf{H_1}\\ \textit{PU present}\end{array} \qquad x = \begin{cases} h_p p + n, & \mathrm{H}_{10}\ \text{SU silent,} \\ h_p p + \chi s + n, & \mathrm{H}_{11}\ \text{SU busy.} \end{cases} \tag{4.2}$$

Notice here, Equations (4.1) and (4.2) are way more complicated than the basic mathematical expression in Equation (2.1), due to the consideration of the RSI from FD mode. However, like before, x, p and n are the received signal at the FD SU terminal, the original transmitted signal from PU terminal and the AWGN, respectively. The power of p and n are then expressed as σ_p^2 and σ_n^2. s stands for the original transmitted signal from the base station SU terminal to ordinary SU with the power of σ_s^2 which is assumed to be calculated before the self-interference suppression (SIS). h_p denotes the channel from p to x, and h_s is omitted here since a perfect channel ($h_s = 1$) is considered from s_{tx} to s_{rx}. Only RSI is considered through this dissertation meaning some effective SIS must be carried out, where χ denotes the suppression level. $\chi \in [0, 1]$, if $\chi = 0$ means there will be RSI; else if $\chi \neq 0$ RSI power equals to $\chi^2 \sigma_s^2 / \sigma_n^2$. The interference-to-noise ratio (INR) as σ_s^2 / σ_n^2.

4.2.2 Implementation Framework

For establishing the converted classification model, $\mathbf{H_0}$ and $\mathbf{H_1}$ can be treated as two types, or classes, of data represented by $\mathbf{C_0}$ and $\mathbf{C_1}$.

Even though the SS is the priory, and its results only are to decide $\mathbf{C_0}$ or $\mathbf{C_1}$. However, the subdivision of these classes as expressed as H_{00}, H_{01}, H_{10}, and H_{11} are able to help upgrade the sensing performance in the to-be-discussed adversarial training step.

4.3 Data Collection: Extraction of Cyclostationarity

4.3.1 Cyclostationarity

Assuming the autocorrelation of $x(t)$:

$$R_{xx}(t,\tau) = E\left\{x(t+\tau/2)\cdot x^*(t-\tau/2)\right\}. \tag{4.3}$$

The periodicity of R_{xx} reflected on t, where the cycle value is T_x. R_{xx} can also be expressed by a series of Fourier expressions as:

$$R_{xx}(t,\tau) = \sum_{\alpha} R_{xx}^{\alpha}(\tau)\cdot e^{j2\pi\alpha t}, \tag{4.4}$$

where $\alpha = z/T_x, z \in \mathbb{Z}$. Subsequently, R_{xx}^{α} are expressed as:

$$R_{xx}^{\alpha}(t,\tau) = \lim_{T\to\infty}\frac{1}{T}\int_{-T/2}^{T/2} R_{xx}(\tau)\cdot e^{-j2\pi\alpha t}dt. \tag{4.5}$$

If there is an α value guarantees $R_{xx}^{\alpha} \neq 0$, $x(t)$ is said to possessing a second order cyclostationarity. The Fourier transformation of R_{xx}^{α} is:

$$S_{xx}^{\alpha}(f) = \int_{-\infty}^{\infty} R_{xx}^{\alpha}(\tau)\cdot e^{-j2\pi f\tau}d\tau, \tag{4.6}$$

which can also be regarded as the spectral correlation density (SCD) function, whose magnitude, $|S_{xx}^{\alpha}(f)|$ can be expressed as a bi-frequency plane with X-axis of cycle frequency α and Y-axis of spectrum frequency f. Such graphical expression can be later utilized as the input for data processor.

4.3.2 Model of OFDM Signals

Starting from one OFDM symbol, $x_k(t_s)$ (with index k and $t_s \in [0,T)$) consists of N subcarriers, and resulting in an N-point iFFT where f_n is $f_n = n/T_s$ for $n \in [0, N/2]$ and $f_n = (n-N)/T_s$ for $n \in [N/2+1, N-1]$, where T_s stands for the pulse-shaping period. The pulse shaping procedure is realized by using

$p(t_s)$ with a length of T. Concatenating $x_k(t_s)$ with $t_s \in [0, T)$ and $k \in [-\infty, \infty)$ yields:

$$x(t) = \sum_{n=0}^{N} \sum_{k=-\infty}^{\infty} a_{n,k} p(t - kT) \cdot e^{j2\pi f_n (t-kT)}. \tag{4.7}$$

Assume the filter $q_n(t)$ has the duration of $t_s \in [0, T)$, then

$$q_n(t) = p(t) \cdot e^{j2\pi f_n t}, \tag{4.8}$$

Equation (4.8) can be rewritten as

$$x(t) = \sum_{n=0}^{N} x_n(t) = \sum_{n=0}^{N} \sum_{k=-\infty}^{\infty} a_{n,k} \cdot q_n(t - kT), \tag{4.9}$$

with the discrete-time input $a_{n,k}$ [81]. Combining $a_{n,k}$ with a series of Dirac impulses $\delta(t)$, the impulse sampled auxiliary signal is as:

$$b_n(t) = \sum_{k=-\infty}^{\infty} a_{n,k} \cdot \delta(t - kT) \tag{4.10}$$

Equation (4.10) is then expressed as

$$x(t) = \sum_{n=0}^{N} b_n(t) * q_n(t). \tag{4.11}$$

Furthermore, the OFDM modulation with a focus of pilot structure is as [82]

$$x(t) = \sqrt{\frac{\sigma_p^2}{N}} [x_{data}(t) + x_{pilot}(t)], \tag{4.12}$$

where,

$$x_{data}(t) = \sum_{n=0}^{N-1} \underset{data}{b_n(t)} \cdot * q_n(t), \tag{4.13}$$

and

$$x_{pilot}(t) = \sum_{n=0}^{N-1} \underset{pilot}{b_n(t)} \cdot * q_n(t). \tag{4.14}$$

4.3.3 Pilot-induced Cyclostationarity in FD Mode

Normally, cross-spectral density of the data carrying subcarriers $b_{n-data}(t)$ is expected to be 0 due to their independent and identical characteristics. Conversely, the $b_{n-pilot}(t)$ data are correlated and parallelly inserted into designated subcarriers, which is able to offer the required cyclostationarity in this study. Then to make the derivation process easier to understand, $b_{n-pilot}(t)$ will be rewritten to $b_{n,t}$ from here on. According to the considered IEEE 802.11g protocol, a pilot symbol in the kth OFDM symbol is subsequently as:

$$b_{n,k} = b_{m,k}e^{i\varphi}, \tag{4.15}$$

where $\varphi \in [-\pi, \pi]$. For exhibiting the joint cyclostationarity of multi-pilots, its discrete-time cyclic cross-correlation function is expressed as

$$R_{xy}^{\alpha}(k,u) = \lim_{M\to\infty} \frac{1}{2M+1} \sum_{k=-M}^{M} \sum_{\alpha} R_{xy}(k,u) \cdot e^{-j2\pi\alpha k}. \tag{4.16}$$

By substituting (4.4) and (4.16) in (4.17), obtain:

$$R_{b(nm)}^{\alpha}(k,u) = \lim_{M\to\infty} \frac{1}{2M+1} \sum_{k=-M}^{M} \sum_{\alpha} E\left\{b_{n,k} \cdot b_{m,k}^{*}\right\} \cdot e^{-j2\pi\alpha k}, \tag{4.17}$$

where,

$$E\left\{b_{n,k} \cdot b_{m,k}^{*}\right\} = \sigma_b^2 e^{i\varphi} \sum_{\iota\in\mathbb{Z}} \delta[k - \iota K - k_0]. \tag{4.18}$$

σ_b^2 denotes the power of b_k and k_0 denotes the very first received OFDM symbol. The cross-correlation function for pilot is then expressed as:

$$R_{b_{nm,k}}^{\alpha} = \frac{\sigma_b^2 e^{-j(2\pi\alpha k_0 + \varphi)}}{K} \sum_{l\in Z} \delta\left[\alpha - \frac{l}{K}\right], \tag{4.19}$$

If $\alpha \in [(l - \lfloor K/2 \rfloor)/K, l \in \{0, 1, ..., K-1\}]$ ($\lfloor\cdot\rfloor$ is integer flooring), then $R_{b_{nm}}^{\alpha} \neq 0$, where $\alpha \in [-1/2, 1/2]$. Subsequently, the local maximum value is localed at:

$$S_{b_{nm,k}}^{\alpha}(f) = \left\{(n, m, K) \mid R_{b_{nm,k}}^{\alpha} \neq 0\right\}, \tag{4.20}$$

where (n, m) is a pilot-tone pair. When $2K$ pilots are symmetrically distributed, local maximum value are localed on the SCD figure according to following coordinates:

$$\alpha = \pm(n-m)\cdot\Delta f, \quad f = \pm(n+m)\cdot\Delta f/2. \tag{4.21}$$

As in IEEE 802.11g, $n, m = \{\pm 7, \pm 21 \mid n \neq m\}$, and the subcarrier interval Δf would be 312.5 kHz. The SCD of IEEE 802.11g protocol is shown in Figure 4.2.

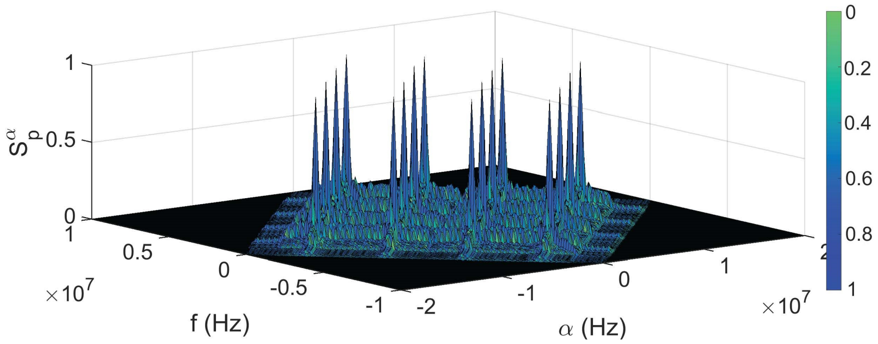

Figure 4.2: Pilot-induced SCD of IEEE 802.11g protocol signal.

For FD mode, the SU signal can be designed based on IEEE 802.11g protocol, specifically the pilot structure, to borrow the robustness in channel equalization. The pilot specific positions of the SU should be changed from those of the PU for distinguishing SU and PU during the sensing:

$$b^s_{n,k} = b^s_{m,k}e^{i\varphi_1} = b^p_{r,k}e^{i\varphi_2}. \tag{4.22}$$

For sensing under RSI, the condition of H_{11} is written as:

$$S_x^\alpha(f) = S_p^\alpha(f) + S_s^\alpha(f) + S_{ps}^\alpha(f), \tag{4.23}$$

where S_p and S_p are the auto-SCD term of the PU and SU signals, respectively. S_{ps} denotes their cross-SCD term. Subsequently, the peaks in the pilot-generated SCD plane are as:

$$S^\alpha_{b_{nm,k}}(f) = \left\{((n_p, m_p), (n_p, m_s), (n_s, m_s), K) | R^\alpha_{b_{nm,k}} \neq 0\right\}, \tag{4.24}$$

at the coordinates:

$$\begin{aligned} \alpha &= \pm\left\{(n_p - m_p), (n_p - m_s), (n_s - m_s)\right\}\cdot\Delta f, \\ f &= \pm\left\{(n_p + m_p), (n_p + m_s), (n_s + m_s)\right\}\cdot\Delta f/2. \end{aligned} \tag{4.25}$$

If a certain pilot design is applied by the SU signal, then its SCD plane is shown in Figure 4.3(a). Under such circumstance, the received data with mixed signal as in H_{11} is shown in Figure 4.3(b). The result figures again prove the accuracy of the mathematical derivation. The SCD peaks standing for the maximum value in the correlation should show themselves at both the auto-term and cross-term coordinates.

4.4 Classification: Utilization Scheme of CNN

As stated in Chapter 2, the SCD transformation is in the form of two-dimensional figure, where α, f, and $|S^{\alpha}_{xx}(f)|$ are as the "x" and "y" pixel coordinates and the pixel value, respectively. Therefore, to deeply exploit the image features, the convolutional neural network is applied here for data processing.

4.4.1 Convolutional Neural Networks Architecture

Suppose that input SCD plane expresses as:

$$\mathbf{X}_b = [\mathbf{x}_{f,\alpha}, ..., \mathbf{x}_{F,A}], b \in [1, B], \tag{4.26}$$

where b is the dataset index. The CNN processes the image data through the convolution and pooling layer: the former is for extracting region characteristic of one input image using a decided kernel; the latter is to generalize the information from extracted feature maps as well as reduce the oversize convolution layer output at some level. These two steps are as:

$$\mathbf{o}_l = pool\,(\sigma\,(\mathbf{w}^v_l \cdot \mathbf{o}_{l-1} + \mathbf{b}^v_l)), v \in [1, c_l], l \in [1, L-1] \tag{4.27}$$

where supposing $\mathbf{o}_0 = \mathbf{x}_b$. L stands for the total layer number of the complete processor network; c, w, and b stand for the number of the convolutional filters, weight, and bias parameters, respectively. σ stands for the nonlinear activation function, which can map the output into certain acceptable range.

The full connected layer will be used as final decision making layer after integrate the convolutional output to a vector. The complete execution flow is as:

$$\mathbf{y}_{l-1} = \sigma(\mathbf{w}_f(f(pool\,(\sigma(\mathbf{w}^v_l \cdot \mathbf{o}_{l-1} + \mathbf{b}^v_l)))) + \mathbf{w_f}). \tag{4.28}$$

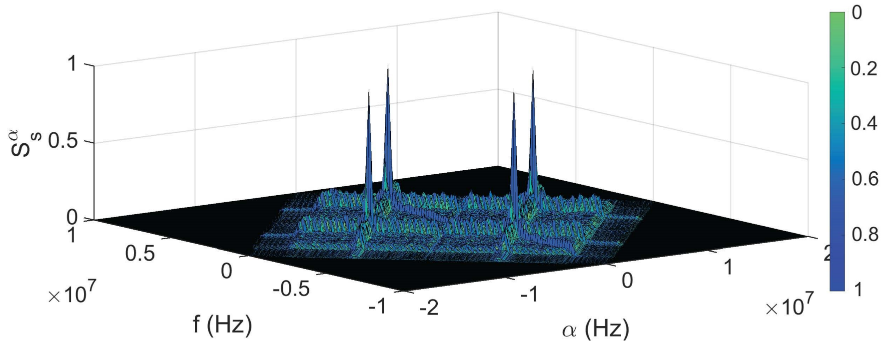

(a) Pilot-induced SCD peaks of one particular SU signal

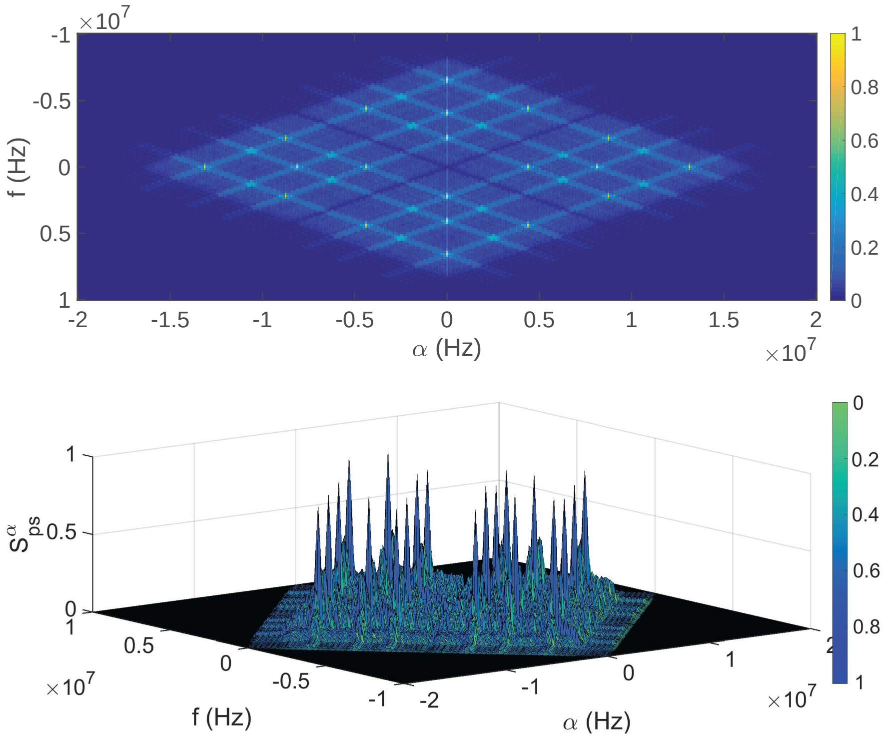

(b) Pilot-induced SCD peaks of PU signl under self-interference

Figure 4.3: Pilot-induced SCD peaks in FD mode.

As one type of the full connected layer, the sensing results will be provided by the softmax layer. It quantifies a given probability and integrate the vector expression for giving the probability of each class, as in:

$$\Psi_i = e^{y_i} / \sum e^{y_k}, \tag{4.29}$$

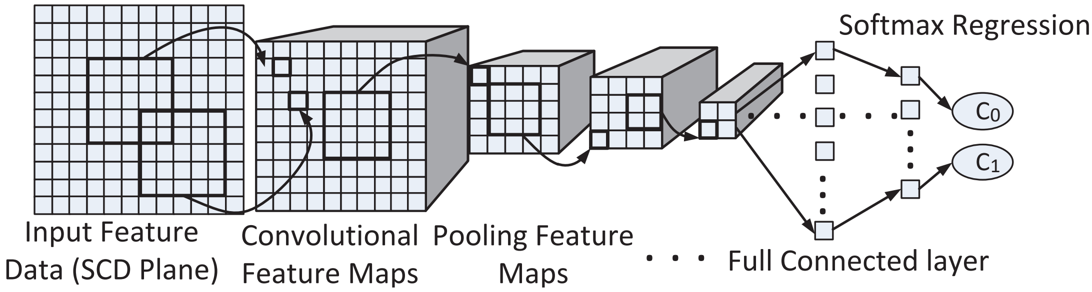

Figure 4.4: CNN architecture.

where y_i stands for the class predictions while k is the number of classes. It is noteworthy that long with the changing in the network structure such as layer number, kernel size, etc., the final classification will be altered. Therefore, in this dissertation, CNN architecture with various parameters will be tested to find out the performance pattern and decide the most suitable one. The CNN architecture is shown in Figure 4.4.

4.4.2 Training Strategy

Most of the related research usually establish two training databases of clean PU signal and pure background noise [76, 77, 78]. However, when receiving data under hash transmission conditions, such data samples are considered as adversarial data that will severely disturb the spectrum sensing, let alone the existing RSI. Even so, when proper training can be executed, the deeply polluted adversarial sample can still be guaranteed an accurate classification. Generally, two adversarial schemes can be used to improve the accuracy: modifying the processor structures or modifying the training strategies, for example, establishing a new, more robust database. In this dissertation, adjusting the training strategy is adopted for following reasons: due to the utilization of open information about IEEE protocol, the simulation of PU transmitting signal under any environments can be done and used to build the training database; for regular image processing using machine learning, considering the complicated inner relationship among pixels, the CNN may face a tough job but still be qualified. Comparing to such situation, the processing of the comparatively organized SCD planes is too easy a task for CNN, where the adversarial samples will not cause any extra trouble;

modifying the processor architecture seems easy, however, more often, the price of cost more computing power must be paid. Table 4.1 gives the concrete establishing plan of the adversarial training databases. The power of the simulated AWGN data remains the same and the PU and SU signal power are changed according to the exhibiting values to build the training database.

Table 4.1: Training databases

Class	**Component**	**Subcomponent**			
			PU (fading effect)	SU (χ^2)	AWGN (in dB)
$\mathbf{C_0}$	1 (H_{00})	1	×	×	◯
	2 (H_{01})	1	×	0.1	INR 10
		2	×	0.2	INR 20
$\mathbf{C_1}$	1r (H_{10})	1	◯ (no fading)	×	×
		2	◯ (Rayleigh)	×	×
		3	◯ (no fading)	×	SNR -15
		4	◯ (Rayleigh)	×	SNR -15
	1m (H_{10})	1	◯ (no fading)	×	×
		2	◯ (multi-path)	×	×
		3	◯ (no fading)	×	SNR -15
		4	◯ (multi-path)	×	SNR -15
	2r (H_{11})	1	◯ (Rayleigh)	◯	×
		2	◯ (Rayleigh)	0.1	SNR -5
		3	◯ (Rayleigh)	0.1	SNR -15
		4	◯ (Rayleigh)	0.2	SNR -15
	2m (H_{11})	1	◯ (multi-path)	◯	×
		2	◯ (multi-path)	0.1	SNR -5
		3	◯ (multi-path)	0.1	SNR -15
		4	◯ (multi-path)	0.2	SNR -15

As illustrated in Table 4.1, a multicomponent database is built to carry out a more suitable training plan. The smallest unit of data group (subcomponent) will contain N sets of data (N equaling 10,000 in this research). However, to reach a balance training which demands an even number of datasets, H_{00} component will contain $4 * N$ sets of data while each subcomponent of H_{01} will contain $2 * N$ sets of data. Here two fading channel effects are considered for the PU transmission, where components 1r and 2r form the $\mathbf{C_1}$ training database for the Rayleigh fading effect and components 1m and 2m form the $\mathbf{C_1}$ training database for multi-path fading effect (the channel tap numbers are 4,6, and 8 and the channel coefficient is set randomly). After the CNN reaching a fitting mode for the training data, the data originally belongs specified label will be accurately classified to the same class no matter how bad the data condition is. Under this circumstance, the sensing/classification performance is expected to rise as long as training the CNN to learn that the polluted adversarial data samples should be labeled to $\mathbf{C_1}$. The execution flowchart is shown in Figure 4.5.

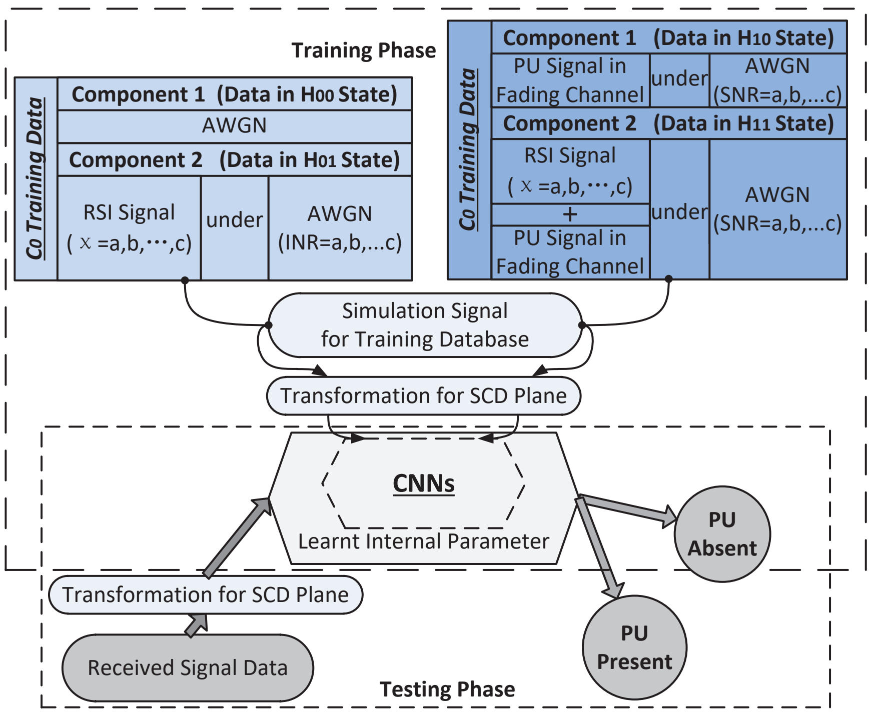

Figure 4.5: Implementation flow-chart.

Because the classifier structure is undecided, for different accuracy and complexity requirements, one can establish the CNN architectures accordingly.

4.5 Simulation and Results

4.5.1 Simulation Setup

This research assumes that PU uses IEEE 802.11g protocol with 16QAM to transmit data under both AWGN as well as Rayleigh/multi-path fading effect. GPU acceleration is utilized via Nvidia GeForce GTX 1080. Other working platforms contain a 3.20-GHz Intel Core i7-6900K CPU and MATLAB R2016b.

As multiple pilots inserted into SU signal structure,

Since multiple pilots may be inserted into the SU OFDM signal, the SCD planes of the received signal at the SU terminal with the FD mode may peak at many coordinate points, as shown in Figure 4.3. A relatively high resolution of the SCD plane is desired for the input image. Meanwhile, the CNN possesses the capability of deeply exploring the inner feature of a comparatively dim input image. The size and formation of the input image may be reduced to reduce the computing ability and the time complexity, which means that an input image with an overly high resolution may not fully utilized. Combining these two points, 10 OFDM symbols are utilized to transform into the input SCD image. For every piece of the input image, the original plane is rotated and abandoned pixels equaled to zero. Data preparation steps are executed too, including principal component analysis and mean elimination. It should be noted that compared with traditional sensing schemes, such as the energy sensing and cyclostationary feature detection which need to calculate the accumulated energy value or cyclostationarity, the sensing schemes proposed are able to save a lot of observation time. Furthermore, if one is willing to invest more computing power to perform the spectrum sensing with more complex CNN structures and larger size input image formation, high sensing performance can be achieved fewer symbols.

4.5.2 Results Analysis

4.5.2.1 Input Formation and CNN Structure

According to the results of the previous formula derivation, as the number of built-in pilots increases, their SCD peaks will also increase. Therefore, to clearly exhibit the peaks in the input plane, three input formations of low-resolution (Low-R), high-resolution (High-R) and extra-high-resolution (XHigh-R) SCD planes are presented. Figure 4.6 shows the detailed expressions of the three input formations for IEEE 802.11g protocol.

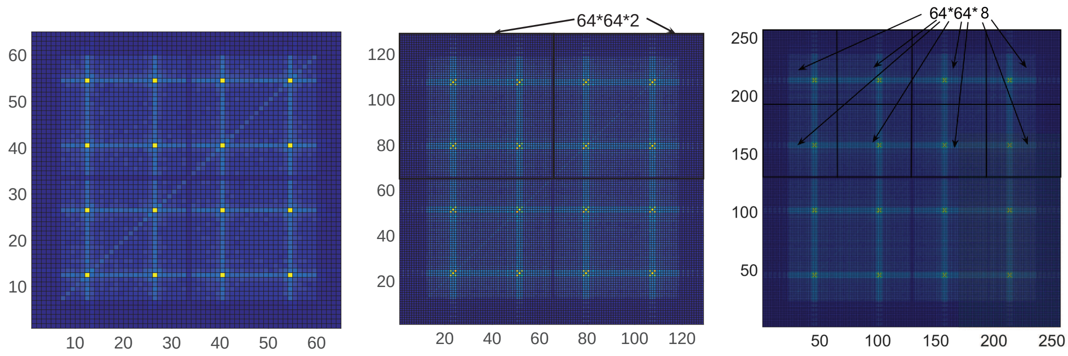

(a) Input formation with low resolution (Low-R) (b) Input formation with high resolution (High-R) (c) Input formation with extra high resolution (XHigh-R)

Figure 4.6: Input image formations.

As shown, the Low-R plane is of the size of 64×64. Subsequently, to save computation power, the plane of High-R and XHigh-R will be divided into small parts with the same size of 64×64. For High-R one, two parts that contain the entire pilots-induced information owing to the symmetry of the SCD feature, will be jointly plugged into the classifier through two input channels; meanwhile, as for XHigh-R one, eight parts will be plugged into the classifier through eight input channels

The CNN architecture can vary according to the equipped computing power and the demanded classification accuracy. Therefore, several CNN models are discussed to provide a ready-to-use architecture for further reference. For better analysis and comparison, this proposal firstly focus on the situation where the SU is always silent or perfect self-interference suppression is in place, instead of a thorough consideration of the FD mode sensing. Hence, similar to the traditional half-duplex, only the sensing results of H_{00} and H_{10} will be obtained. Therefore, only component 1 of C_0/C_1 in Table 4.1 is plugged into the classifier as input training data. Firstly, the Low-R input formation is used to locate a CNN architecture with better image-feature-exploiting capability. Five architectures of

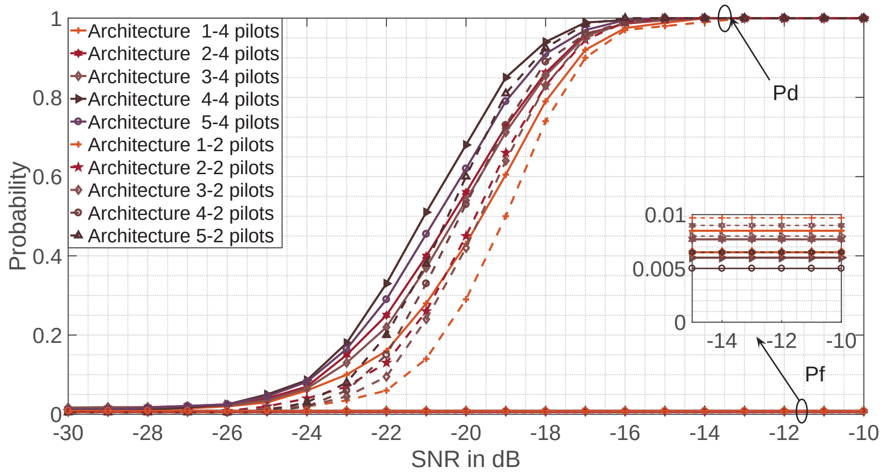

Figure 4.7: Performance comparison between different CNN architecture with Low-R input formation under various SNR of non-fading transmission environment, where the SU is always silent or a perfect self-interference suppression is in place. IEEE 802.11g protocol with 2 and 4 pilots are considered to be the PU signals.

the CNNs are tested in this study, and their detailed conditions are exhibited in Table 4.2.

Figure 4.7 shows p_d, p_f curves for the purposed five CNN architectures. As one can imagine, for p_f curves, the perfectly fitting training cannot be reached with the proposed training database since we increase the training samples as many as possible. In another word, when the databases in Table 4.1 are used in the training phase, some samples in $\mathbf{C_0}$ will be misclassified into $\mathbf{C_1}$ and vice versa. After executing training, a pretesting process is necessary to see if the training is successfully done; this is done by utilizing sets of generated data with the same condition as the training data. The misclassification probability, which is calculated by misclassifying $\mathbf{C_0}$ to $\mathbf{C_1}$, is p_f. Therefore, p_f is entirely determined by every training/pretesting phase instead of being set randomly. Hence, even though a receiver-operating characteristic (ROC) curve is commonly used to evaluate the performance of the spectrum sensing, the inability to change p_fs or p_d along p_f means that only a separated result analysis of p_d and p_f is possible.

The SCD peaks exhibit certain distribution rules that allow one to alter the hyper-parameters such as strike, padding, and feature map channel number ac-

Table 4.2: Conditions of 5 CNN architectures

Architecture	Time Complexity	Parameters
1	2.85×10^5	1 convolution layer (6*6) 1 pooling layer 1 full connection layer
2	4.25×10^5	1 convolution layer (10*10) 1 pooling layer 1 full connection layer
3	4.21×10^5	2 convolution layers (6*6) 2 pooling layers 2 full connection layers
4	6.87×10^5	2 convolution layers (10*10) 2 pooling layers 2 full connection layers
5	7.02×10^5	3 convolution layers (6*6) 3 pooling layers 2 full connection layers

cordingly. If a large kernel value is used, one is able to choose a large strike while still obtain excellent performance, while saving computing power. In Figure 4.7, as the convolution kernel becomes larger, the detection accuracies significantly increase. Meanwhile, the depth of the CNN architecture increases and a large amount of computation is required; however, p_d curves do not increase as expected. Furthermore, even though Architectures 1 and 4 give the lowest time complexity and the best performance, the low p_d and the computing power conditions may not be met for every SU terminal. Therefore, the CNN architecture of Architecture 2 is applied.

To further prove our determination of the CNN architecture, Figure 4.8 shows the sensing performances (p_d, p_f) of five CNN architectures versus their time complexities. The horizontal axis indicates the index of five proposed CNN architecture, and the vertical axis indicates the p_d/p_f to the time complexity ratio, where the p_ds are the values at an SNR of -20 dB in Figure 4.7. As shown in Table 4.2 and Figure 4.7, different sensing performance are provided by different architectures, or time complexity, of CNN; therefore, it is unfair to compare the p_d and p_f values directly. At this point, Figure 4.8 calculates the p_d (p_f) vs. time complexity ratio, i.e. how much the sensing ability can a unit time complexity provide for each architecture, to conduct a fair competition and find out the most economical and practical architecture. All the vertical coordinates are normalized by the maximum value, i.e. the p_d (p_f) vs. time complexity for Architecture 1. The value beside every double arrow indicates the difference between the two ratio values for the corresponding architecture, which can be obtained as:

$$Difference_i = \frac{p_{di}/time\ comlexity_i}{(p_{d1}/time\ comlexity_1)} - \frac{p_{fi}/time\ comlexity_i}{(p_{f1}/time\ comlexity_1)}, \tag{4.30}$$

where i is the index for each CNN architecture. As one can expect, for p_d, the higher value the better the performance; however, for p_f, the lower value the better the performance. It means the greater the difference values between these two curves, the better CNN architecture it is. Once again, Architectures 1 and 4 show their advantages in the cases of p_f and p_d, respectively. However, combining these two curves enables final determination the CNN architecture with the biggest difference value, which best balances the general performance and the time complexity. According to the above analysis and evaluation, this is the CNN of Architecture 2. Meanwhile, from the performance comparison between IEEE 802.11g protocol with 2 and 4 pilots, one can conclude that, with certain limits, the SCD plane with more pilot peaks can contribute a better sensing capability since it will have more image feature for the CNN classifier to capture and be easier to distinguish itself from AWGN transmission environment.

In Figure 4.9, the detection results for the Low-R/High-R/XHigh-R scheme and the conventional cyclostationary feature detection (CFD) [16] under non-fading, Rayleigh fading, and multi-path fading channels with AWGN are subsequently compared. p_f of CFD is 0.01. As shown, in the perfect self-interference suppression condition or half-duplex mode, the proposed method shows superior capability in PU sensing. Furthermore, the High-R and XHigh-R schemes provide better sensing performances than the Low-R scheme. However, for High-R and

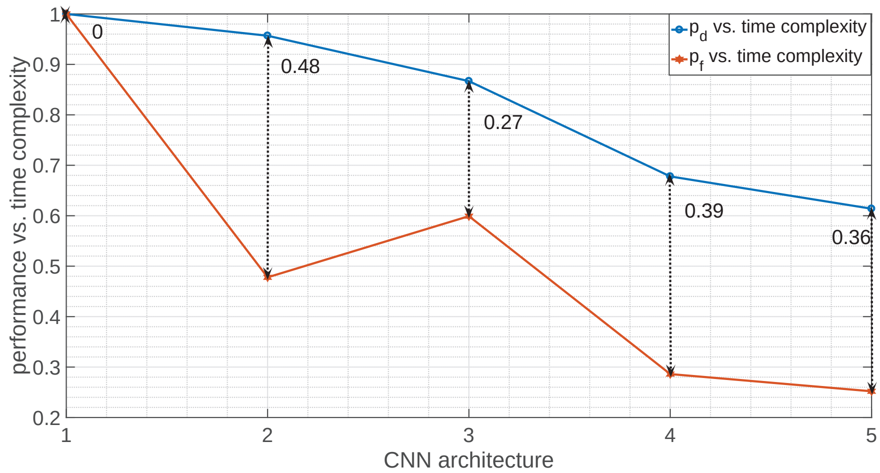

Figure 4.8: Performance vs. time complexity ratio for five CNN architecture

XHigh-R schemes, with two and eight input channels, their time complexity of CNN Architecture 2 increase to 7.59×10^5 and 3.65×10^6. As shown in Figure 4.10, when comparing the raised p_d versus the costing computing complexity values, such improvements are not sufficient enough, especially the one from XHigh-R formation. Even though for the sensing task in the FD mode, the improvement is expected to be higher; to balance the sensing performance and costing computing power, the testing will be conducted only between the High-R and Low-R input formations.

The time complexity comparison between the proposed CNN classification and conventional CFD is exhibited in Table 4.3. When considering the computation situation, the proposed method with such a deep artificial intelligent neural network indeed requires higher computing power. However, as mentioned earlier, only applying 10 OFDM symbols to calculate the SCD input plane helps sufficiently reduce the observation time compared to the conventional method, in order to obtain a satisfactory performance. When sufficient OFDM symbols are provided for these methods, their time complexity will increase by a large margin.

4.5.2.2 Pilot Structure Evaluation for SU Signal Selection

Since the SU is able to design its signal formation by itself to facilitate SS and own transmission, it can consult the efficiency proved IEEE 802.11g protocol. The

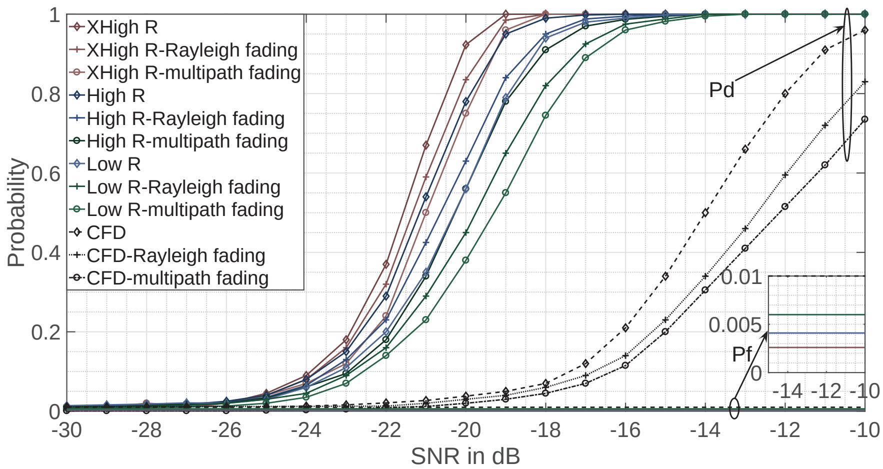

Figure 4.9: Performance comparison between three input formations and CFD under various SNR of transmission environment where, still, the SU is always silent or a perfect self-interference suppression is in place.

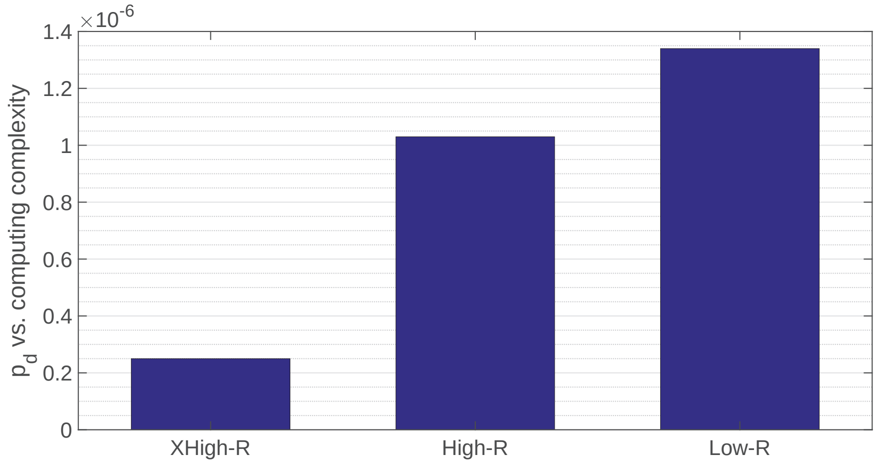

Figure 4.10: p_d vs. computing complexity comparisons for non-fading transmission at SNR of -20 dB among three input resolutions.

Table 4.3: Time complexity comparison with silent SU

	Proposed scheme	**CFD**
Time complexity	4.25×10^5 Low-R 7.59×10^5 High-R	6.16×10^4

investigation is based on the pilot induced cyclostationarity; therefore, only the number and location of the pilot need to be designed. Let us focus on the number first. Three pilot number is proposed including two (Design 1), four (Design 2), and six (Design 3). This research considers these three plans are suitable, since too few or too many will drag on the frequency band utilization and equalization. However, in order to distinguish Design 2 with the PU signal, their specific pilot arrangements will be different from each other. Firstly, to confirm that the SU can be distinguished from both the PU and AWGN, the t-SNE technique [83] is used to exhibit the clustering situation of different SU signal designs. Figure 4.10(a) shows the feature clustering maps for clean SU signals of a certain design, IEEE 802.11a protocol, and the AWGN. Figure 4.10(b) subsequently shows their re-extraction feature after being plugged into the CNNs. The input image formation is in Low-R and the CNN of Architecture 2 is applied. Notice, the SU signals are assumed to be synchronized with the PU signals. As stated in Chapter 4.3, one can learn that the relative location of the pilot subcarriers decide the cross-term peak coordinates on the SCD plane. If the synchronization is assumed between the SU and PU signals, then the relative locations of their pilot subcarriers are fixed, so are the cross-term peaks. At this point, the training database can be established accordingly, and be utilized to train the classifier. However, if the relative location is changed due to the random arrangement of the pilot subcarriers, the training database should be modified, too.

As it shown, the SCD features of the designed signals with two and six pilots are projected into a different feature space compared to IEEE 802.11g protocol, which is beneficial to the spectrum sensing. After the CNN feature re-extraction, the signals can again be expressly separated from the AWGN, which will benefit the SUs own transmission. However, both results suggest that a four-pilot structure is not compatible with the SU signal as its feature space is intertwined with IEEE 802.11g protocol. Even though the two-dimensional t-SNE mapping is a narrow feature space and the CNN training process can be further improved, this confusion cannot be ignored.

Then quantified test should conduct for more valuable reference. Firstly, the misclassification probability of misclassifying SU into PU and AWGN are provided, i.e., whether the SU with the designed signal will successfully execute

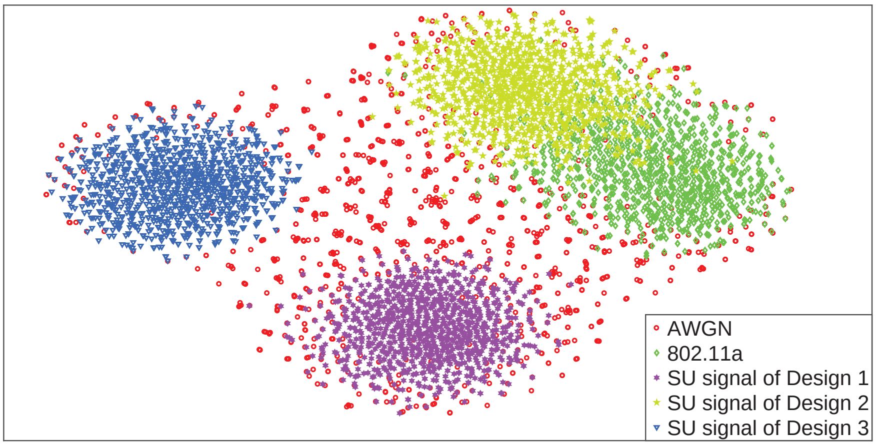

(a) t-SNE feature mapping before CNNs

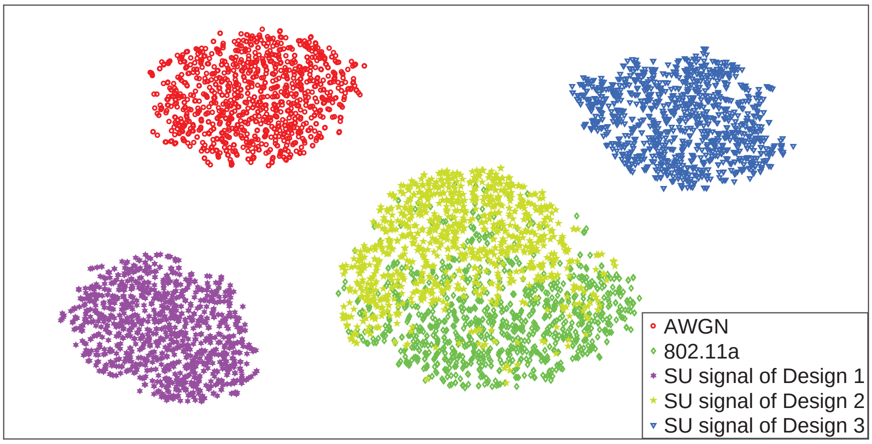

(b) t-SNE feature mapping after CNNs

Figure 4.11: t-SNE feature mapping of SU signal designs and AWGN in Low-R formation.

self-transmission and PU-detection. Figure 4.10 shows the mean and variance of the misclassification probability of misclassifying SU into PU and AWGN. Here, the training data of the clean PU signal, clean SU signal, and pure AWGN are utilized as training data to distinguish the SU signal from the AWGN and the PU signal. Subsequently, the SU signals under different SNRs become the testing data to test how far the designed SU signal can help the CNNs with the distinction and self-transmission. Notice that, the adversarial training scheme is not applied in this section. The SU pilot design determination is, in reality, a testing setup

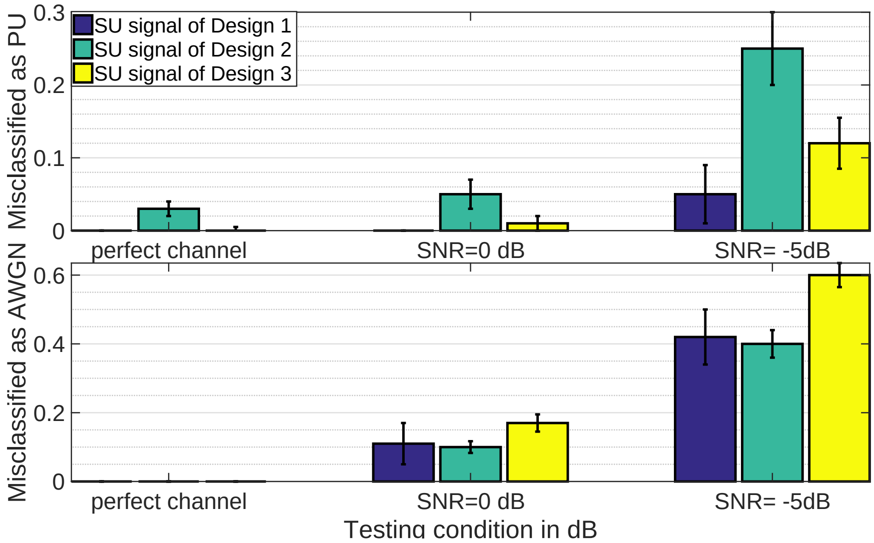

Figure 4.12: Mean and variance values of misclassification for each considered pilot number in Low-R input formation.

before the final performance evaluation for the FD mode; therefore, to determine the most suitable design, the adaptation competence of the pilot designs are explored deeply. If the designed SU signal is accurately adapted without the help of the adversarial training, this will result in an even better performance during the final testing. Different design of pilot positions are tested, which gives the mean and variance values shown in Figure 4.11. The input image formations are in Low-R and the CNN of Architecture 2 is applied.

As shown in Figure 4.12, SU different pilot number will be more easily to be distinguished from PU. Design is firstly dropped. Design 1 is more easily distinguished from the AWGN than Design 3. However, when the transmission condition is worse than the SNR of -5 dB, p_fs of the SU self-transmission becomes unacceptably high. Such results are caused by the fact the adversarial training is not applied and only the clean PU/SU/AWGN data is plugged into the CNN for training. Even though the CNN is a powerful tool for image processing and is able to withstand image shifting and distortion, it cannot classify a highly polluted AWGN signal into the right class. This result also shows the importance of the proposed training scheme and limitations of simple applications of the CNN. Therefore, the high misclassification probability of Design 3 can be reduced using adversarial training. The value of variances and means shows that the actual pilot position will not affect the sensing result as the pilot number do. Fortunately, Design 1 is the most promising design, and the limited position can allow us provide an optimal complete design plan ($p = \{\pm 13\}$).

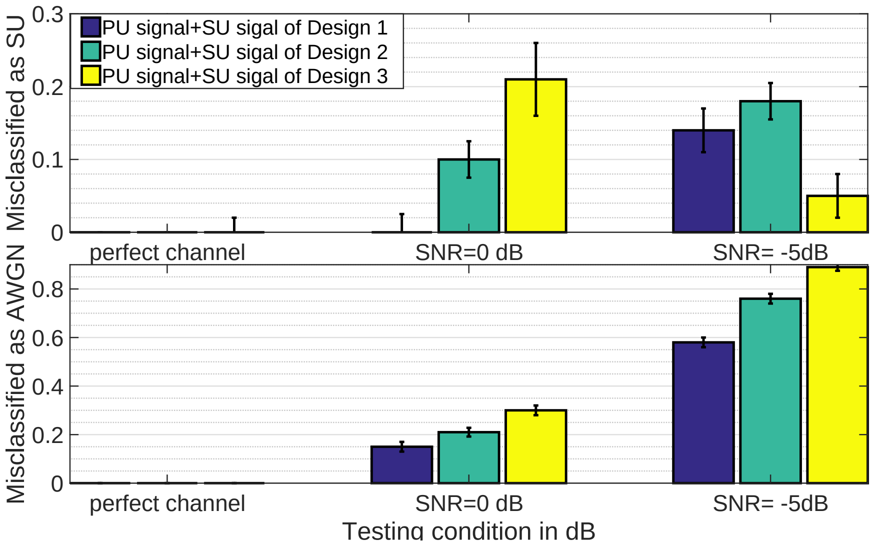

Figure 4.13: Mean and variance values of misclassification for each considered pilot number in Low-R input formation.

When considering the FD mode, the design should ensure the PU interfered by the SU (H_{11}) is able to be adequately identified from the two components of Class C_0: the AWGN (H_{00}) and the SU signal (H_{01}). Therefore, these three data kinds, i.e., received data of PU interfered by SU, SU, and AWGN, are used as the three training databases. Again, the adversarial training is still not applied here. Subsequently, the PU signal interfered by the designed SU signal and AWGN are regarded as the testing data. Here, one should focus on whether the designed SU signal is able to improve the sensing of the PU signal; therefore, the transmission environment is set to prioritize this situation. With or without AWGN, for the PU signal interfered by or mixed with the designed SU signal of the same power, i.e., the INR remains at a relatively high value of 0dB for the training and testing data collection at this step. The SNRs are again changed to analyze how far the designed SU can help the CNNs with the distinction and execution of the PU-detection. Figure 4.13 shows the misclassification probability concerning SU or AWGN. The input image formation is in Low-R and the CNN of Architecture 2 is applied.

Consistent with Figure 4.12 results, Design 1 shows the most superior distinguishability, in the perfect channel and with an SNR of 0dB; hence, Design 1 is the decided plan of the SU design. It is noteworthy that for all proposed pilot numbers, the mean value of the misclassification with regard to the AWGN at an SNR of −5dB appears to be too high. Even though the adversarial training scheme can fix such a high misclassification probability, when considering that the many pilot peaks in the SCD plane are clearly shown with a Low-R input formation, a high-resolution condition should be tested.

Figure 4.14 shows the misclassification probability with regard to SU and AWGN category in High-R input formation. The conditions of the training and testing data are similar to those in Figure 4.13.

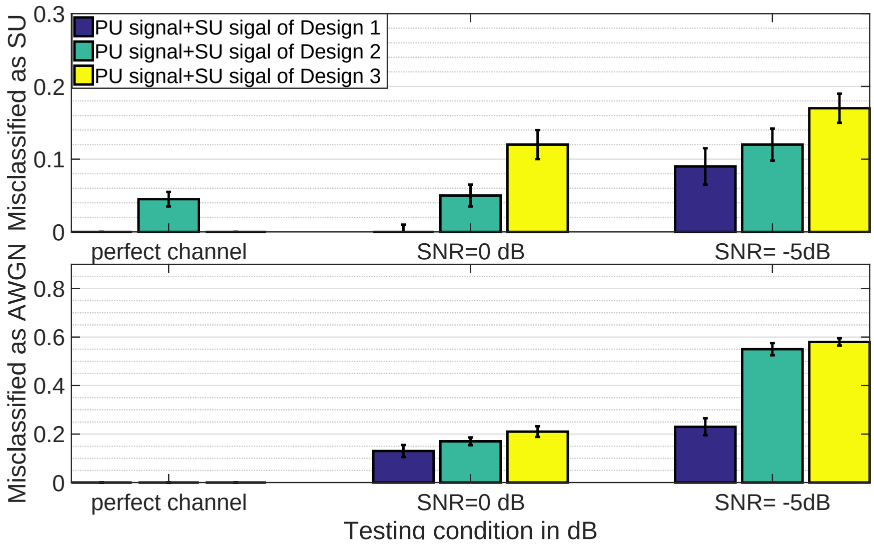

Figure 4.14: Mean and variance values of misclassification for each considered pilot number in High-R input formation.

As shown, the previous result is again proven, in that a High-R can contribute significantly to the increase of the classification/sensing performance. When processing the SCD feature plane with more pilot-induced peaks, such as a six-pilot built-in OFDM signal for powerful channel estimation ability, the High-R is subsequently recommended.

4.5.2.3 Spectrum Sensing in FD Mode

Figure 4.15 gives comparisons between the performance of the proposed method and the cyclic prefix (CP)-based detection, which utilizes cyclostationarity and conventional energy detection [75][72]. Both the p_fs of CFD and energy detection are 0.01, and INR is $20dB$ while the Rayleigh or multipath fading effect is used for the PU signal. Except for when $\chi^2 = 0$, all the other simulation conditions are considered for testing the performance under H_{10} (p_f) and H_{10} (p_d), which is the focusing point for the full-duplex mode. The complete adversarial training is applied here, which means that the training data is prepared and collected exactly according to Table 4.1. Although the detection performance decreases with the increase in χ^2, the proposed method exhibits an outstanding advantage over traditional methods. Even though the sensing accuracies decrease when χ^2 value becomes bigger, the proposed method is still able to contribute a better performance. Notice here, as stated in Table 4.1, the training data component does not contain a $\chi^2 = 0.3$ data; therefore, the performance drops greatly comparing to others. However, thanks to the anti-distortion ability of CNN, the performance can still be satisfied.

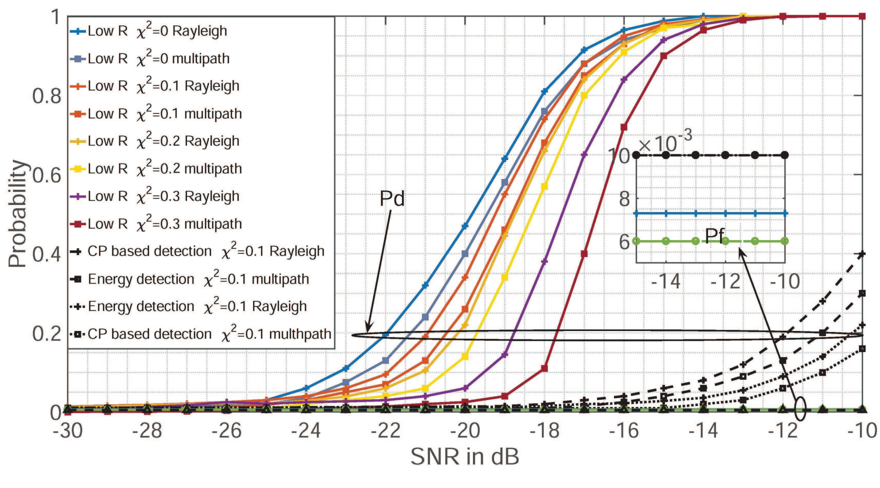

Figure 4.15: Performance comparison between the proposed Low-R input formation and CFD, energy detection under various SNR of transmission environment.

In order to test the sensing limitation of the proposed scheme, training strategies of training database under various conditions are considered, as shown in

Table 4.4. Databases A, B, C, D and E contains several components of data, for example, Database E contains Subcomponent 1 from H_{00}, Subcomponents 1 and 2 from H_{01}, Subcomponents 1-2 from H_{10} and Subcomponents 1-3 from H_{11}. The sensing results are shown in Figure 4.16. For the training database containing data with worse condition, the p_d and p_f values both rise. In another word, advantage and disadvantage both come along with new harsh training strategies, so it is not easily and precisely decided which one can present the maximum achievable performance.

Table 4.4: Training databases

<table>
<tr><th colspan="5" rowspan="2">Database</th><th rowspan="2">Class</th><th rowspan="2">Component</th><th colspan="4">Subcomponent</th></tr>
<tr><th></th><th>PU</th><th>SU (χ^2)</th><th>AWGN (in dB)</th></tr>
<tr><td rowspan="3">A</td><td rowspan="3">B</td><td rowspan="3">C</td><td rowspan="3">D</td><td rowspan="3">E</td><td rowspan="3">$\mathbf{C_0}$</td><td>1 (H_{00})</td><td>1</td><td>$\times$</td><td>$\times$</td><td>$\bigcirc$</td></tr>
<tr><td rowspan="2">2 (H_{01})</td><td>1</td><td>$\times$</td><td>0.1</td><td>INR 10</td></tr>
<tr><td>2</td><td>$\times$</td><td>0.2</td><td>INR 20</td></tr>
<tr><td rowspan="6">A</td><td rowspan="5">B</td><td rowspan="4">C</td><td rowspan="3">D</td><td rowspan="2">E</td><td rowspan="15">$\mathbf{C_1}$</td><td rowspan="6">1 (H_{10})</td><td>1</td><td>$\bigcirc$</td><td>$\times$</td><td>$\times$</td></tr>
<tr><td>2</td><td>$\bigcirc$</td><td>$\times$</td><td>SNR -10</td></tr>
<tr><td rowspan="4"></td><td>3</td><td>$\bigcirc$</td><td>$\times$</td><td>SNR -15</td></tr>
<tr><td rowspan="3"></td><td>4</td><td>$\bigcirc$</td><td>$\times$</td><td>SNR -20</td></tr>
<tr><td rowspan="2"></td><td>5</td><td>$\bigcirc$</td><td>$\times$</td><td>SNR -25</td></tr>
<tr><td></td><td>6</td><td>$\bigcirc$</td><td>$\times$</td><td>SNR -30</td></tr>
<tr><td rowspan="9">A</td><td rowspan="8">B</td><td rowspan="7">C</td><td rowspan="5">D</td><td rowspan="3">E</td><td rowspan="9">2 (H_{11})</td><td>1</td><td>$\bigcirc$</td><td>$\bigcirc$</td><td>$\times$</td></tr>
<tr><td>2</td><td>$\bigcirc$</td><td>0.1</td><td>SNR -5</td></tr>
<tr><td>3</td><td>$\bigcirc$</td><td>0.1</td><td>SNR -10</td></tr>
<tr><td rowspan="6"></td><td>4</td><td>$\bigcirc$</td><td>0.1</td><td>SNR -15</td></tr>
<tr><td>5</td><td>$\bigcirc$</td><td>0.2</td><td>SNR -15</td></tr>
<tr><td rowspan="4"></td><td>6</td><td>$\bigcirc$</td><td>0.2</td><td>SNR -20</td></tr>
<tr><td>7</td><td>$\bigcirc$</td><td>0.3</td><td>SNR -20</td></tr>
<tr><td rowspan="2"></td><td>8</td><td>$\bigcirc$</td><td>0.3</td><td>SNR -25</td></tr>
<tr><td></td><td>9</td><td>$\bigcirc$</td><td>0.3</td><td>SNR -30</td></tr>
</table>

The time complexity comparison between the proposed CNN classification and

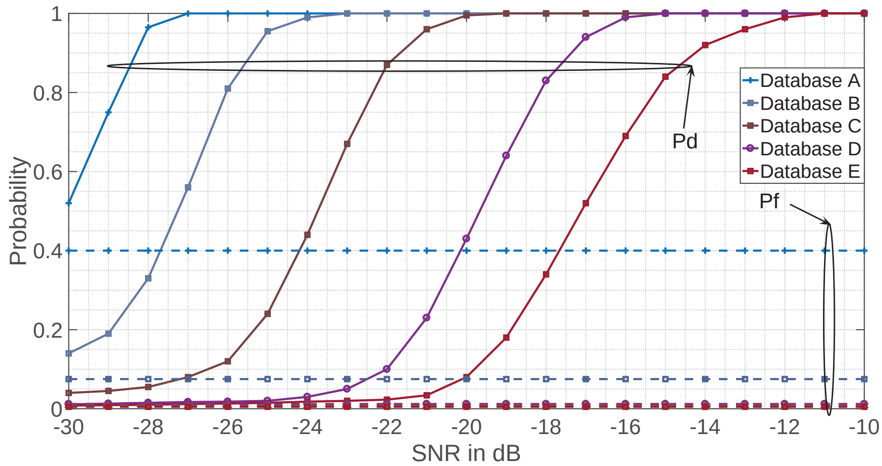

Figure 4.16: Performance comparison between the proposed Low-R input formation and CFD, energy detection under various SNR of transmission environment.

the ED as well as the CP-based detection for the FD mode is exhibited in Table 4.5. The unsatisfactory large computation cost is still present. However, the proposed scheme with the adversarial training may continue to further increase p_d; a surprisingly good detection performance may be attained by adding deeper polluted PU signal data samples to the training database. Such an excellent and robust sensing capability should be weighed greater against the time complexity for further development.

Table 4.5: Time complexity comparison with busy SU

	Proposed scheme	**Energy detection**	**CP based detection**
Time complexity	4.25×10^5 Low-R 7.59×10^5 High-R	1.60×10^3	4.50×10^4

In Figure 4.17, the comparison between the performance of High-R and Low-R are shown. The INR is 20dB and the Rayleigh or multipath fading is applied for the PU signal. The proposed adversarial training is again applied according to Table 4.1. A High-R can provide a much better sensing performance than a Low-R. A p_d of $\chi^2 = 0.2$ with High-R is even better than a perfect self-interference implemented in Low-R. Furthermore, as the χ^2 values increase, the decreasing performance rate of the High-R scheme is not as fast as that of the Low-R scheme. Therefore, when a superior sensing performance is required and large computing power can be disregarded, a High-R is highly recommended.

Then, let us focus on the channel situation of the PU transmission with a multi-path fading effect. The collected training data is difficult to truly simulate the actual transmission, since only numerable channel tap numbers can be set up to build the training database. After a satisfactory fitting is reached, even though the SCD feature is sensitive to the frequency selective fading, the immunity of image distortion and shifting of CNN as well as the excellent competence of the proposed adversarial training can help with executing the spectrum sensing and reach a high p_d value. However, the fact is that the condition of the multipath is highly dependent on the transmission environment and hard to predict. The simulation training data cannot be transferred to the actual situation testing. In this case, a mentioned two-step sensing scheme can be used; then, the multi-path fading condition will be learned by the classifier and utilized to realize the final FD sensing [63].

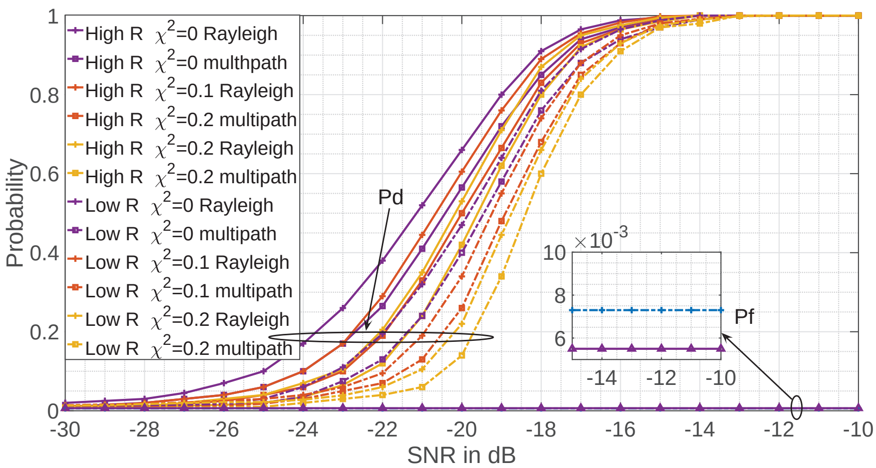

Figure 4.17: Performance comparison between Low-R and High-R input formation under various SNR of transmission environment.

4.6 Chapter Summary

This research suggests a novel SS method when the SU is equipped with FD module. The machine learning algorithm is adopted here to assist in raising the detection performance, by converting the signal recognition into classification. The prior information about the PU signal, the supervised learning is conducted with two steps: data collecting of extracting cyclostationarity plane induced by pilot structure; data processing of modifying and localizing the CNN and its corresponding adversarial training. Different input formation, as well as SU signal design, are tested to decide the most suitable set for this research. The final simulation results prove the superiority of the proposed method.

Chapter 5

Ensemble Learning Based Cooperative Spectrum Sensing

An ensemble learning (EL) framework is proposed, in this chapter, to overcome the difficulty of the OFDM signal based cooperative spectrum sensing (CSS). A local spectrum sensing scheme is achieved by considering each secondary user as a base learner, where the convolution neural networks play a role of classifier, as it does in image recognition. And a feature termed cyclic spectral correlation is used as network input. For the global decision, fusion centers learn the SU output that is obtained from the probability predictions of the PU status. This proposal shows superiority in the detection probability or false alarm probability, compared with conventional CSS methods [84].

This chapter contains following sections. Section 5.1 provides an introduction of the background and the proposed scheme. Section 5.2 explains the system model and the implementation framework of the proposed method. Section 5.3 presents the specific implementation scheme for both of the local sensing and global decision method. In Section 5.4, the local sensing performances given by the different CNN architectures is analyzed and balanced the limited computing capability at each cooperative user. Meanwhile the integrate detection performances of each proposed fusion center plans are compared with the conventional methods. Section 5.5 summarizes this chapter.

5.1 Introductions

As stated before, the spectrum sensing is able to maintain bands entitlement of the licensed (primary) user, meanwhile helps the unlicensed (secondary) user search for opportunities to access the interested bands. However, the shadowing [38] and multi-path fading [85] definitely impact on the detection performance of an non-cooperative spectrum sensing scheme. Cooperative spectrum sensing scheme, in contrast, locates multiple spatial distributed SUs [86]. Therefore, it can get rid of the hidden terminal problem. For final decision of PU's activity status, a typical CSS scheme will merge a series of local detection results which can be obtained by some of the non-CSS efficient approaches, such as energy detection [87] and cyclostationary feature detection [88]. Till date, there are two main global decision schemes: hard fusion and soft fusion. The former allow its SU makes one-bit decision of 0/1 (inactive/active PU) [89]. The latter centralized processes those estimated parameters collected from SUs [90].

It is far from new that machine learning has become quite popular in CSS. However, the unsatisfactory capability of learner or system structure [77, 89] will definitely degrade the sensing performance that is provided by CSS. Therefore, a more stereoscopic and cyber structure for CSS should be considered. It must require an efficient processor as each SU and a sound network to connect and bound them to realize a spectrum sensing system with high performance. It comes naturally that ensemble learning can be relied on as a modification of machine learning to compensate the mentioned defectiveness. In [91], a strong learner is formed by an integration of weak learners by certain ensemble strategy.

On one hand, it is suitable to consider the SUs as weak learners when used to predict the probability of PU activity status. On the other hand, the convolution neural network, constrained by simple structure, can be adopted locally due to its fine image processing ability. In [92], bagging-strategy formed databases were used for the CNN training. [55] input the cyclostationary feature plane induced by pilots tones to aid learning process. A particular ensemble strategy can achieve the FC, e.g. another learner of the full connected neural network can make the global decision from EL [93]. Both a hard fusion and semi-soft fusion can be performed by inputting the classification prediction of PU status given by softmax regression.

5.2 System Model and Framework

5.2.1 System Fundament of CSS

An OFDM signal based CSS scheme is proposed by this article. We assume that a spectrum channel which belonged to one PU has been temporarily allocated to a cooperative system. The PU alternates between active and inactive states.

The centralized CSS network contains M SUs, where $i = 1, ..., M$. For each SU, its status can be considered as an effective binary hypothesis, which is

$$\begin{aligned} &\mathrm{H}_0 : x_i = n, \qquad \text{Inactive PU} \\ &\mathrm{H}_1 : x_i = p + n, \quad \text{Active PU} \end{aligned} \tag{5.1}$$

Here, n represents the sampling index, p denotes the transmitted signal from PU. x denotes the received signal at one SU end. And n denotes the additive white Gaussian noise. After the local sensing decision of each SU is made, the FC will use those decisions to make the global decision according to certain combination rule. In Figure 5.1, the system model is given.

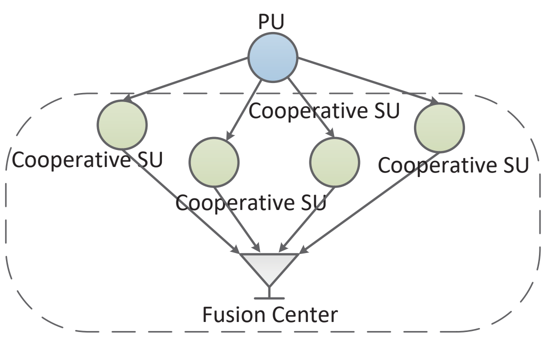

Figure 5.1: Cooperative spectrum sensing system model.

5.2.2 Framework of proposed CSS scheme

5.2.2.1 Ensemble Learning

EL combines the outputs of a collection of base/weak learners to improve a prediction. Specifically, EL can be built by altering algorithms of a set of learners or altering learners of the same algorithm. Either way, overlapped datasets or independent databases will be learned respectively. Although the prediction of each single learner is biased, those biased prediction can be calibrated by an "ensemble" strategy.

5.2.2.2 Establishment of proposed CSS scheme

As we mentioned above, the advantage of CR system is that it can integrate the decision results of each SU, and then calculate the global decision results according to a certain weight. EL also has a similar mechanism, that is, each weak learner is combined based on a certain strategy to form a strong learner to give the final decision. The commonness of the two impels us to implement EL in CSS. Therefore, the advantages of the former can be translated into the improvement of the latter in detection performance.

The proposed EL based CSS scheme is depicted in Figure 5.2.

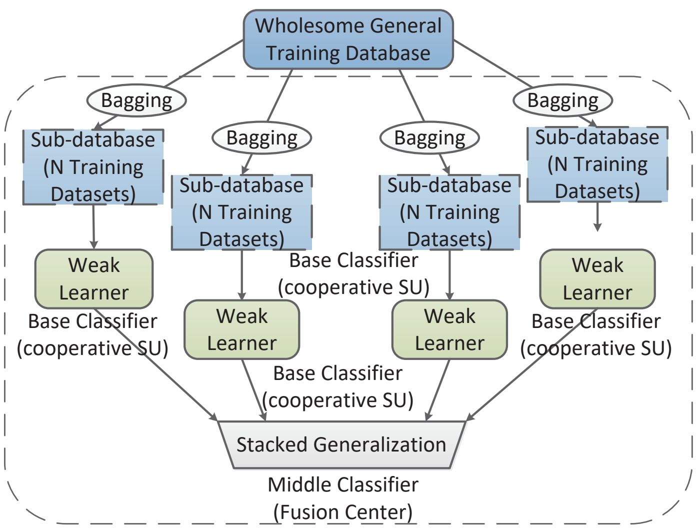

Figure 5.2: Cooperative spectrum sensing system model.

Although the strength of each SU in CSS will be compensated and corrected, we prefer to choose a relatively good SU in the selection process of weak learners. Since CNN has been proven to be able to be used by CR systems, we can use it as a weak learner to improve accuracy. Furthermore, since the base learner has to classify inactive and active PU before study, apparently the base learner is acting as a weak/base classifier. Figure 5.2 shows that using sub-databases independently, the bagging strategy in EL improves the accuracy by training each weak learner. In this proposal, the training database is built in advance, and then a fixed predetermined number of datasets is randomly extracted to form a series of sub-databases for classifier training. In fusion center, hard fusion and semi-soft fusion schemes are considered. The stacking strategy combines all the predictions of the other learners to make a final decision.

In this chapter, for the above stacked generalization scheme, a full connected neural network is used. And the final decision is made by this full connected neural network as well.

5.3 Scheme of proposed CSS

5.3.1 Local Sensing - Classification to Spectrum Sensing

In the El based CSS, the probability perditions of PU's statuses which are sent from each SU learner is required by FC for the global decision. Firstly, to better understand this scheme, the concept of signal classification should replace the term–local detection. According to Equation (5.1), H_0 and H_1 are treated as two categories to state the PU as: C_0: PU is inactive; C_1: PU is active. Then, as for the final classification outputs, on one hand, when performing a hard fusion, the classification decision of C_0 or C_1 will be sent to the fusion center including the information of 0/1; on the other hand, when performing a semi-soft fusion center, the probability predictions of the classification of C_0 or C_1 will be reported to the fusion center, where the probability sum of two classes equals 1.

5.3.1.1 Data Collection

As we mentioned in Chapter 2, OFDM signals include a preamble, framed data packages and inserted pilot tones. Therefore, the OFDM signal has a powerful anti-multi-path ability. Naturally, for supervised feature extraction machine learning, PU can provide usable features as input to classifiers.

Generally speaking, if the data on the individual sub-carriers are random, the spectral correlation is expected to be zero. However, we can rely on the spectral relationship of built-in pilot tones. When the correlated data is transmitted in parallel on the subcarriers, signal detection and identification can be achieved due to the spectral feature contributions to the cyclic signature.

One can realize statistical spectrum analysis by decomposing a signal into sinusoidal waveforms. The relationship between the cyclic spectral analysis and the second-order unearthly expression can be established. Assuming that we have a signal $x(t)$ which is second order periodical. Then the cyclic correlation spectral periodogram which is a crucial expression to measure its spectral correlation is given by

$$S^{\alpha}_{X_T}(f) = \left[X_T\left(t, f + \frac{\alpha}{2}\right) \cdot X^*_T\left(t, f - \frac{\alpha}{2}\right)\right]/T, \tag{5.2}$$

with frequency $f + \alpha/2$, $f - \alpha/2$, where f is coordinates spectral location (shift center). α is spectral separation (shift amount). Then, we can define the spectral coherence density as :

$$S^{\alpha}_{X_T}(f)_{\Delta t} = \frac{1}{\Delta t}\int_{-\Delta t/2}^{\Delta t/2} \frac{1}{T} X_T\left(t, f + \frac{\alpha}{2}\right)^* X^*_T\left(t, f - \frac{\alpha}{2}\right) dt, \tag{5.3}$$

where X_T is the local spectral representation as:

$$X_T(u, v) = \int_{u-T/2}^{u+T/2} x(t)^* e^{-i2vft} dt. \tag{5.4}$$

According to equations above, second-order cyclic spectral correlation feature can be visualized by plotting the SCD over the bi-frequency plane (with f and α), which can be considered as expert feature for classification. The problem of PU detection of OFDM signal is replaced by a task of image classification on SCD plane.

5.3.1.2 Base Learner of CNN

In EL based CSS, regarding the selection of the local classifier or PU-detector, one should be more concerned about the contribution of valuable information rather than an potent classification capacity.

Similar to conventional image recognition tasks, image preprocessing of SCD of OFDM signal, is necessary. As a deep forward network, CNN is widely used in image field. In order to simplify the preprocessing process, we redesigned the CNN into a variation version. Specifically, individual units only respond to a local region, where units overlap partially, thus ensuring coverage of the entire input field.

Supervised learning requires training input database to train the network, so as to determine network parameters. At the same time, we need a testing input database to test the network performance. The network input data forms a feature plane of SCD, which can be expressed as:

$$\mathbf{x}_b = [x_{i,j}, ..., x_{F,A}], i \in [i, F], j \in [i, A], b \in [i, B], \tag{5.5}$$

where b denotes the index of dataset in the training/testing database, and F express the total pixel resolution of SCD feature plane. After convolution and pooling of SCD features, the output is as:

$$\mathbf{o}_l = pool\left(\sigma\left(\mathbf{w}_l^v \cdot \mathbf{o}_{l-1} + \mathbf{b}_l^v\right)\right), v \in [1, c_l], l \in [1, L-1] \tag{5.6}$$

where we assume $\mathbf{o}_0 = \mathbf{x}_b$, L is the layer number of the CNN structure. c denotes the number of convolutional filters. w denotes the weight in each layer, and b denotes the bias parameters in each layer. σ is a non-linear function known as the activation function. A manageable and measurable data range can be mapped to from the input of network. Then, the final output is expressed as:

$$\mathbf{y}_b = \mathbf{w}_f(f(pool\left(\sigma\left(\mathbf{w}_l^v \cdot \mathbf{o}_{l-1} + \mathbf{b}_l^v\right)\right))) + \mathbf{w_f}, b \in [i, B], \tag{5.7}$$

where f denotes a linear function for the concatenation process including $\mathbf{w}_f$ and $\mathbf{w_f}$. The former denotes the weight parameters and the latter denotes bias parameters of the full connection layers.

The softmax regression is, finally, used for the class-predicting layer. The softmax regression is a kind of activation function that considers the posterior probability to quantity classification confidence, as

$$\Psi_\theta(\mathbf{y}_b) = \frac{e^{\theta_i \mathbf{y}^i}}{\sum_K e^{\theta_i \mathbf{y}^k}}, \tag{5.8}$$

where y_i represents the label predictions of each class $i = 1, 2, ..., K$, (we have $K = 2$ here because only two classes are considered). θ can be optimized in the gradient descent by minimizing the cost function. Normally, the output of the entire network will be the classification prediction of C_0 and C_1, which will be considered as the hard fusion for all the base learner has already made its own final decision. However, thanks to the characteristic of the softmax layer, the local classifier can also export a in-process set of value, i.e. the probability predictions of C_0 and C_1, and send to the fusion center. Such local report scheme of providing a comparatively soft decision can contribute to a better performance.

At the same time, we need to emphasize that we need not excessively pursue the accuracy of the classifier, but consider the limited computing power of the equipment in practical application. Therefore, on the premise of guaranteeing the performance, we should simplify the network structure as much as possible to improve the realizability of the system.

5.3.2 Global Decision-Stacking to Fusion Center

5.3.2.1 Hard Fusion center

For each secondary user, it detects the status of the interested channel independently, which means the received signal is different from each other. Meanwhile, considering the utilization of the bagging strategy to train the local classifier, this leads different CNN model for each classifier. Each local sensor of the CNN performs a complete sensing process using the unique received data and classifier model, and makes its own decision of either C_0 or C_1. One bit of information, i.e. 0 or 1 is fed back to the FC, as the same as the conventional hard fusion.

Unlike the powerful process capability required for the image data in local sensing, the middle classifier requires to process a small number of datasets. The full connected neural network is applied as the middle classifier to process the report data, due to the comparatively simple formation of the local report. Even though the reporting scheme is rigid, the final decision made by the center still can be expected to be satisfying.

5.3.2.2 Semi-soft Fusion center

The same as the hard fusion scheme, the model of the base classifier and the received data are still different and a set of independent local decisions can still be made. However in this time, since the classification results can be exhibited as the probability predictions for C_0 and C_1, FC are fed by outputs of the SU local sensing information and makes a semi-soft global decision. The term "semi-" is used here because each SU reports mild version of the output that the classifier should give. It is neither a hard "0 or 1" classification decision nor some estimated parameters as in common soft fusion.

As mentioned above, a machine learning is required to achieve the stacking generalization strategy and integrate the local outputs.

To meet this requirement, a full connected neural network is adopted once more as a middle classifier which gives the C_0 or C_1 classification decision. Notice that, since each SU only reports two probability values to the FC, only a small number of collected data is needed to be processed through the middle classifier unlike the analysis of the SCD plane. Therefore, a fully connected network can achieve high performance while avoiding unrealistic computational requirements to the FC. The stacking strategy combining with the CNN is shown in Figure 5.3.

5.4 Result Evaluations

5.4.1 Simulation and Training Setup

5.4.1.1 Experimental Parameters

In this study, we assume that there is a single PU that transmits OFDM signals according to the 802.11g protocol with 16QAM. At the same time, there are

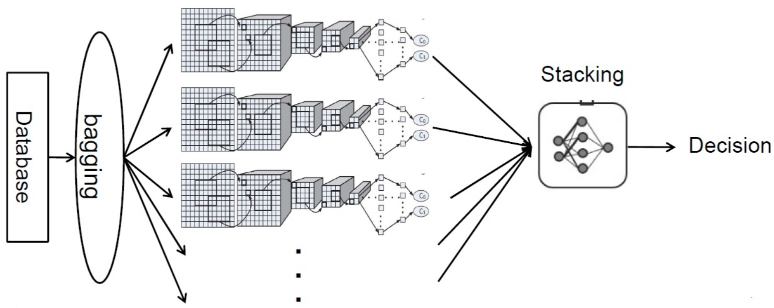

Figure 5.3: The stacking generalization.

multiple SUs with fixed positions, which perceive the state of PU in AWGN environment and send the results to FC without error, thus forming a CSS system. In order to investigate the relationship between SU number and performance, we tried several different SU number configurations.

The hardware environment is with a 3.20 GHz Intel Core i7-6900K CPU and Nvidia GeForce GTX 1080 GPU. Simulations software is MATLAB R2016b on a 64-bit Windows operating system. Relu activation function and average pooling layers are used for CNN structure, which contains several dense full connection layers with Relu activation function. The softmax layer is built in the end to provide C_0 and C_1 probability predictions. The batch size is 100, and the learning rate is 0.01 In order to make the results more valuable, we investigated the performance of several different structures of SU classifiers. Details are given later.

5.4.1.2 Training Process

Notice, only one OFDM symbol is used for the SCD-plane, which could help each SU to save sensing time and make near real-time decision. It should be emphasized that the input SCD feature is only a 64×64 pixel image, so the computational load of the system is very small. Under low such resolution, the deep CNN for high efficient image processing instead of simple full connected network, is indispensable to obtain and analyze the hyper-connection between each pixel.

Then we need to prepare two wholesome general training databases who share the same structure. The first is for training SU classifiers, and the second is for middle training the FC classifier.

In both wholesome general training databases, the C_0 and C_1 classes both have 100,000 mentioned input datasets for their own learning.

However, in order to find a balance between accuracy and computational complexity, all cooperative weights are equal, and all training data are derived from random extraction of the general training database. The extracted sub-databases have the same size of: 10,000 for C_0 and 10,000 for C_1. Notice that, the training database for C_1 is not pure but polluted by Gaussian noise (SNR $= -10$dB) to improve the robustness of classification.

The training flow is as follows:

1. to decide the parameters of CNN structure, extract sub-databases from the 1st general training database and use individual sub-database to train corresponding SU classifier;
2. testify the classification performance of trained base learners using the 2nd general training database;
3. collect training results and train FC to determine the structure;
4. The entire architecture of proposed method is fully decided. Perform overall performance evaluation using test databases.

After observation, each SU feedback its sensing prediction to the FC and the input of the base classifier only transforms from only one OFDM modulation signal. Regarding the report size, for the hard fusion scheme, only one bit of information is sent to the center. Assume CSS includes M SUs, the middle data has M dimensions; for the semi-soft fusion scheme, information of the probability prediction of the classification is sent to the center. Assume CSS includes M SUs, the middle data has $M \times 2$ dimensions. These two types of data are used to then train the middle classifier.

In order to better evaluate the system performance, 5,000 datasets were tested under each SNR.

5.4.2 Results Analysis

We tested three CNN architectures of local base classifiers to gain insight into the relationship between local sensing and the global decision. The parameters are shown in Table 5.1.

Table 5.1: three CNN architectures

Architecture	**Time Complexity**	**Structure**
1	1.27×10^6	1 convolution layer (3*3) 1 pooling layer 1 full connection layer
2	1.74×10^6	1 convolution layer (5*5) 1 pooling layer 1 full connection layer
3	4.29×10^6	2 convolution layer 2 pooling layer 1 full connection layer

Notice that, the local sensing performance curves in Figure 5.4 are obtained when each SU classifier gives a final hard classification decision of 0 or 1 when the entire classification process is completed. As is shown in Figure 5.4, with the increasing complexity of structure, the training fitting degree of classifier increases, resulting in the ascent of the local p_d and the descent of the local p_f.

Firstly, let us on the hard fusion center. As is shown in Figure 5.5, in the same trend with the local sensing result, architecture 3 shows the highest p_d since it combines base CNN classifiers. However, a trade-off has to be made to balance the local computation complexity with the sensing performance. Moreover, all three curves drop to low p_d no matter how they behave in the local sensing. It means that the ability of stacking strategies to compensate for performance deficiencies in underlying classifiers is limited.

Figure 5.6 shows performance variation curves of p_d and p_f. To better evaluate proposed method, a comparison with FC based cyclostationary feature detection

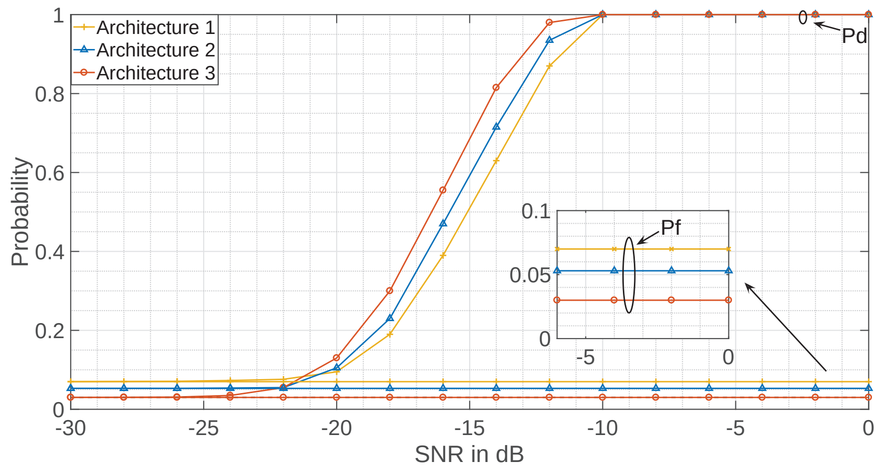

Figure 5.4: Local sensing performance comparison of p_d and p_f. The SUs number $M = 4$.

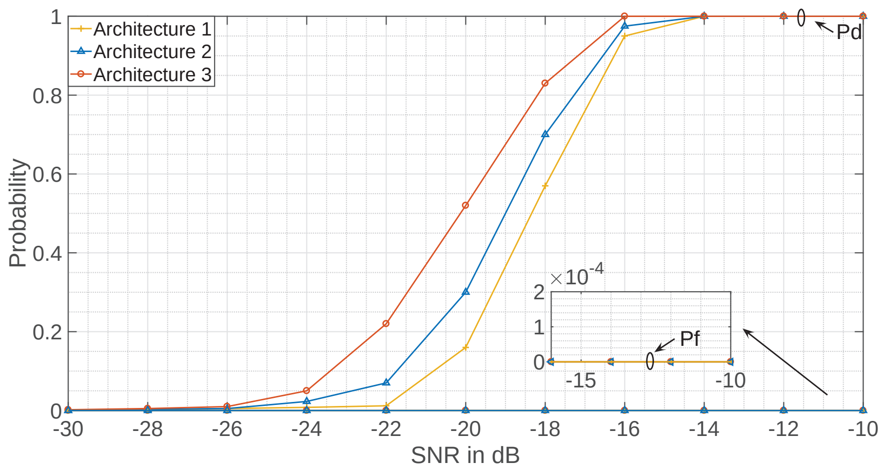

Figure 5.5: Global sensing performance comparison of p_d and p_f variation curve for different base classifier architectures in hard fusion scheme. The SUs number M is 4.

and FC based energy detection are exhibited where $p_f = 0.001$. In order to prove the superiority and promise of this research, the architecture with the poorest performance, Architecture 1 is used for the comparison.

If we pay attention to the p_d curves, we can find that the performance of the energy detection method cannot meet the detection requirements under low signal-to-noise ratio. The performance of cyclostationary feature detection is

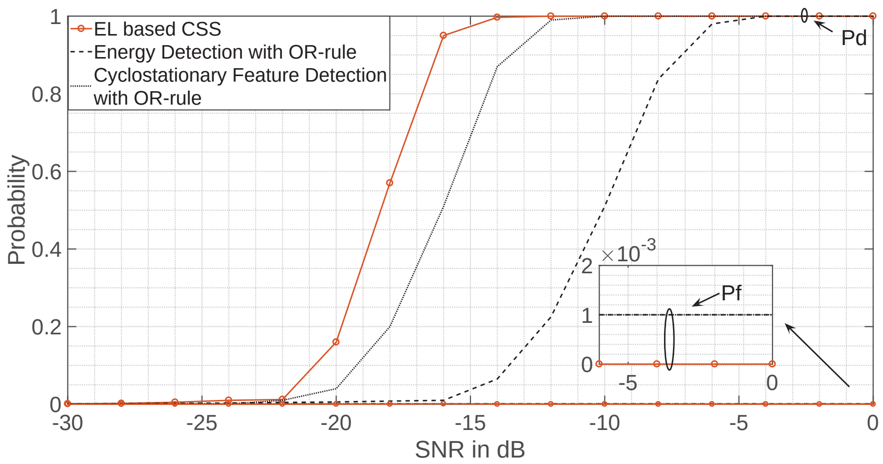

Figure 5.6: General performance comparison of p_d and p_f variation curve with the conventional sensing methods in hard fusion scheme. The SUs number M is 4.

much better. This is due to the robustness of the efficient cyclic spectral feature. Therefore, this paper also makes use of the cyclic spectral feature. However, the performance of the proposed method is better than that of the conventional cyclostationary feature method, which is attributed to the ensemble learning structure and superior strategies. For the p_f curves, although the false alarm of the conventional methods are very low, the proposed method can further reduce the false alarm probability to0.00005 for the hard FC. This excellent false alarm performance is attributed to the stacking strategy in the FC, where adequate training samples ensure the fitting performance of the system. Although the ROC curves are commonly used to evaluate the system performance in spectrum sensing studies, p_fs in the proposed scheme can only be provided by the training process and cannot be set randomly as one may be needed. It means once the training database and execution are determined, one can only expect p_f naturally given by the fitting training result, i.e., the misclassification proportion. The network and the training database can be further refined to get lower p_f value, however since the nonlinear mapping is included in the CNN for each training, p_f is hard to calculate in a common method.

Finally, the performance comparison of the proposed method under different SU numbers is shown in Figure 5.7. Apparently, when the number of cooperative SUs increases from 4 to 32, the p_d continues to rise. This is because the increase in the number of SUs enhances the dimension of the input data of the middle classifier, thus carrying more signal features and allows a better learning. However, when the number of SUs exceeds 32, the performance basically does not change. This is because the improvement of data dimension cannot provide more signal features. Therefore, when CSS contains a large number of SUs, splitting SUs into groups may further improve performance.

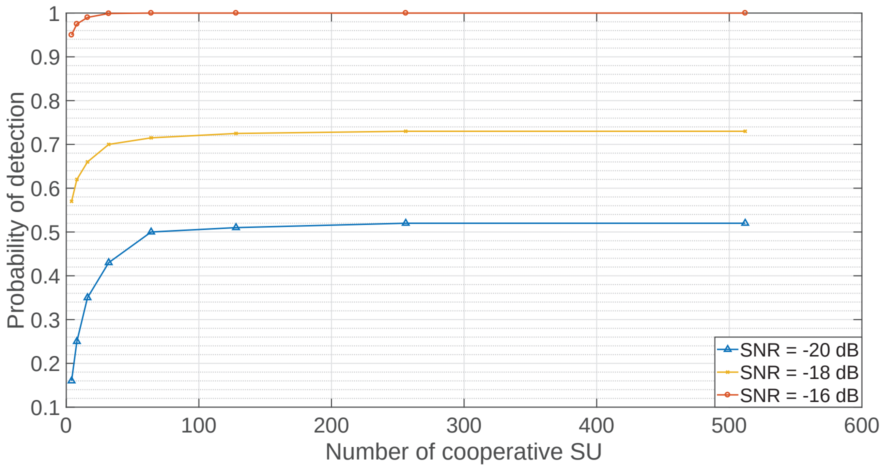

Figure 5.7: Performance comparison of p_d variation curve for different numbers of SUs where Ms equal 4, 8, 16, 32, 64 and 128, respectively.

Then, turn our eyes to the semi-soft fusion center. As is shown in Figure 5.8, still, architecture 3 shows the highest p_d since it combines base CNN classifiers. However, a trade-off has to be made to balance the local computation complexity with the sensing performance. Moreover, all three curves drop to low p_d no matter how they behave in the local sensing. It means that the ability of stacking strategies to compensate for performance deficiencies in underlying classifiers is limited.

Figure 5.9 shows performance variation curves of p_d and p_f. To better evaluate proposed method, a comparison with FC based cyclostationary feature detection and FC based energy detection are exhibited where $p_f = 0.001$. In addition, to reveal the advantage of the semi-soft strategy, the evaluation also compares it with a hard FC of the same stacking classifier structure, where the reported results from SUs are simply 0 or 1.

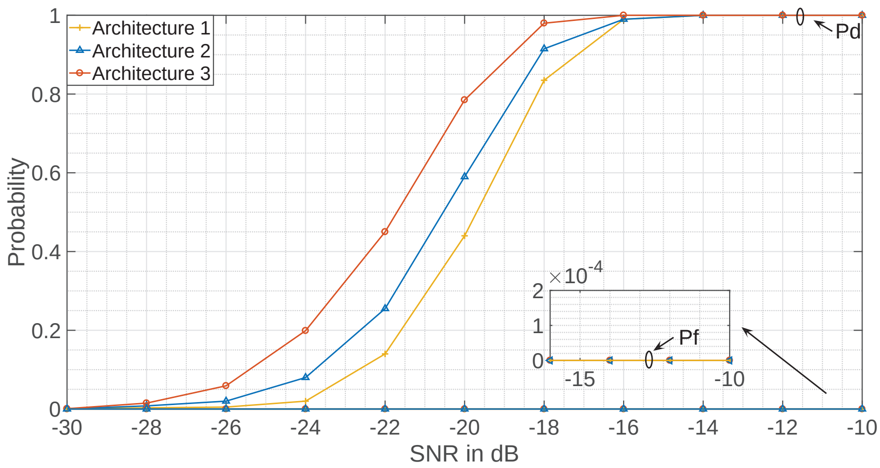

Figure 5.8: Global sensing performance comparison of p_d and p_f variation curve for different base classifier architectures in semi-soft fusion scheme. The SUs number M is 4.

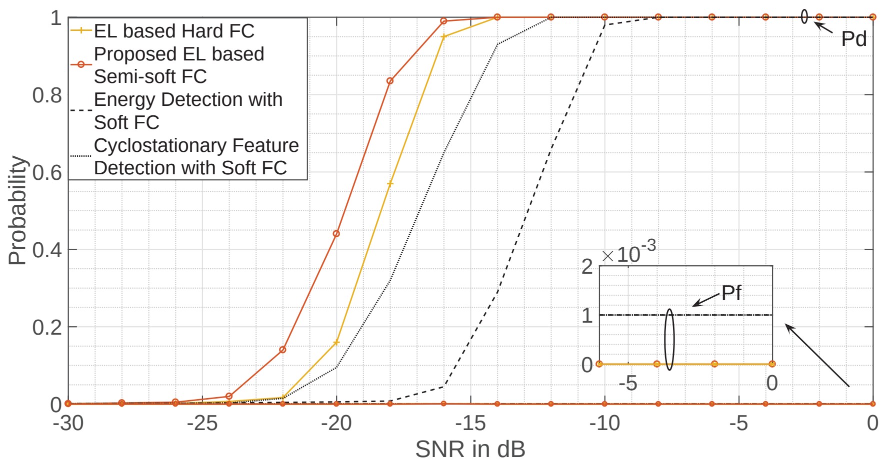

Figure 5.9: General performance comparison of p_d and p_f variation curve with the conventional sensing methods in semi-soft fusion scheme. The SUs number M is 4.

As the hard fusion scheme, if we pay attention to the p_d curves, we can find that the performance of energy detection method cannot meet the detection requirements under low signal-to-noise ratio. The performance of cyclostationary feature detection is much better. This is due to the robustness of the efficient cyclic spectral feature. Therefore, this paper also makes use of the cyclic spectral feature. However, the performance of the proposed method is better than that of the conventional cyclostationary feature method, which is attributed to the ensemble learning structure and superior strategies. In addition, our proposed CSS with semi-soft FC can provide the best detection performance with the additional help of the mild decision-making scheme. Besides of the generally better performance, the downtrend is more moderate against the hard FC methods, and it ensures a higher p_d at low SNR values where specifically the proposed method is 25% better at SNR of -20 dB.

For the p_f curves, although the false alarm of the conventional methods are very low, the proposed method can further reduce the false alarm probability to0.00005 for the hard FC and 0.000075 for the semi-soft FC from the middle training results. This excellent false alarm performance is attributed to the stacking strategy in the FC, where adequate training samples ensure the fitting performance of the system.

Then this research considers more complicated condition for PU transmission: the training sample are collected not only under AWGN but also Rayleigh effect, while the testing data is in the same condition. Figure 5.10 show that even the performances of the conventional sensing methods is high degraded under the Rayleigh effect, the proposed method can still provide a satisfactory sensing ability owing to the adversarial training.

Finally, the performance comparison of the proposed method under different SU numbers is shown in Figure 5.11. Apparently, when the number of cooperative SUs increases from 4 to 32, the p_d continues to rise. This is because the increase in the number of SUs enhances the dimension of the input data of the middle classifier, thus carrying more signal features and allows a better learning. However, when the number of SUs exceeds 32, the performance basically does not change. This is because the improvement of data dimension cannot provide more signal features. Therefore, when CSS contains a large number of SUs, splitting SUs into groups may further improve performance.

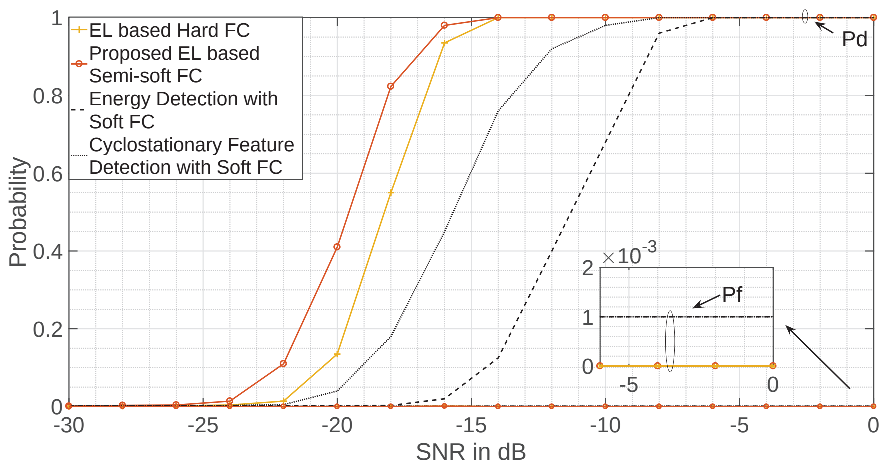

Figure 5.10: General performance comparison of p_d and p_f variation curve with the conventional sensing methods in semi-soft fusion scheme. The SUs number M is 4. The PU transmission is under Rayleigh effect.

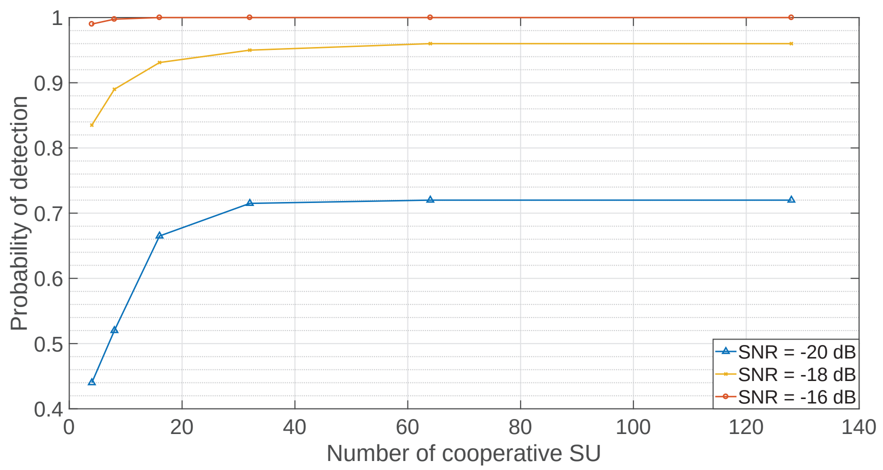

Figure 5.11: Performance comparison of p_d variation curve for different numbers of SUs where Ms equal 4, 8, 16, 32, 64 and 128, respectively.

5.5 Chapter Summary

In this study, a novel ensemble learning based CSS method is proposed. Both hard and semi-soft FCs are considered. The EL model is used for cooperative SU and FC respectively, and the final decision comes from the integration result. The local sensing scheme is transformed into a signal classification based on CNN deep network and cyclic spectral correlation feature. The bagging strategy is also adopted to build the training database. The semi-soft FC integrates the reported predictions to make the global decision. The results show that the proposed method has obvious advantages over traditional methods in terms of p_d and p_f. In addition, increasing the number and complexity of SU can further improve the detection performance of the proposed method.

Chapter 6

Conclusion

This chapter summarizes the research work on applying the machine learning into the spectrum sensing system. The contributions and discussions of two proposed schemes, i.e., "full-duplex spectrum sensing using convolutional neural network" and "ensemble learning based cooperative spectrum sensing" is provided first. Then the directions for related future work is presented at the end.

6.1 Contribution and Discussion

The cognitive radio is inspired by cognition cycle to minimize the burden in terms of the spectrum efficiency. It can observe and understand its operating environment, make an in-place decision based on observations and experiences, and perform a reasonable adjustment. The CR helps secondary user recycle and reuse the vacant spectrum channels, while the primary user possesses entitlement of spectrum channels. The spectrum sensing operating from the PHY layer performs an inspection to confirm whether some or all of the frequency band resource is free. According to the sensed results, the secondary user adjusts its radio parameters to be able to access these free spectrum bands to complete its own transmission. In this dissertation, the basic idea is to invite the machine learning to assist the spectrum sensing, and built the intelligent sensing scheme. The reasons are: on one hand, there are some problems of uncertainty of the signal, noise and channel, external or inner interference, spectrum mobility, etc. resulting in problems of requiring for high sensibility for signal recognition, hidden terminal, inaccurate estimation of parameters, high false alarm, difficulty of spectrum hand-off, etc.; on the other hand, there is a similarity between the artificial intelligence with cognitive radio since both of them obtain knowledge and comprehension by perception, learning, reasoning to problem-solving automatically.

Firstly, this research suggests a novel SS method when the SU is equipped with FD module. A machine learning algorithm is adopted here to assist in raising the detection performance, by converting the signal recognition into classification. The prior information about the PU signal, the supervised learning is conducted with two steps: data collecting of extracting cyclostationarity plane induced by pilot structure; data processing of modifying and localizing the CNN and its corresponding adversarial training. Different input formation, as well as SU signal design, are tested to decide the most suitable set for this research. The final simulation results prove the superiority of the proposed method.

Secondly, an ensemble learning based CSS method is proposed. Each SU perform its own local sensing and gives elementary sensing results using a simplified CNN network for its ability in image processing. A full connected neural network performs the combination task and acting as the FC to integrate reports from all the secondary users and upgrade performance by strong integrate capability. The bagging strategy is adopted for the establishment of the local training database to generalize each classifier model of the weak learner. The semi-soft FC integrates the reported predictions to make the global decision. The results show that the proposed method has obvious advantages over traditional methods in terms of p_d and p_f. In addition, increasing the number and complexity of SU can further improve the detection performance of the proposed method.

6.2 Function Extensions

With the continuous improvement of computer processing power and the latest developments in the field of cloud storage, the science fiction concept of artificial intelligence is becoming an attractive reality. Many industries are currently exploring how to make better use of artificial intelligence, and the wireless communications industry is no exception. Artificial intelligence is often compared to the "brain", while communication carries the role of "brain stem", like the brain stem controls the movement of people's breathing, heartbeat, etc. Communication also supports the transmission of data and the normality of various types of artificial intelligence hardware. Operation. At the same time, communication itself is one of the industries that have been transformed by artificial intelligence.

Recent survives in the wireless communications industry, there is a strong desire to start implementing artificial intelligence solutions, but the industry has not reached a consensus on the best path to apply artificial intelligence). From network management to predictive maintenance, there are some fledgling AI application cases, but one has to admit that the wireless communications industry faces many challenges in adopting AI. It offers unparalleled opportunities in two broad categories: network management and operations, and customer focus. Clearly, network management actually has many possible requirements that can benefit from artificial intelligence solutions to cope with the rapidly expanding number of connected devices and users. Even the customer-oriented communications service providers terminal services can benefit greatly from artificial intelligence technology, as customers will increasingly need personalized services.

The form of the communication network will be decentralized, no longer have complex levels. And it can modify, self-heal, and process large amounts of data in parallel. Technological innovations are bound to drive the transformation of wireless communications. For a long time in the past, communication operators have continued a relatively simple business model. After the completion of the artificial intelligence transformation, operators are likely to turn to provide data services for all walks of life. After all, communication operators are sitting in the gold mine of big data. The massive sensors in the Internet of Things era are the source of massive data. Using user data to improve services, using network data to improve operation and maintenance, and using data to support innovation will be The trend of the times. Moreover, in the 5G network, the huge investment in infrastructure construction and the decline in network revenue are suddenly contradictory. In other words, to solve such contradictions, artificial intelligence and data services are inevitable choices. Dealing with large-scale data is precisely inseparable from artificial intelligence.

References

[1] Joseph Mitola, Gerald Q Maguire, et al. Cognitive radio: Making software radios more personal. *IEEE Personal Communications*, 6(4):13–18, 1999. 2

[2] Federal Communications Commission et al. Notice of proposed rule making and order: Facilitating opportunities for flexible, efficient, and reliable spectrum use employing cognitive radio technologies. *ET Docket*, (03-108):73, 2005. 2

[3] Hongjian Sun, Arumugam Nallanathan, Cheng-Xiang Wang, and Yunfei Chen. Wideband spectrum sensing for cognitive radio networks: A survey. *IEEE Wireless Communications*, 20(2):74–81, 2013. 3

[4] Erik Axell, Geert Leus, Erik G Larsson, and H Vincent Poor. Spectrum sensing for cognitive radio: State-of-the-art and recent advances. *IEEE Signal Process. Mag.*, 29(3):101–116, 2012. 3

[5] Tevfik Yucek and Huseyin Arslan. A survey of spectrum sensing algorithms for cognitive radio applications. *IEEE Communications Surveys and Tutorials*, 11(1):116–130, 2009. 3

[6] Yonghong Zeng, Ying-Chang Liang, Anh Tuan Hoang, and Rui Zhang. A review on spectrum sensing for cognitive radio: challenges and solutions. *EURASIP Journal on Advances in Signal Processing*, 2010(1):381465, 2010. 3

[7] Kishor Patil, Ramjee Prasad, and Knud Skouby. A survey of worldwide spectrum occupancy measurement campaigns for cognitive radio. In *International Conference on Devices and Communications, 2011 (ICDeCom)*, 2011. 4

[8] Shree Krishna Sharma, Tadilo Endeshaw Bogale, Symeon Chatzinotas, Björn Ottersten, Long Bao Le, and Xianbin Wang. Cognitive radio techniques under practical imperfections: A survey. *IEEE Communications Surveys and Tutorials*, 17(4):1858–1884, 2015. 4, 6, 16

[9] Ian F Akyildiz, Won-Yeol Lee, Mehmet C Vuran, and Shantidev Mohanty. A survey on spectrum management in cognitive radio networks. 2008. 4, 33

[10] Jianfeng Wang, Monisha Ghosh, and Kiran S. Challapali. Emerging cognitive radio applications: A survey. *IEEE Communications Magazine*, 49(3):74–81, 2011. 4

[11] Beibei Wang and K J R Liu. Advances in cognitive radio networks: A survey. *IEEE Journal of Selected Topics in Signal Processing*, 5(1):5–23, 2011. 4, 6

[12] Moshe Timothy Masonta, Mjumo Mzyece, and Ntsibane Ntlatlapa. Spectrum decision in cognitive radio networks: A survey. *IEEE Communications Surveys and Tutorials*, 15(3):1088–1107, 2013. 4

[13] Antonio De Domenico, Emilio Calvanese Strinati, and Maria-Gabriella Di Benedetto. A survey on mac strategies for cognitive radio networks. *IEEE Communications Surveys and Tutorials*, 14(1):21–44, 2012. 4

[14] K. Ben Letaief and Wei Zhang. Cooperative communications for cognitive radio networks. *Proceedings of the IEEE*, 97(5):878–893, 2009. 6

[15] Tevfik Ycek and Hseyin Arslan. A survey of spectrum sensing algorithms for cognitive radio applications. *IEEE Communications Surveys and Tutorials*, 11(1):116–130, 2009. 6

[16] Simon Haykin, David J. Thomson, and Jeffrey H. Reed. Spectrum sensing for cognitive radio. *Proceedings of the IEEE*, 97(5):849–877, 2009. 6, 64

[17] Yonghong Zeng and Ying-Chang Liang. Covariance based signal detections for cognitive radio. In *IEEE 2nd International Symposium on New Frontiers in Dynamic Spectrum Access Networks, 2007*, pages 202–207, 2007. 6

[18] Jun Ma, Geoffrey Ye Li, and Biing Hwang Juang. Signal processing in cognitive radio. *Proceedings of the IEEE*, 97(5):805–823, 2009. 6

[19] Wei Zhang, Ranjan K. Mallik, and Khaled Ben Letaief. Optimization of cooperative spectrum sensing with energy detection in cognitive radio networks. *IEEE Transactions on Wireless Communications*, 8(12):5761–5766, 2009. 6

[20] J. Lunden, V. Koivunen, A. Huttunen, and H.V. Poor. Collaborative cyclostationary spectrum sensing for cognitive radio systems. *IEEE Transactions on Signal Processing*, 57(11):4182–4195, 2009. 6

[21] Amod V. Dandawate and Georgios B. Giannakis. Statistical tests for presence of cyclostationarity. *IEEE Transactions on Signal Processing*, 42(9):2355–2369, 1994. 6

[22] Changlai Du, Huacheng Zeng, Wenjing Lou, and Y Thomas Hou. On cyclostationary analysis of wifi signals for direction estimation. In *IEEE International Conference on Communications, 2015 (ICC '15)*, pages 3557–3561, 2015. 6, 29

[23] Yoshua Bengio, Aaron Courville, and Pascal Vincent. Representation learning: A review and new perspectives. *IEEE Transactions on Pattern Analysis and Machine Intelligence*, 35(8):1798–1828, 2013. 6

[24] G. Ganesan and Li Ye. Cooperative spectrum sensing in cognitive radio, part ii: multiuser networks. *IEEE Transactions on Wireless Communications*, 6(6):2214–2222, 2007. 7

[25] Matteo Gandetto and Carlo S. Regazzoni. Spectrum sensing: A distributed approach for cognitive terminals. *IEEE Journal on Selected Areas in Communications*, 25(3):546–557, 2007. 7

[26] Jayakrishnan Unnikrishnan and Venugopal Varadachari Veeravalli. Cooperative sensing for primary detection in cognitive radio. *IEEE Journal of Selected Topics in Signal Processing*, 2(1):18–27, 2008. 7

[27] Charles Clancy, Joe Hecker, Erich Stuntebeck, and Tim O'Shea. Applications of machine learning to cognitive radio networks. *IEEE Wireless Communications*, 14(4):47–52, 2007. 7

[28] Xiqi Gao, Bin Jiang, Xiaohu You, Zhiwen Pan, Yisheng Xue, and Egon Schulz. Efficient channel estimation for mimo single-carrier block transmission with dual cyclic timeslot structure. *IEEE Transactions on Communications*, 55(11):2210–2223, 2007. 7

[29] Yuqing Huang, Hong Jiang, Hong Hu, and Yuancheng Yao. Design of learning engine based on support vector machine in cognitive radio. In *International Conference on Computational Intelligence and Software Engineering, 2009*, 2009. 8

[30] Xu Dong, Ying Li, Chun Wu, and Yueming Cai. A learner based on neural network for cognitive radio. In *IEEE 12th International Conference on Communication Technology, 2010*, pages 893–896, 2010. 8

[31] Manel Martinez Ramon, Thomas Atwood, Silvio Barbin, and Christos G Christodoulou. Signal classification with an svm-fft approach for feature extraction in cognitive radio. In *SBMO/IEEE MTT-S International Microwave and Optoelectronics Conference, 2009 (IMOC)*, pages 286–289, 2009. 8

[32] William A. Gardner. Exploitation of spectral redundancy in cyclostationary signals. *IEEE Signal Processing Magazine*, 8(2):14–36, 1991. 17

[33] Yuan Yuan, Paramvir Bahl, Ranveer Chandra, Philip A. Chou, John Ian Ferrell, Thomas Moscibroda, Srihari Narlanka, and Yunnan Wu. Knows: Cognitive radio networks over white spaces. In *IEEE 2nd International Symposium on New Frontiers in Dynamic Spectrum Access Networks, 2007*, pages 416–427, 2007. 17

[34] G. Ganesan and Ye Li. Agility improvement through cooperative diversity in cognitive radio. In *IEEE Global Telecommunications Conference, 2005 (GLOBECOM '05)*, volume 5, page 5, 2005. 17

[35] N.S. Shankar, C. Cordeiro, and K. Challapali. Spectrum agile radios: utilization and sensing architectures. In *IEEE First International Symposium on New Frontiers in Dynamic Spectrum Access Networks, 2005 (DySPAN)*, pages 160–169, 2005. 17

[36] Danijela Cabric, Artem Tkachenko, and Robert W. Brodersen. Spectrum censing measurements of pilot, energy, and collaborative detection. In *IEEE Military Communications conference, 2006 (MILCOM)*, pages 2342–2348, 2006. 17

[37] Ghurumuruhan Ganesan and Ye (Geoffrey) Li. Cooperative spectrum sensing in cognitive radio networks. In *IEEE First International Symposium on New Frontiers in Dynamic Spectrum Access Networks, 2005 (DySPAN)*, pages 137–143, 2005. 17

[38] Danijela Cabric, Shridhar Mubaraq Mishra, and Robert W. Brodersen. Implementation issues in spectrum sensing for cognitive radios. In *Conference Record of the Thirty-Eighth Asilomar Conference on Signals, Systems and Computers, 2004*, volume 1, pages 772–776, 2004. 17, 18, 78

[39] Harry Urkowitz. Energy detection of unknown deterministic signals. *Proceedings of the IEEE*, 55(4):523–531, 1967. 18

[40] Haiyun Tang. Some physical layer issues of wide-band cognitive radio systems. In *IEEE First International Symposium on New Frontiers in Dynamic Spectrum Access Networks, 2005 (DySPAN)*, pages 151–159, 2005. 18

[41] Tevfik Yucek and Huseyin Arslan. Spectrum characterization for opportunistic cognitive radio systems. In *IEEE Military Communications conference, 2006 (MILCOM)*, pages 1805–1810, 2006. 18

[42] Fadel F. Digham, Mohamed-Slim Alouini, and Marvin K. Simon. On the energy detection of unknown signals over fading channels. In *IEEE International Conference on Communications, 2003 (ICC '03)*, volume 55, pages 3575–3579, 2003. 18

[43] Deepa Bhargavi and Chandra R. Murthy. Performance comparison of energy, matched-filter and cyclostationarity-based spectrum sensing. In *IEEE 11th International Workshop on Signal Processing Advances in Wireless Communications, 2010 (SPAWC)*, pages 1–5, 2010. 19

[44] Shipra Kapoor, Svrk Rao, and Ghanshyam Singh. Opportunistic spectrum sensing by employing matched filter in cognitive radio network. In *International Conference on Communication Systems and Network Technologies, 2011*, pages 580–583, 2011. 19

[45] Liangping Ma, Yingxue Li, and Alpaslan Demir. Matched filtering assisted energy detection for sensing weak primary user signals. In *IEEE International Conference on Acoustics, Speech and Signal Processing, 2012 (ICASSP)*, pages 3149–3152, 2012. 19

[46] Xinzhi Zhang, Rong Chai, and Feifei Gao. Matched filter based spectrum sensing and power level detection for cognitive radio network. In *IEEE Global Conference on Signal and Information Processing, 2014 (GlobalSIP)*, pages 1267–1270, 2014. 19

[47] Menguc Oner and Friedrich Jondral. Cyclostationarity-based methods for the extraction of the channel allocation information in a spectrum pooling system. In *Proceedings. 2004 IEEE Radio and Wireless Conference*, pages 279–282, 2004. 20

[48] Nilesh Khambekar, Liang Dong, and Vipin Chaudhary. Utilizing ofdm guard interval for spectrum sensing. In *IEEE Wireless Communications and Networking Conference, 2007*, pages 38–42, 2007. 20

[49] Peng Qihang, Zeng Kun, Wang Jun, and Li Shaoqian. A distributed spectrum sensing scheme based on credibility and evidence theory in cognitive radio context. In *IEEE 17th International Symposium on Personal, Indoor and Mobile Radio Communications, 2006*, pages 1–5, 2006. 20

[50] Ning Han, SungHwan Shon, Jae Hak Chung, and Jae Moung Kim. Spectral correlation based signal detection method for spectrum sensing in ieee 802.22 wran systems. In *8th International Conference Advanced Communication Technology, 2006*, volume 3, 2006. 20

[51] Danijela Cabric and Robert W. Brodersen. Physical layer design issues unique to cognitive radio systems. In *IEEE 16th International Symposium on Personal, Indoor and Mobile Radio Communications, 2005*, volume 2, pages 759–763, 2005. 20

[52] Jarmo Lundn, Visa Koivunen, Anu Huttunen, and H. Vincent Poor. Spectrum sensing in cognitive radios based on multiple cyclic frequencies. In *2nd International Conference on Cognitive Radio Oriented Wireless Networks and Communications, 2007*, pages 37–43, 2007. 20

[53] Kyouwoong Kim, I. A. Akbar, K. K. Bae, Jung sun Urn, C. M. Spooner, and J. H. Reed. Cyclostationary approaches to signal detection and classification in cognitive radio. In *2nd IEEE International Symposium on New Frontiers in Dynamic Spectrum Access Networks, 2007*, pages 212–215, 2007. 20

[54] Yonghong Zeng and Ying-Chang Liang. Maximum-minimum eigenvalue detection for cognitive radio. In *IEEE 18th International Symposium on Personal, Indoor and Mobile Radio Communications, 2007*, 2007.

[55] Hou-Shin Chen, Wen Gao, and David G Daut. Spectrum sensing for ofdm systems employing pilot tones. *IEEE Transactions on Wireless Communications*, 8(12):5862–5870, 2009. 29, 78

[56] François-Xavier Socheleau, Philippe Ciblat, and Sébastien Houcke. Ofdm system identification for cognitive radio based on pilot-induced cyclostationarity. In *IEEE Wireless Communications and Networking Conference, 2009 (WCNC)*, pages 1–6, 2009. 29

[57] Andrea Mariani, Andrea Giorgetti, and Marco Chiani. Effects of noise power estimation on energy detection for cognitive radio applications. *IEEE Transactions on Communications*, 59(12):3410–3420, 2011. 33

[58] Carl R Stevenson, Gerald Chouinard, Zhongding Lei, Wendong Hu, Stephen J Shellhammer, and Winston Caldwell. Ieee 802.22: The first cognitive radio wireless regional area network standard. *IEEE Communications Magazine*, 47(1):130–138, 2009. 33, 34

[59] ECMA TC48-TG. Standard ecma-392: Mac and phy for operation in tv white space. *ECMA Std., Dec*, 2009. 33

[60] Pavlo Molchanov, Stephen Tyree, Tero Karras, Timo Aila, and Jan Kautz. Pruning convolutional neural networks for resource efficient inference. *arXiv preprint arXiv:1611.06440*, 2016. 40

[61] Hang Liu, Xu Zhu, and Takeo Fujii. Cyclostationary based full-duplex spectrum sensing using adversarial training for convolutional neural networks. In *International Conference on Artificial Intelligence in Information and Communication, 2019 (ICAIIC)*, pages 369–374, 2019. 47

[62] Hang Liu, Xu Zhu, and Takeo Fujii. Adversarial training for low-complexity convolutional neural networks using in spectrum sensing. In *International Conference on Artificial Intelligence in Information and Communication, 2019 (ICAIIC)*, pages 478–483, 2019. 47

[63] Hang Liu, Xu Zhu, and Takeo Fujii. A new classification-like scheme for spectrum sensing using spectral correlation and stacked denoising autoencoders. *IEICE Transactions on Communications*, page 2017EBP3447, 2018. 47, 75

[64] Jung Il Choi, Mayank Jain, Kannan Srinivasan, Phil Levis, and Sachin Katti. Achieving single channel, full duplex wireless communication. In *Proceedings of the 16th Annual International Conference on Mobile Computing and Networking*, 2010. 48

[65] Mayank Jain, Jung Il Choi, Taemin Kim, Dinesh Bharadia, Siddharth Seth, Kannan Srinivasan, Philip Levis, Sachin Katti, and Prasun Sinha. Practical, real-time, full duplex wireless. In *Proceedings of the 17th Annual International Conference on Mobile Computing and Networking*, pages 301–312, 2011. 48

[66] Bozidar Radunovic, Dinan Gunawardena, Peter Key, Alexandre Proutiere, Nikhil Singh, Vlad Balan, and Gerald Dejean. Rethinking indoor wireless mesh design: Low power, low frequency, full-duplex. In *IEEE Fifth Workshop on Wireless Mesh Networks, 2010 (WIMESH 2010)*. 48

[67] Achaleshwar Sahai, Gaurav Patel, and Ashutosh Sabharwal. Pushing the limits of full-duplex: Design and real-time implementation. *arXiv preprint arXiv:1107.0607*, 2011. 48

[68] Evan Everett, Achaleshwar Sahai, and Ashutosh Sabharwal. Passive self-interference suppression for full-duplex infrastructure nodes. *IEEE Transactions on Wireless Communications*, 13(2):680–694, 2014. 48

[69] Gan Zheng, Ioannis Krikidis, and Bjdotrm orn Ottersten. Full-duplex cooperative cognitive radio with transmit imperfections. *IEEE Transactions on Wireless Communications*, 12(5):2498–2511, 2013. 48, 49

[70] Yun Liao, Tianyu Wang, Lingyang Song, and Zhu Han. Listen-and-talk: Protocol design and analysis for full-duplex cognitive radio networks. *IEEE Transactions on Vehicular Technology*, 66(1):656–667, 2017. 48

[71] Wessam Afifi and Marwan Krunz. Exploiting self-interference suppression for improved spectrum awareness/efficiency in cognitive radio systems. In *2013 IEEE Proceedings INFOCOM*, pages 1258–1266. 48

[72] Taneli Riihonen and Risto Wichman. Energy detection in full-duplex cognitive radios under residual self-interference. In *9th International Conference on Cognitive Radio Oriented Wireless Networks and Communications, 2014 (CROWNCOM)*, pages 57–60. 48, 72

[73] Wenchi Cheng, Xi Zhang, and Hailin Zhang. Full duplex spectrum sensing in non-time-slotted cognitive radio networks. In *Military Communications Conference, 2011 (MILCOM)*, pages 1029–1034. 48

[74] Ville Syrjala, Mikko Valkama, Markus Allén, and Koji Yamamoto. Simultaneous transmission and spectrum sensing in ofdm systems using full-duplex radios. In *IEEE 82nd Vehicular Technology Conference, 2015 (VTC Fall)*. 48

[75] Qingqing Cheng, Eryk Dutkiewicz, Gengfa Fang, Zhenguo Shi, Diep N Nguyen, and Huiyang Wang. A novel full-duplex spectrum sensing algorithm for ofdm signals in cognitive radio networks. In *IEEE Global Communications Conference, 2017 (GLOBECOM)*. 48, 72

[76] Naim Bitar, Siraj Muhammad, and Hazem H Refai. Wireless technology identification using deep convolutional neural networks. In *IEEE 28th Annual International Symposium on Personal, Indoor, and Mobile Radio Communications, 2017 (PIMRC)*. 49, 57

[77] Woongsup Lee, Minhoe Kim, Dong-Ho Cho, and Robert Schober. Deep sensing: Cooperative spectrum sensing based on convolutional neural networks. *arXiv preprint arXiv:1705.08164*, 2017. 49, 57, 78

[78] Ming Zhang, Ming Diao, and Limin Guo. Convolutional neural networks for automatic cognitive radio waveform recognition. *IEEE Access*, 5:11074–11082, 2017. 49, 57

[79] Sachin Chaudhari, Visa Koivunen, and H Vincent Poor. Autocorrelation-based decentralized sequential detection of ofdm signals in cognitive radios. *IEEE Transactions on Signal Processing*, 57(7):2690–2700, 2009. 49

[80] Naveed Akhtar and Ajmal Mian. Threat of adversarial attacks on deep learning in computer vision: A survey. *arXiv preprint arXiv:1801.00553*, 2018. 49

[81] Marc Adrat, Jan Leduc, Stefan Couturier, Markus Antweiler, and Harald Elders-Boll. 2nd order cyclostationarity of ofdm signals: Impact of pilot tones and cyclic prefix. In *IEEE International Conference on Communications, 2009 (ICC'09)*, 2009. 52

[82] Yonghong Zeng, Ying-Chang Liang, and The-Hanh Pham. Spectrum sensing for ofdm signals using pilot induced auto-correlations. *IEEE Journal on Selected Areas in Communications*, 31(3):353–363, 2013. 52

[83] Laurens van der Maaten and Geoffrey Hinton. Visualizing data using t-sne. *Journal of Machine Learning Research*, 9(Nov):2579–2605, 2008. 67

[84] Hang Liu, Xu Zhu, and Takeo Fujii. Ensemble deep learning based cooperative spectrum sensing with stacking fusion center. In *Asia-Pacific Signal and Information Processing Association Annual Summit and Conference, 2018 (APSIPA ASC)*, pages 1841–1846, 2018. 77

[85] Anant Sahai, Rahul Tandra, Shridhar Mubaraq Mishra, and Niels Hoven. Fundamental design tradeoffs in cognitive radio systems. In *Proceedings of the First International Workshop on Technology and Policy for Accessing Spectrum*, 2006: 2. 78

[86] Ian F Akyildiz, Brandon F Lo, and Ravikumar Balakrishnan. Cooperative spectrum sensing in cognitive radio networks: A survey. *Physical Communication*, 4(1):40–62, 2011. 78

[87] Fadel F Digham, Mohamed-Slim Alouini, and Marvin K Simon. On the energy detection of unknown signals over fading channels. *IEEE Transactions on Communications*, 55(1):21–24, 2007. 78

[88] A Fehske, J Gaeddert, and Jeffrey H Reed. A new approach to signal classification using spectral correlation and neural networks. In *IEEE First International Symposium on New Frontiers in Dynamic Spectrum Access Networks, 2005 (DySPAN 2005)*, pages 144–150, 2005. 78

[89] Karaputugala Madushan Thilina, Kae Won Choi, Nazmus Saquib, and Ekram Hossain. Machine learning techniques for cooperative spectrum sensing in cognitive radio networks. *IEEE Journal on Selected Areas in Communications*, 31(11):2209–2221, 2013. 78

[90] Jingwen Tong, Ming Jin, Qinghua Guo, and Youming Li. Cooperative spectrum sensing: A blind and soft fusion detector. *IEEE Transactions on Wireless Communications*, 2018. 78

[91] Xiao-Lei Zhang and DeLiang Wang. A deep ensemble learning method for monaural speech separation. *IEEE/ACM Transactions on Audio, Speech and Language Processing (TASLP)*, 24(5):967–977, 2016. 78

[92] Mikel Galar, Alberto Fernandez, Edurne Barrenechea, Humberto Bustince, and Francisco Herrera. A review on ensembles for the class imbalance problem: bagging-, boosting-, and hybrid-based approaches. *IEEE Transactions on Systems, Man, and Cybernetics, Part C (Applications and Reviews)*, 42(4):463–484, 2012. 78

[93] Gang Wang, Jinxing Hao, Jian Ma, and Hongbing Jiang. A comparative assessment of ensemble learning for credit scoring. *Expert Systems with Applications*, 38(1):223–230, 2011. 78

Publications

List of Publications Directly Related to Thesis

Journal Papers

1. Hang Liu, Xu Zhu and Takeo Fujii, **"Convolutional neural networks for pilot-induced cyclostationarity based OFDM signals spectrum sensing in full-duplex cognitive radio",** IEICE Transactions on Communications.

2. Hang Liu, Xu Zhu and Takeo Fujii, **"A new classification-like scheme for spectrum sensing using spectral correlation and stacked denoising autoencoders",** IEICE Transactions on Communications 2018, vol. E101-B, no. 11, pp 2348-2361.

International Conference Papers

1. Hang Liu, Xu Zhu and Takeo Fujii, **"Ensemble Deep Learning Based Cooperative Spectrum Sensing with Semi-soft Stacking Fusion Center"**, in Proceedings of *2019 IEEE Wireless Communications and Networking Conference (WCNC)*, Apr. 2019.

List of Publications for References

Journal Paper

1. Xiukun Li, Xiangxia Meng, Hang Liu and Mingye Liu, **"Classification of Underwater Target Echoes Based on Auditory Perception Characteristics",** Journal of Marine Science and Application, 2014.13(2), 218-224.

International Conference Papers

1. Hang Liu, Xu Zhu and Takeo Fujii, **"Cyclostationary based full-duplex spectrum sensing using adversarial training for convolutional neural networks"**, in Proceedings of *2019 IEEE International Conference on Artificial Intelligence in Information and Communication (ICAIIC)*, Feb. 2019.

2. Hang Liu, Xu Zhu and Takeo Fujii, **"Adversarial training for low-complexity convolutional neural networks using in spectrum sensing"**, in Proceedings of *2019 IEEE International Conference on Artificial Intelligence in Information and Communication (ICAIIC)*, Feb. 2019.

3. Hang Liu, Xu Zhu and Takeo Fujii, **"Ensemble Deep Learning Based Cooperative Spectrum Sensing with Stacking Fusion Center"**, in Proceedings of *2018 IEEE Asia-Pacific Signal and Information Processing Association Annual Summit and Conference (APSIPA ASC)*, Nov. 2018.

4. Hang Liu, Xu Zhu and Takeo Fujii, **"Primary User Detection in Cognitive Radio Using Spectral-Correlation Features and Stacked Denoising Autoencoder"**, in Proceedings of *2017 IEEE International Symposium on Personal, Indoor and Mobile Radio Communications (PIMRC)*, Oct. 2017.

5. Hang Liu and Takeo Fujii, **"Second Order Blind Identification based Spectrum Sensing for Cognitive Radio"**, in Proceedings of *2016 IEEE*

Eighth International Conference on Ubiquitous and Future Networks (ICUFN), July 2016.

Domestic Conference Papers

1. Hang Liu, Xu Zhu, and Takeo Fujii, **"Primary user detection in cognitive radio using spectral-correlation features and stacked denoising autoencoders based on signal classification"**, IEICE Technical conference on Softwared Radio (IEICE SR 2017), May. 2017.

2. Hang Liu and Takeo Fujii, **"Single Channel Blind Source Separation of Energy Detection Using EMD for Cognitive Radio"**, IEICE Technical conference on Softwared Radio (IEICE SR 2016), Mar. 2016.